



Scuola Internazionale Superiore di Studi Avanzati - Trieste

Role of frustration in quantum spin chains and ladders: A field theory approach

Thesis submitted for the degree of Doctor Philosophiae

CANDIDATE

Mahdi Zarea Ahmadabadi

SUPERVISORS

Alexander A. Nersesyan
Michele Fabrizio

SISSA - Via Beirut 2-4 - 34014 TRIESTE - ITALY

Role of frustration in quantum spin chains and
ladders: A field theory approach

Candidate: **Mahdi Zarea Ahmadabadi**

Supervisors: **Alexander A. Nersesyan, Michele Fabrizio**

Thesis submitted for the degree of Doctor Philosophiae

Acknowledgments

I would like to warmly thank my supervisors Prof. M. Fabrizio and Prof. A. Nersesyan for giving me the opportunity of working with them, teaching me many things, their patient, the constant attention and the time they devoted to me. I thank them deeply and sincerely.

I also appreciate highly Prof. A. Gogolin for his invaluable remarks and critical analysis of the work.

I would like also to thank my friend Y. J. Wang for useful discussions and remarks.

Contents

1	Introduction	6
I	Bound states of standard spin ladder	12
2	Review of quantum spin chain	13
2.1	Continuum Limit	14
2.2	Bosonization	16
3	Standard Ladder	20
3.1	Non-conventional Haldane phase	23
3.2	Bound states in the standard spin ladder	25
3.3	Conclusion	30
4	Appendix I: Quantum Ising chain	32
5	Appendix II: Breathers in the sine-Gordon model	36
5.1	Bare propagators	37
5.2	Perturbation Series	40
6	Appendix III: The bosonized form of four-spin interaction	47
II	Ordered phase of XXZ-zigzag spin-1/2 Heisenberg ladder	49
7	The model and its low-energy limit	50
8	Twistless ladder	57
9	Critical spin nematic phase	61
10	Massive spin nematic and dimerized phases	64
11	Ferromagnetic phase	68
12	RG approach at A-D boundary	71

13	Conclusions	75
14	Appendix I: More about sector C	77
15	Appendix II: Twist Interacting Term	80
16	Conclusion	84

List of Figures

1	Particle-hole spectrum of the spin-1/2 AF Heisenberg chain. . .	14
2	The standard ladder with in-chain coupling J and inter-chain coupling J_{\perp}	20
3	The phase diagram of the generalized spin ladder.	24
4	The in-phase (the above figure) and alternating-phase (the lower figure) vacuum state of the dimerized spin liquid.	25
5	The bare singular correlation function at $s = 2m$ (dashed line). In the presence of the interaction, instead of singularity a bound state will appear (solid line).	29
6	The kink excitations of the in-phase dimerized spin liquid (the above figure) and the alternating dimerized phase (the lower figure).	30
7	The triplet excitations in the rung-singlet phase (the above figure) and in the Haldane phase (the lower figure). Along the line spins have a tendency to form singlets.	31
8	The zigzag ladder with in-chain coupling J and inter-chain coupling J' . For small J it can be viewed as a single ladder (along the dashed line) with next nearest neighbor interaction.	50
9	The parameter space of the model	56
10	Possible phase transitions in the ladder: the left one is when $z_{\perp} < z_1$, MSN phase is very narrow, and the right one is for $z_{\perp} > z_1$	68

- 11 The first path shows one possible way of going through CSN, MSN and D phases when $z_{\perp} < z_1$, by increasing Δ and keeping Δ' to be a constant. The right figure shows the qualitative change of the spin current (solid line) and the dimerization order parameter (dashed line) following this path. In the second path by decreasing Δ' and keeping Δ at constant value, the ladder enters the F phase. 70

1 Introduction

Antiferromagnetic Heisenberg (AFH) spin chains and ladders have attracted notable theoretical and experimental interest in recent years because they may provide some insights into the physics of high- T_c superconductors. It is believed in many quarters that some aspects of cuprates superconductors might be understood if one assumed that the *parent* normal phase is not a conventional Fermi-liquid metal but rather some spin-liquid phase which emerges by the spin-frustration induced by doping holes in the Mott antiferromagnetic insulator at half-filling, for a recent brief review paper see [1].

Spin-liquid insulating phases are known to exist in one-dimensional models, like spin-ladders [2, 3] or single chains with competing nearest and next-nearest neighbor exchanges [4]. Even more, there are several evidences that doped holes in those model produce an enhancement of superconducting fluctuations [5, 6]

From this viewpoint, it would be desirable to have a unique theoretical framework which would allow to properly describe on equal footing frustrated and un-frustrated spin-chains, which is still lacking in one-dimension, not to speak about higher dimensions. That would represent not only an important achievement in the theory of one-dimensional systems, but it might also represent a first step towards a generalization in higher dimensions.

In low dimensions quantum fluctuations play an important role, even if frustration is not considered. Indeed, Mermin-Wagner theorem states that quantum fluctuations prevent any Neel-type of long range order in spin-isotropic Heisenberg chains. Therefore conventional methods to study spin-models, like the spin-wave theory, are useless in one-dimensions. Fortunately, we have at our disposal not only the exact Bethe Ansatz solution of the simplest Heisenberg chain with only nearest neighbor coupling, but also other powerful techniques like bosonization (a short review of the latter being given in the next section). What we know about the Heisenberg spin-chain is that it has a gapless spectrum and is critical, namely all spin correlation functions decay algebraically. Remarkably, the conventional spin-wave excitations, i.e. the $S=1$ magnons, are not coherent as they decompose into two massless $S=1/2$ domain walls (spinons): a realization of fractionalized excitations. A carton of magnon excitation can be visualized as $\uparrow\downarrow\uparrow\downarrow:\downarrow\uparrow\downarrow\uparrow$ in which the domain walls are free to move, thus creating two $S=1/2$ objects $\uparrow\downarrow:\downarrow\uparrow\downarrow\uparrow:\downarrow\uparrow\downarrow$.

The spin dynamical structure factor, which describes the spectrum of $S=1$ excitations, comprises therefore a gapless two-particle continuum, which was indeed observed in neutron scattering experiments on $KCuF_3$ [7].

In the route from one to higher dimension, a first step may be represented by n -rung spin ladders, namely n weakly coupled AFH spin-chains. Indeed, already in these simple cases interesting phenomena occur. For instance, spin ladders with n odd or even behave differently. While the former remain critical, the latter are gapped with exponentially decaying spin-spin correlation function [5]. This prediction has been confirmed experimentally in a series of compounds, $Sr_{n-1}Cu_{n+1}O_{2n}$, which realize n -rung spin ladders [8]. This gap should vanish, presumably as a power law when $n \rightarrow \infty$, namely in the two-dimensional case, where it is believed that the ground state is Neel ordered with gapless magnon-excitations.

The simplest model to investigate the properties of ladders is the $n = 2$ case in which each spin interact with only one spin in the other chain either by a ferromagnetic or antiferromagnetic interchain exchange interaction J_{\perp} . It is known that this ladder is gapped in both strong and weak interchain coupling limit (as compared with the AF intrachain coupling J_{\parallel}). The existence of the gap is obvious in the large AF interchange coupling limit, at which a singlet is formed along the rung, and the triplet excitations are separated from the singlets by a large gap, of the order of J_{\perp} . Yet this gap persists even when $J_{\perp} \ll J_{\parallel}$. Therefore, in the presence of J_{\perp} two massless spinons get confined to form a coherent massive magnon. The presence of the spin gap is also confirmed in $Cu_2(C_5H_{12}N_2)_2Cl_4$, in which the Cu^+ ions with $S = 1/2$ are coupled antiferromagnetically along and across the chains [9].

Besides the single magnon excitation, a continuum of two-magnons can be observed in the $n = 2$ ladder, which is highly sensitive to the interchain spin interaction: an antiferromagnetic interchain coupling can bind two magnons and create a bound state with a well defined excitation peak at an energy slightly below the two particles threshold. In the strong coupling limit, $J_{\perp} \gg J_{\parallel}$, the singlet bound state has been observed in optical measurements on $(La, Ca)_{14}Cu_{24}O_{41}$ [11], in agreement with the theoretical predictions [10].

On the contrary, an interchain ferromagnetic coupling can not confine two magnons to form a bound state.

The second step towards more realistic models which might be relevant

for higher dimensions, is to include frustration. Indeed, when frustration comes into play, quantum fluctuations get even more pronounced leading to novel physical behaviors. The appearance of unconventional spin-liquid phases in frustrated Heisenberg models around a critical point separating different magnetic ordered phases is a long standing intriguing issue which has attracted notable theoretical and experimental interest in recent years[12]. From a theoretical point of view, this is quite a challenging problem which calls for a deep reexamination of standard theories. Conventionally, the stability of a spin-ordered phase may be investigated by spin-wave theory or by more sophisticated field-theoretical approaches based on the non-linear σ -model. Spin-wave theory is in principle able to detect instabilities at any wave-vector, although a reliable description would require a systematic $1/S$ expansion, S being the magnitude of the spin. The non-linear σ -model offers a better description of the critical behavior close to an instability point, yet it has a major limitation. Namely, it takes into account only the long-wavelength Goldstone modes of the ordered state under consideration, but fails to describe the excitations at the wave-vector of the competing ordered state. Hence it does not provide any information about the phase which can emerge under increasing the effect of frustration.

The simplest example of one-dimensional frustrated spin model is the spin-1/2 Heisenberg chain with antiferromagnetic nearest neighbor exchange J' and frustrating next nearest neighbor exchange J (for a recent review and references therein, see Ref.[13]). Besides the general interest, this model is also relevant for realistic materials, such as Cs_2CuCl_4 , in which magnetic Cu ions get arranged into a zig-zag fashion.[14]

In the classical limit, the J - J' spin chain has a Neél long range order for $j = J/J' < 1/4$, with characteristic momentum $q = \pi/a_0$. In the Neél phase time reversal symmetry is preserved if combined with a translation by one lattice spacing a_0 . For larger values of j , a spiral ordering at momentum satisfying $\cos(q a_0) = -1/4 j$ is stabilized at the classical level. There parity and time reversal symmetries are separately broken.

Quantum fluctuations modify the classical phase diagram [18]. As we said, spin rotational symmetry cannot be broken in one dimension: the Neél long-range ordered phase turns into the quasi-long range ordered one characterized by power-law decaying correlations of the staggered magnetization. The low-energy effective critical theory is the level-1 Wess-Zumino-Novikov-Witten (WZNW) model (free massless bosons with central charge $C = 1$). On the contrary, the spiral order disappears completely in favor of a sponta-

neously dimerized phase. The transition point is slightly shifted with respect to the classical value, $j_c \simeq 0.241$ [19, 20]. Within the WZNW model formalism, the transition is driven by a perturbation which is marginally irrelevant (relevant) at $j < j_c$ ($j > j_c$). At $j = j_c$ a Berezinskii-Kosterlitz-Thouless transition takes place, and an exponentially small spectral gap opens up in the region $j > j_c$ [21]. The system continuously passes to a two-fold degenerate, spontaneously dimerized, massive phase. Upon further increasing j , the gap reaches its maximum at the exactly solvable Majumdar-Ghosh point [22], $j = 1/2$, after which it slowly decreases [21]. Even though the ground state of the J - J' chain remains dimerized at all $j > j_c$, above the Majumdar-Ghosh point the system reveals signatures of the classical spiral phase: the spin-spin correlations become incommensurate, as it was shown numerically in Refs.[21, 23]. Since this occurs far away from the region of applicability of the $SU(2)_1$ WZNW model, there is little scope to improve the field-theoretical description of the gapless phase at $j < j_c$ to account for incommensurate correlations that emerge well above j_c . More promising is to approach this problem from the opposite side, $j \gg 1$. If $J' = 0$, the even and odd sublattices of the spin chain decouple, and the model effectively describes two decoupled Heisenberg chains, one for each sublattice. Classically this corresponds to the case when the spiral wave number is equal to $q = \pi/2a_0$. Switching on a small J' transforms the model to a weakly coupled two-chain zigzag spin ladder, with the interchain coupling giving rise to a marginally relevant perturbation that opens up a gap and brings the system back to the dimerized phase. In addition it should also move the relevant momentum q away from $\pi/2a_0$ towards π/a_0 . Therefore incommensuration and the spectral gap are supposed to appear together in this limit, which makes a field-theoretical description more plausible.

Indeed, in the limit $j \gg 1$, a novel, parity-breaking (twist) perturbation was identified in Ref. [24] as a natural source of the spin incommensurabilities. The twist term has a tendency to support a finite spin current along the chains which would account for the expected shift of the momentum. However, for the $SU(2)$ -symmetric zigzag ladder, the situation still remains rather unclear. Apparently, the appearance of a nonzero spin current is not compatible with the requirement of unbroken spin rotational symmetry (see, however, the discussion in sec.VII). On the other hand, no reliable information about the actual role of the twist operator at the strong-coupling fixed point can be extracted from the Renormalization Group (RG) analysis [24] because of the perturbative nature of this approach. Thus, the structure of

the low-energy effective field theory for the $SU(2)$ -symmetric $S=1/2$ zigzag ladder still remains unknown.

The situation changes much to the better in the presence of strong spin anisotropy. Namely, close to the XX limit, a self-consistent, symmetry-preserving mean-field approach shows that the twist operator can stabilize a new, spin-nematic (chiral) phase [24]. In this doubly degenerate phase a nonzero spin current polarized along the easy axis flows along the ladder, and the transverse spin-spin correlations are incommensurate and may even decay algebraically within some parameter range, as it is the case at the XX point. This picture is supported by recent numerical simulations [25, 26, 27, 28]. In particular, the numerical work by Hikihara *et al* [25, 26] has indeed confirmed the existence of the critical spin-nematic phase in a broad region of the phase diagram for spin-anisotropic chains, both for integer and half-integer spins. NMR experiments on CaV_2O_4 [29], which physically realizes a spin-1 zigzag ladder, have indeed revealed the gapless nature of the spectrum, which may be an indication in favor of a critical chiral state. On the other hand, numerical simulations also show the existence of a new gapped chiral state in a very narrow region between the dimerized and the critical chiral phases, but, within numerical accuracy, only for integer spins. In that gapped phase, the spin current coexists with dimerization; accordingly, the spin-spin correlations are incommensurate but decay exponentially. The phase diagram for general spin S has also been studied analytically by bosonization technique [30] and through the non-linear σ -model [31], verifying the existence of both critical and gapped chiral phases for integer spin.

In this thesis we aim to clarify some aspects which are still obscure or controversial, both for unfrustrated and for frustrated spin-ladder.

In Part I we deal with the problem of bound states in the standard ladder. That will also give us the opportunity to briefly review quantum spin chains and bosonization technique, which is done in Section 2. The standard ladder is instead introduced in the section 3. There we review the analysis of Ref. [2] which allows, in the limit of small interchain exchange interaction $J_\perp \ll J_\parallel$, to characterize the ground state and part of the spectrum. Upon taking into account the residual interaction between singlet and triplet magnon excitations, we study for the first time the bound states which can appear in the ladder at weak coupling.

Part II of this thesis contains most of our original work. Here we present a detailed study of the phase diagram of the XXZ frustrated spin-1/2 chain in the limit $J' \ll J$. Using a variational analysis of the bosonized Hamiltonian

we identify possible phases of the model. In addition to the critical spin-nematic phase and to the commensurate spontaneously dimerized one, we find conditions for the existence of a massive spin-nematic region for the $S = 1/2$ case. We also characterize the topological excitations which occur in each region of the phase diagram.

In section 7 we introduce the model and discuss the bosonization approach. In section 8 we demonstrate how the variational approach can be applied to the twistless ladder, in which only the dimerization operator plays a role. Critical spin nematic phase, driven only by the twist operator, is studied in section 9. The interplay between dimerization and twist operator and other emerging phases is discussed in section 10. In section 11 we analyse the ferromagnetic phase dual to the critical spin nematic phase, while in section 12 we perform an RG approach to study the interplay between different twist operators at the border of these mutually dual phases. The last section contains conclusions.

Part I

Bound states of standard spin ladder

This part is devoted to the weakly coupled standard spin ladder, its spectrum, ground state and excitations. Special emphasis has been put on the possible bound states of the ladder, the formation of which prominently changes the nature of spin-spin correlation functions. Bound states of magnons has been observed in some compounds [11] in which the interchain and inchain coupling are of the same order. Since the theoretical work is restricted to strong coupling limit [10], a weak coupling analysis seems to be useful.

2 Review of quantum spin chain

In one dimensional (1D) quantum systems the role of quantum fluctuations is dominant. We consider the antiferromagnetic (AF) Heisenberg spin-1/2 chain

$$\mathcal{H} = J \sum_{n=1}^N (S_n^x S_{n+1}^x + S_n^y S_{n+1}^y + \Delta S_n^z S_{n+1}^z) \quad (S_{N+1}^\alpha = S_1^\alpha). \quad (1)$$

with $-1 < \Delta \leq 1$ being the exchange anisotropy parameter. This model can be mapped to spin-less fermions on a lattice, by means of the Jordan-Wigner transformation

$$S_n^z = a_n^\dagger a_n - \frac{1}{2}, \quad S_n^+ = a_n^\dagger \exp[-i\pi \sum_{j=1}^{n-1} a_j^\dagger a_j], \quad S_n^- = [S_n^+]^\dagger \quad (2)$$

in which a and a^\dagger are fermionic operators. As two spin operators anti-commute on the same sites but commute on different sites, the nonlocal string operator $\exp[-i\pi \sum_{j=1}^{n-1} a_j^\dagger a_j]$ is implemented to guarantee correct commutation relations. In fermionic language the Hamiltonian reads

$$\mathcal{H}_f = \frac{J}{2} \sum_n (a_n^\dagger a_{n+1} + h.c.) + J\Delta \sum_n (a_n^\dagger a_n - 1/2)(a_m^\dagger a_m - 1/2). \quad (3)$$

At the XX-point, $\Delta = 0$, these fermions are free with

$$\mathcal{H}_f^0 = \sum_k \varepsilon(k) a_k^\dagger a_k, \quad (4)$$

where the single-particle spectrum is given by

$$\varepsilon(k) = J \cos ka. \quad (5)$$

When the total magnetization is zero, (2) implies that the fermionic model is at half-filling $N_f = \frac{N}{2}$. The particle-hole excitation spectrum is shown in Fig(1). The system is gap-less (critical) so all its correlation functions show a power law decay and there is no long range order. This can be seen from the simple observation that $\langle S_n \rangle = 0$ and $\langle S_n S_m \rangle = -\frac{1}{2\pi^2} \frac{1-(-1)^{n-m}}{(n-m)^2}$.

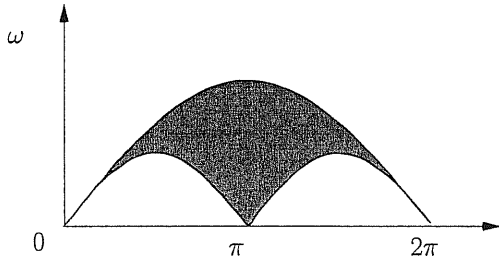


Figure 1: Particle-hole spectrum of the spin-1/2 AF Heisenberg chain.

2.1 Continuum Limit

At low energies compared to the band-width J or large distances compared to the lattice constant, universal properties emerge which can be approached by an appropriate continuum limit. It consists in taking $J \rightarrow \infty$, $a \rightarrow 0$ but $Ja = v_f = \text{constant}$, so that the original bounded spectrum $\varepsilon(p)$ will transform onto two linear branches $\varepsilon_R(p + \frac{\pi}{2}) = v_F p$ and $\varepsilon_L(p - \frac{\pi}{2}) = -v_F p$ near the two Fermi points $k_F = \pm \frac{\pi}{2}$. In this limit, the Hamiltonian (5) becomes

$$\mathcal{H}_f^0 = \text{const} + \sum_{|p| < \Lambda} p v_F [R^\dagger(p)R(p) - L^\dagger(p)L(p)] \quad (6)$$

in which R (L) is the right (left) fermion near $k = \frac{\pi}{2}$ ($k = -\frac{\pi}{2}$). The momentum cutoff Λ is supposed to be very large. All negative energy states are supposed to be filled. In the following, any operator is considered as the normal ordered one, in order to avoid the contribution from the unphysical infinity of filled and empty states. Associated with the operators $R(p)$ and $L(p)$ are the slowly varying fields $R(x)$ and $L(x)$

$$R(x) = \frac{1}{\sqrt{Na}} \sum_{|p| < \Lambda} e^{ipx} R(p), \quad L(x) = \frac{1}{\sqrt{Na}} \sum_{|p| < \Lambda} e^{ipx} L(p), \quad (7)$$

which satisfy the canonical anti-commutation relations

$$\begin{aligned} \{R(x), R^\dagger(x')\} &= \{L(x), L^\dagger(x')\} = \delta(x - x'), \\ \{R(x), L(x')\} &= \{R(x), L^\dagger(x')\} = 0, \end{aligned} \quad (8)$$

in the limit when $\Lambda \rightarrow \infty$. In Fourier representation

$$a_n \rightarrow \sqrt{a} [(-i)^n R(x) + i^n L(x)]. \quad (9)$$

and the Hamiltonian reads

$$\mathcal{H}_f^0 = -iv_F \int dx [R^\dagger(x) \partial_x R(x) - L^\dagger(x) \partial_x L(x)]. \quad (10)$$

The equation of motion for the right fermion $\partial_t R(x, t) = -v_F \partial_x R(x, t)$ guarantees that for the free right mover $R(x, t) = R(x - t) = R(x_-)$. In the same way $L(x, t) = L(x + t) = L(x_+)$. On the other hand as $\langle R(p) R^\dagger(p') \rangle = \theta(p) \delta_{pp'}$ one concludes that

$$\begin{aligned} \langle R^\dagger(x^-) R(y^-) \rangle &= \langle R(x^-) R^\dagger(y^-) \rangle = \frac{i}{2\pi(y^- - x^- + i\delta)} \\ \langle L^\dagger(x^+) L(y^+) \rangle &= \langle L(x^+) L^\dagger(y^+) \rangle = \frac{i}{2\pi(y^+ - x^+ + i\delta)} \end{aligned} \quad (11)$$

At each Fermi point we define the densities of the right and left fermions through

$$J_R(q) = \sum_p R_p^\dagger R_{p+q}, \quad J_L(q) = \sum_p L_p^\dagger L_{p+q}, \quad (12)$$

The most striking property of these operators is the so-called anomaly, namely if we calculate the commutator e.g. of the right-mover density

$$[J_R(q), J_R(q')] = \sum_{pp'} [R_p^\dagger R_{p+q}, R_{p'}^\dagger R_{p'+q'}] = \sum_p (R_p^\dagger R_{p+q+q'} - R_{p-q'}^\dagger R_{p+q}),$$

by the shift $p \rightarrow p + q'$ it seems naively to vanish. Yet, by assuming that all negative energy states in the infinite Dirac sea are filled, the ground state average of this commutator turns instead finite:

$$\langle F | [J_R(q), J_R(q')] | F \rangle = \delta_{q+q',0} \sum_p [n_R^0(p) - n_R^0(p+q)] = \frac{Lq}{2\pi} \delta_{q+q',0} \quad (13)$$

where $n_R^0(p) = \theta(-p)$ is the vacuum Fermi distribution function for the right-movers and $|F\rangle$ is the Fermi vacuum. For the L -density operators one similarly finds

$$\langle F | [J_L(q), J_L(q')] | F \rangle = -\frac{Lq}{2\pi} \delta_{q+q',0}. \quad (14)$$

Therefore it is not correct that the commutator is zero; instead it is equal to the constant which represents its vacuum average. In real space the above equations realize a $U(1)$ Kac-Moody algebra

$$[J_L(x^+), J_L(0)] = \frac{i}{2\pi} \partial_- \delta(x^+) \quad [J_R(x^-), J_R(0)] = \frac{i}{2\pi} \partial_- \delta(x^-). \quad (15)$$

Now we consider the retarded Green functions for the right and left densities defined as

$$D_{R,L}(x, t) = -i\theta(t) \langle [J_{R,L}(x, t), J_{R,L}(0, 0)] \rangle$$

$$D(\mathbf{q}, \omega) = L^D \int \frac{d^D \mathbf{k}}{(2\pi)^D} \frac{n_{\mathbf{k}} - n_{\mathbf{k}+\mathbf{q}}}{\omega - \epsilon(\mathbf{k} + \epsilon(\mathbf{k} + \mathbf{q})) + i\delta}. \quad (16)$$

In one dimension this function has a pole structure and represents the Green function of one dimensional massless bosons with linear dispersion relation $\omega = v_F q$:

$$D_{R,L}(q, \omega) = \pm \frac{Lq}{2\pi} \frac{1}{\omega \mp qv_F + i\delta} \quad (17)$$

The poles indicate that we are dealing with two coherent bosonic modes which are particle-hole excitations near the same Fermi point Fig(1). Such bosons are called Tomonaga bosons.

2.2 Bosonization

Now we try to express the density operators J_R, J_L and the free Hamiltonian (10) in term of bosonic fields. The free massless boson Hamiltonian is

$$\mathcal{H}_{bosons} = \frac{v_F}{2} \int dx [(\partial_x \Theta)^2 + (\partial_x \Phi)^2] = v \int dx [(\partial_x \varphi_R)^2 + (\partial_x \varphi_L)^2]. \quad (18)$$

in which v_F is the particle velocity, $\Phi = \varphi_R + \varphi_L$ and $\Pi = \partial_x \Theta = \partial_x (-\varphi_R + \varphi_L)$ are two canonical conjugate fields with

$$[\Phi(x), \Pi(x')] = \delta(x - x') \quad [\Phi(x), \Phi(x')] = [\Theta(x), \Theta(x')] = 0. \quad (19)$$

The vacuum expectation values of these fields are given by

$$\langle\langle \Phi(x)\Phi(0) \rangle\rangle = \langle\langle \Theta(x)\Theta(0) \rangle\rangle = -\frac{1}{4\pi} \ln \left(\frac{x^2 + a^2}{a^2} \right)$$

$$\langle\langle \Phi(x)\Theta(0) \rangle\rangle = -\frac{i}{2\pi} \arctan \frac{x}{a} \rightarrow -\frac{i}{4} \text{sign } x. \quad (20)$$

If the following relations between right and left fermion density operators and bosonic fields are assumed

$$J_R(x) = \frac{1}{\sqrt{\pi}} \partial_x \varphi_R(x), \quad J_L(x) = \frac{1}{\sqrt{\pi}} \partial_x \varphi_L(x). \quad (21)$$

then we recover the anomaly (15) as well as the correct equations of motion $(\partial_t + v_F \partial_x)J_R(x, t) = 0$, $(\partial_t - v_F \partial_x)J_L(x, t) = 0$.

We need also to express the fermionic operator R, L in term of bosonic fields. The relation is not trivial (see[15]) and we only quote the final expression

$$\begin{aligned} R^\dagger(x) &\Rightarrow \frac{1}{\sqrt{2\pi a}} \exp[i\sqrt{\pi}\{-\Phi(x) + \Theta(x)\}], \\ L^\dagger(x) &\Rightarrow \frac{1}{\sqrt{2\pi a}} \exp[i\sqrt{\pi}\{\Phi(x) + \Theta(x)\}], \end{aligned} \quad (22)$$

Considering (20) the above correspondence will give the right fermionic commutation relation (8) and the fermionic correlator (11).

We can now bosonize the spin operator which according to the JW transformation (2) and the continuum form of the fermion operators (9), is

$$\begin{aligned} S_n^z &= : a_n^\dagger a_n : \rightarrow a S^z(x), \\ S^z(x) &= J^z(x) + (-1)^{x/a} n^z(x) \end{aligned} \quad (23)$$

where the slowly varying (smooth) part of the spin density

$$J^z(x) = J_R(x) + J_L(x) = \frac{1}{\sqrt{\pi}} \partial_x \Phi(x) \quad (24)$$

while the staggered part is

$$n^z(x) = R^\dagger(x)L(x) + L^\dagger(x)R(x) = -\frac{1}{\pi a} \sin \sqrt{4\pi} \Phi(x). \quad (25)$$

Bosonization of the transverse spin operators S_n^\pm is a more complicated problem due to the presence of the string operator in (2). The reader can follow the details in [16], here we just write the final result:

$$\begin{aligned} S_n^+ &\rightarrow a S^+(x) = J^+ + (-1)^{x/a} n^+(x) \\ J^+(x) &\simeq -\frac{1}{\sqrt{2\pi a}} \sin \sqrt{4\pi} \Phi(x) \exp[i\sqrt{\pi}\Theta(x)] \quad n^+(x) \simeq -\frac{1}{\sqrt{2\pi a}} \exp[i\sqrt{\pi}\Theta(x)] \end{aligned} \quad (26)$$

Our last goal is to see how the interacting term $: a_n^\dagger a_n :: a_{n+1}^\dagger a_{n+1} :$ in (3) transform in bosonization language. Using (23) in the the continuum, we

get:

$$H_{int} = v_F \Delta \int dx [: J^z(x) J^z(x+a) : - : n^z(x) n^z(x+a) :]. \quad (28)$$

The bosonization of the first term is trivial and gives : $J^z(x) J^z(x+a) : \rightarrow \frac{1}{\pi} (\partial_x \Phi(x))^2$. This perturbation can be absorbed in the free bosonic Hamiltonian (18) by rescaling the bosonic field according to

$$\Phi(x) \rightarrow \sqrt{Q} \tilde{\Phi}(x), \quad \Pi(x) \rightarrow \frac{1}{\sqrt{Q}} \tilde{\Pi}(x) \quad (29)$$

where Q is a Δ -dependent parameter. This transformation preserve the bosonic commutation relation. The exact value of Q can be computed by the Bethe ansatz solution of the XXZ chain:

$$Q = \frac{1}{2 - 2\arccos(\Delta)/\pi}. \quad (30)$$

At the XX -point $Q = 1$ and at $SU(2)$ point we get $Q = 1/2$.

All together we get

$$H_{XXZ} = \frac{u}{2} \int dx [Q \Pi^2 + \frac{1}{Q} (\partial_x \Phi)^2] \quad (31)$$

where $u = v_F/Q$. The transformation of the second term in (28) is more subtle. In the fermionic language this term contain the so called Umklapp term in which two left movers scatter onto two right movers or vice versa. The bosonic form is given by

$$n^z(x) n^z(x+a) = -\frac{1}{2(\pi a)^2} : \cos \sqrt{16\pi} \Phi(x) : .$$

Adding the above term to (31) we finally get a sine-Gordon Hamiltonian for which the Umklapp term turns out to be an irrelevant operator, which only affect the proper dependence of Q upon Δ . Consequently in the whole region $-1 < \Delta \leq 1$ the spin-1/2 AF Heisenberg chain is in a critical phase described by a free bosonic Hamiltonian (18)

Taking into account the rescaling of the fields, the spin operators are bosonized as follows

$$\begin{aligned} J^z(x) &= \sqrt{\frac{Q}{\pi}} \partial_x \tilde{\Phi}(x), & J^+(x) &\simeq -\frac{1}{\sqrt{2\pi a}} \sin \sqrt{4\pi Q} \tilde{\Phi}(x) \exp[i\sqrt{\frac{\pi}{Q}} \tilde{\Theta}(x)] \\ n^z(x) &= -\frac{\lambda}{\pi a} \sin \sqrt{4\pi Q} \tilde{\Phi}(x), & n^+(x) &= -\frac{\lambda}{\pi a} \exp[i\sqrt{\frac{\pi}{Q}} \tilde{\Theta}(x)] \end{aligned} \quad (32)$$

where λ is a non-universal constant. These relations are valid for $-1 < \Delta \leq 1$. At the $SU(2)$ point a more appropriate mapping is needed, see e.g. [17].

Now we can calculate spin correlation functions for the XXZ spin chain. For the the total magnetization, through (20) and (32), we get:

$$\langle J^z(x)J^z(0) \rangle = -\frac{Q}{2\pi^2} \frac{1}{x^2}, \quad (33)$$

while for the staggered magnetization

$$\langle n^z(x)n^z(0) \rangle \sim \frac{1}{|x|^{2Q}}, \quad \langle n^x(x)n^x(0) \rangle \sim \frac{1}{|x|^{1/2Q}}. \quad (34)$$

Note that at the $SU(2)$ point $Q = \frac{1}{2}$ and two critical exponents become equal, as they should .

Finally it is instructive to bosonize the the dimerization field $\epsilon(x)$ defined by

$$\epsilon_n \sim (-1)^n \mathbf{S}_n \cdot \mathbf{S}_{n+1}. \quad (35)$$

In the bosnized form it reads

$$\epsilon(x) = \frac{\lambda}{\pi a} \cos \sqrt{4\pi Q} \tilde{\Phi}(x) \quad (36)$$

3 Standard Ladder

A single spin-1/2 chain is critical in whole range $-1 < \Delta \leq 1$. The excitations are massless spinons. The fate of spinons in weakly coupled spin-1/2 chains is an interesting problem. It is expected that ladders with even number of spin-1/2 chains are gapped with exponentially decaying spin-spin correlation functions, in contrary to those with odd number of chains which remain critical. Two weakly coupled spin-1/2 chain forming the standard spin-1/2 Heisenberg ladder are the best candidates to study the crossover from 1D spin chain to 2D spin systems. Moreover there are compounds which are physical realizations of spin ladders, like $Cu_2(C_5H_{12}N_2)_2Cl_4$.

The standard ladder is described by the Hamiltonian :

$$H = J_{\parallel} \sum_{j=1,2} \sum_n \mathbf{S}_j(n) \cdot \mathbf{S}_j(n+1) + J_{\perp} \sum_n \mathbf{S}_1(n) \cdot \mathbf{S}_2(n) \quad (37)$$

in which the in-chain coupling $J_{\parallel} > 0$ is antiferromagnetic but the inter-chain coupling J_{\perp} can take any sign Fig(2).

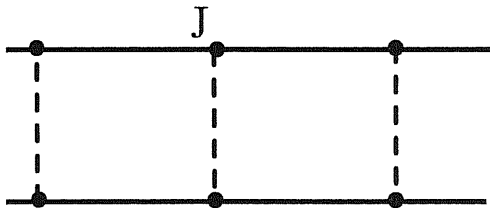


Figure 2: The standard ladder with in-chain coupling J and inter-chain coupling J_{\perp} .

The strong coupling $J_{\perp} \gg J$ analysis of the model reveals the existence of a spin-gap: in the strong ferromagnetic $-J_{\perp} \gg J$ region local triplets formed along each rung effectively leads to spin-1 AF chain with Haldane gap. On the other hand, in the strong AF limit a large gap (of order J_{\perp}) separates rung spin-singlet from spin-triplet configurations. Remarkably, the gap persists down to infinitesimal values of J_{\perp} .

Bosonization approach can be used near the critical point $J_{\perp} = 0$ separating these two massive phases. In the continuum limit the critical properties of each ladder is described by the free Hamiltonian H_0 in (18), which equivalently can be written in term of the total and the relative fields $\Phi_{\pm} = \frac{\Phi_1 \pm \Phi_2}{\sqrt{2}}$.

In the continuum limit each spin is represented by a smooth (total magnetization) and a staggered part, $\mathbf{S} = \mathbf{J} + (-1)^n \mathbf{n}$. The inter-chain interacting term is taken as a small perturbation. The ladder possesses the parity symmetry $P_S^1 \otimes P_S^2$ or $P_L^1 \otimes P_L^2$ (P_L and P_S are the link and site parity) which foretells that the strongly relevant term $\mathbf{n}_1 \cdot \mathbf{n}_2$ plays the leading role in the low energy effective Hamiltonian. The slowly varying part of each spin contributes in the marginal interaction $\mathbf{J}_1 \cdot \mathbf{J}_2$. In bosonized form the total Hamiltonian reads

$$H = H_+ + H_- + H_{int} \quad (38)$$

$$H_+(x) = \frac{v_s}{2} \left(\Pi_+^2 + (\partial_x \Phi_+)^2 \right) + \frac{m}{\pi a_0} \cos \sqrt{4\pi} \Phi_+ \quad (39)$$

$$H_-(x) = \frac{v_s}{2} \left(\Pi_-^2 + (\partial_x \Phi_-)^2 \right) + \frac{m}{\pi a_0} \cos \sqrt{4\pi} \Phi_- + \frac{2m}{\pi a_0} \cos \sqrt{4\pi} \Theta_- \quad (40)$$

Here $m = \frac{J_1 \lambda^2}{2\pi}$ (λ is a non-universal constant) and H_{int} is the marginal perturbation $\mathbf{J}_1 \cdot \mathbf{J}_2$. The (+) channel Hamiltonian is equivalent to a free massive Thirring model and can be mapped onto the model of two Majorana fermions with the same masses (see Appendix). In the same way the (-) channel Hamiltonian can be represented by two free Majorana fermions this time with different masses. The total 'free' Hamiltonian is

$$\begin{aligned} H &= H_m[\vec{\xi}] + H_{3m}[\xi_0] \\ &= \sum_{a=1,2,3} \left[-\frac{iv_s}{2} (\xi_R^a \partial_x \xi_R^a - \xi_L^a \partial_x \xi_L^a) - im \xi_R^a \xi_L^a \right] \\ &\quad + \left[-\frac{iv_s}{2} (\xi_R^0 \partial_x \xi_R^0 - \xi_L^0 \partial_x \xi_L^0) + 3im \xi_R^0 \xi_L^0 \right] \end{aligned} \quad (41)$$

The Majorana fermion $\xi_0, \bar{\xi}_0$ describes the singlet excitations and $\vec{\xi}, \vec{\bar{\xi}}$ accounts for the triplet excitations. The interacting term breaks the $SU(2) \otimes SU(2)$ symmetry of the decoupled ladder down to $SU(2) \otimes Z_2$ which is mirrored in $SO(3) \otimes Z_2$ -symmetric real fermions Hamiltonian (41).

We need to express the smooth and the staggered part of the spin operator in terms of Majorana fermions. Only the chiral components of the smooth part of the total and relative spin can be expressed locally in term of fermions:

$$(\mathbf{S}_1 + \mathbf{S}_2)^a \sim i\epsilon^{abc} (\xi_a \xi_b + \bar{\xi}_a \bar{\xi}_b) \quad (42)$$

$$(\mathbf{S}_1 - \mathbf{S}_2)^a \sim i(\xi_a \xi_0 + \bar{\xi}_a \bar{\xi}_0) \quad (43)$$

The staggered part of the spin and also the dimerization operator, are non-local function of Majorana fermions. The dimerization field $\epsilon(x)$ defined in (35) is the forth relevant field of $SU_1(2)$ WZW model. These fields can be expressed in terms of order (σ) and disorder (μ) Ising operators [2]:

$$\begin{aligned}\mathbf{n}^+ &\sim (\mu_1\sigma_2\sigma_3\mu_0, \sigma_1\mu_2\sigma_3\mu_0, \sigma_1\sigma_2\mu_3\mu_0) \\ \mathbf{n}^- &\sim (\sigma_1\mu_2\mu_3\sigma_0, \mu_1\sigma_2\mu_3\sigma_0, \mu_1\mu_2\sigma_3\sigma_0) \\ \epsilon_+ &\sim \mu_1\mu_2\mu_3\mu_0 \quad \epsilon_- \sim \sigma_1\sigma_2\sigma_3\sigma_0\end{aligned}\tag{44}$$

where $\mathbf{n}^\pm = \mathbf{n}_1 \pm \mathbf{n}_2$ and $\epsilon_\pm = \epsilon_1 \pm \epsilon_2$.

The most important feature of the standard ladder is that the triplet excitations contribute a coherent peak to the dynamical spin susceptibility at $q = \pi$ and $\omega = m_t$. Assuming that $J_\perp < 0$ the Ising phase of the triplet (singlet) fermions is ordered (disordered) $m_t \sim T - T_c < 0$ ($m_s \sim T - T_c > 0$) so that the two-point correlation functions can be simply read from those of the Ising model, see (80). (For the singlet the role of σ and μ is interchanged). The magnon coherent peak will appear in the correlation function

$$\langle \mathbf{n}^+(\mathbf{r}) | \mathbf{n}^+(\mathbf{0}) \rangle \sim K_0(|m_t|r)\tag{45}$$

which in Fourier space describes a free boson propagator. At the same time

$$\langle \epsilon_-(\mathbf{r}) \epsilon_-(\mathbf{0}) \rangle \sim K_0(|m_s|r)\tag{46}$$

implying that the an elementary excitation of relative dimerization is a coherently propagating particle. For antiferromagnetic coupling $J_\perp > 0$ the role of all order and disorder Ising operator are interchanged and the coherent magnon peak is observed in $\langle \mathbf{n}^-(\mathbf{r}) | \mathbf{n}^-(\mathbf{0}) \rangle$ correlation function and the coherent singlet peak in $\langle \epsilon_+(\mathbf{r}) \epsilon_+(\mathbf{0}) \rangle$.

The triplet and singlet massive Majorana fermions are weakly coupled by a marginal perturbation

$$\mathcal{H}_{int} = \frac{aJ_\perp}{4} (\vec{\xi}_R \cdot \vec{\xi}_L)^2 - \frac{aJ_\perp}{2} \vec{\xi}_R \cdot \vec{\xi}_L \xi_{RS}^0 \xi_{LS}^0\tag{47}$$

which, being the spectrum massive, results in a renormalization of the masses and velocities. Moreover it can lead to the formation of two particle bound states depending on its sign as we shall discuss in the next section.

3.1 Non-conventional Haldane phase

The rung-singlet and the Haldane phases, both with coherent magnons, are not the only possible massive spin liquid phases. An example of gapped spin liquid with mass threshold spectrum instead of a coherent peak was proposed by [3] upon introduction of a four-spin interaction

$$H_{scalar} = u(S_1(n).S_1(n+1)(S_2(n).S_2(n+1)) \quad (48)$$

which effectively can be generated from spin-phonon interaction or from orbital degeneracy. This interaction leads to the relevant term $\epsilon_1.\epsilon_2$, and contributes to the renormalization of all the masses equally, reflecting the fact that the $SU(2) \times SU(2) \sim SO(4)$ symmetry of the decoupled ladders is not affected by it. The free Hamiltonian is now

$$\begin{aligned} H(x) &= \frac{v_s}{2} \sum_{s=\pm} \left[(\Pi_s^2 + (\partial_x \Phi_s)^2) + \frac{m}{\pi a_0} \cos \sqrt{4\pi} \Phi_s \right] \\ &= \sum_{\nu=1,2,3,0} \left[-\frac{iv_s}{2} (\xi_R^\nu \partial_x \xi_R^\nu - \xi_L^\nu \partial_x \xi_L^\nu) - im \xi_R^\nu \xi_L^\nu \right] \end{aligned} \quad (49)$$

in which $m = u\lambda^2$. We can't distinguish between triplet and singlet due to $SO(4)$ invariant symmetry. Besides the four-spin interaction contributes the marginal interacting term

$$\mathcal{H}_{scalar} = \frac{a\pi u}{24\pi} \sum_{\nu,\mu=1,2,3,0}^{\nu \neq \mu} \xi_R^\nu \xi_L^\nu \xi_R^\mu \xi_L^\mu$$

to the Hamiltonian, which comes from the smooth part of the spin (see appendix 3).

Including the four-spin interaction, from now on we consider the generalized spin ladder in which the mass of fermions are given by

$$m_t = \frac{J_\perp \lambda^2}{2\pi} (1 - u/J_\perp) \quad m_s = -\frac{J_\perp \lambda^2}{2\pi} (3 + u/J_\perp) \quad (50)$$

and the total interacting terms will be:

$$\mathcal{H}_{int} = \frac{a(J_\perp - u/6)}{4} (\vec{\xi}_R \cdot \vec{\xi}_L)^2 - \frac{a(J_\perp + u/6)}{2} \vec{\xi}_R \cdot \vec{\xi}_L \xi_R^0 \xi_L^0 \quad (51)$$

As long as $m_t m_s < 0$ we are in the rung-singlet phase, but for $m_t m_s > 0$ the role of four-spin term is dominant and the properties of the system change

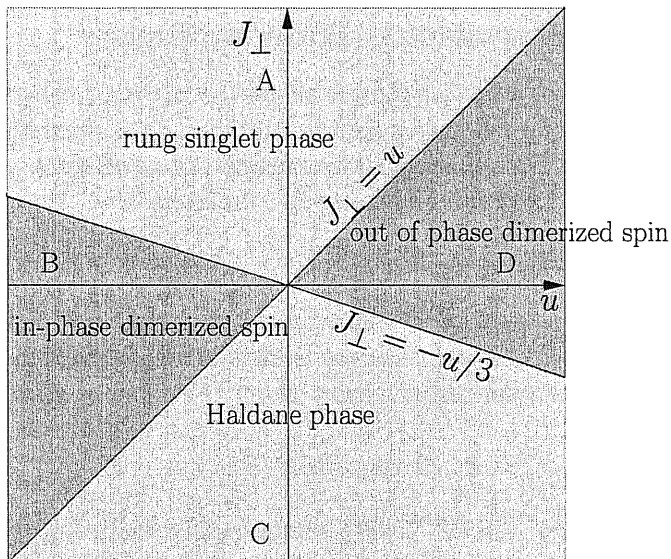


Figure 3: The phase diagram of the generalized spin ladder.

drastically. Fig(3). The phase transition is either a Kosterlitz-Thouless transition (the line of $m_t = 0$) or an Ising one (the line of $m_s = 0$). In the dimerized spin phase the degenerate ground state of the Hamiltonian breaks the translational invariance and is characterized by long-range dimerization ordering along each chain either with zero or π relative phase $\epsilon_1 = \pm\epsilon_2$ depending on the sign of the fermion masses. When the triplet and singlet masses are positive, all Ising models are disordered so that

$$\langle \epsilon_+(\mathbf{r})\epsilon_+(\mathbf{0}) \rangle \approx C[1 + O(\frac{e^{-2|m|r}}{r^2})] \quad (52)$$

while, when all fermion masses are negative, the role of ϵ_- and ϵ_+ is interchanged. The ground state is shown in Fig(4).

The important feature of this so-called non-conventional Haldane phase (or dimerized spin liquid phase) is that the elementary excitations are neither coherent magnons nor massive spinons but propagating massive singlet or triplet kinks. This shows up in the correlation functions of the total and relative staggered magnetization

$$\langle \mathbf{n}^+(\mathbf{r})|\mathbf{n}^+(\mathbf{0}) \rangle \sim K_0^2(m_t r) \quad \langle \mathbf{n}^-(\mathbf{r})|\mathbf{n}^-(\mathbf{0}) \rangle \sim K_0(m_t r)K_0(m_s r). \quad (53)$$

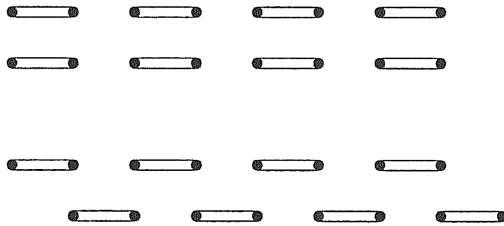


Figure 4: The in-phase (the above figure) and alternating-phase (the lower figure) vacuum state of the dimerized spin liquid.

So at $q \approx \pi$ the total and relative spin correlation functions have singularity at two mass thresholds $s = 2|m_t|$ and $s = |m_t| + |m_s|$ respectively [3]:

$$\begin{aligned} \Im\chi_+(\omega, \pi - q) &\sim \frac{\theta(s - 2m_t)}{m_t\sqrt{\omega^2 - q^2 - 4m_t^2}} \\ \Im\chi_-(\omega, \pi - q) &\sim \frac{\theta(s - m_t - m_s)}{\sqrt{m_t m_s}\sqrt{\omega^2 - q^2 - (m_t + m_s)^2}} \end{aligned} \quad (54)$$

3.2 Bound states in the standard spin ladder

Now we turn to the task of finding the bound states in the standard ladder. Bound states of two magnons has been predicted theoretically [49, 10, 50, 51] in the strong coupling limit of the standard ladder $J_\perp \gg J$ by mapping each spin into triplets and a singlet creation and annihilation operators. These bound states have been observed in the optical spectrum of $(\text{La,Ca})_{14}\text{Cu}_{24}\text{O}_{41}$ [11]. Here we derive various bound states of the standard ladder simply by using Majorana fermions representation of the model (41) in the weak coupling region. Moreover we show in which correlation functions the bound states peak is expected to be seen. In the neutron scattering experiment, the scattering cross section is proportional to the dynamical structure factor. In the case of spin ladder this is given by

$$S^{\alpha\beta}(q, q_\perp, \omega) = \frac{1}{4\pi N} \sum_{a,b=1}^2 \sum_{n,m=1}^N \int_{-\infty}^{+\infty} dt e^{i\omega t} e^{-iq(n-m) - iq_\perp(a-b)} \langle S_{a,n}^\alpha | S_{b,m}^\beta \rangle \quad (55)$$

Information about the low-energy part of the spin fluctuation is contained in the smooth ($q \approx 0$) and the staggered ($q \approx \pi$) parts of the structure factor both for the total $q_{\perp} = 0$ and the relative $q_{\perp} = \pi$ spins.

To this end we need first to identify those correlation functions which are singular near the mass threshold. In the appendix we have discussed the case of simple sine-Gorgon model consisting of two Majorana. The discussion can be easily generalized for the non-Abelian $O(3)$ -case (41) which we are dealing with. So the first group of two-particle propagators consists of those involving two triplet fermions and have the singularity at $s = 2|m_t|$. The second group deals with one triplet and one singlet fermion so that it is singular at $s = |m_s| + |m_t|$. Let first enlist the first group:

- The total spin density is defined in (42) and its correlation function corresponds to the structure factor (55) at $q = 0$, $q_{\perp} = 0$. The bare correlation function is given in (94) and near the $s = 2m = 2|m_t|$ is

$$\begin{aligned}\Re\chi_{\rho} &\approx \frac{q^2 m^2}{s^3} \frac{\theta(s < 2m)}{\sqrt{4m^2 + q^2 - \omega^2}} \\ \Im m\chi_{\rho}(\omega, q) &\sim \frac{2q^2 m^2}{s^3 \sqrt{s^2 - 4m^2}}\end{aligned}\quad (56)$$

The vanishing of χ_{ρ} at $q = 0$ reflects the fact that the total spin density is a conserved quantity (the global $SU(2)$ symmetry of the Hamiltonian). This result is reported in [2].

- The dual of the total spin density (42) is

$$J^a \sim i\epsilon^{abc}(\xi_a \xi_b - \bar{\xi}_a \bar{\xi}_b).$$

and defines the parallel spin current (or vector chirality order parameter)

$$\tilde{\mathbf{J}}_{\parallel} \sim \mathbf{S}_1(n) \times \mathbf{S}_1(n+1) + \mathbf{S}_2(n) \times \mathbf{S}_2(n+1). \quad (57)$$

The z-component of this function is ($\tilde{\mathbf{J}}_{\parallel}^z \sim \partial_x \Theta_+$). The correlator of spin current is given in (94) and its real part singularity reads as

$$\Re[\chi_J] \approx \frac{\omega^2 m^2}{s^3} \frac{1}{\sqrt{4m^2 + q^2 - \omega^2}}. \quad (58)$$

As the total current is not a conserved quantity, it will not vanish at $q = 0$. The bare correlation functions of total density and current are related to each other by continuity equation (95).

- The third singular correlator at $s = 2|m_t|$ consists of any two different triplet fermions with opposite chirality:

$$ie^{abc}(\xi_a\bar{\xi}_b + \bar{\xi}_a\xi_b). \quad (59)$$

The z-component of (59) is $\sin\sqrt{4\pi}\Phi_+ \sim i(\xi_1\bar{\xi}_2 + \bar{\xi}_1\xi_2)$, so is expected to be one of the singular correlators of sine-Gordon model. Its propagator is given in (98) and below the threshold its propagator behaves as

$$\Re[\chi_{\sin\phi}] \sim \frac{m^2}{s\sqrt{4m^2 + q^2 - \omega^2}}. \quad (60)$$

The function (59) can be assigned to

$$\begin{aligned} & (\mathbf{S}_1(n) \cdot \mathbf{S}_1(n+1))\mathbf{S}_2(n) + (\mathbf{S}_2(n) \cdot \mathbf{S}_2(n+1))\mathbf{S}_1(n) \\ & = \epsilon_1\mathbf{n}_2 + \epsilon_2\mathbf{n}_1 \sim \epsilon_+\mathbf{n}_+ - \epsilon_-\mathbf{n}_-. \end{aligned} \quad (61)$$

In the case of rung-singlet and Haldane phase the above function is a three-spin correlation function. However when we are in the non-Haldane phase according to (52) the propagator of (61) effectively reduces to the correlation function of total staggered magnetization $\langle \mathbf{n}_+(\mathbf{r}) | \mathbf{n}_+(\mathbf{0}) \rangle$, namely the structure factor at $q = \pi$, $q_\perp = 0$. So in the dimerized spin liquid phase one gets the result of Ref. [3] for $\Im\chi_+(\omega, \pi - q)$ (54).

The second group of singular two-particle propagators, contain one triplet fermion and one singlet one. In the rung-singlet phase these two Majorana fermions have different masses and opposite sign. By the duality transformation

$$\bar{\xi}_0 \leftrightarrow -\bar{\xi}_0 \quad \Phi_- \leftrightarrow \Theta_- \quad (62)$$

the problem of the sign can be resolved and now we can use the results of the appendix but keeping in mind that the role of $\sin\sqrt{4\pi}\Theta_-$ and $\sin\sqrt{4\pi}\Phi_-$ is interchanged and moreover the duality transformation changes the sign of singlet-triplet interaction in (51). Obviously in the non-Haldane phase no duality transformation is necessary. In both cases the singularity can be observed at $s = |m_t| + |m_s|$ in the following function:

- The relative spin density defined in (43). The propagator is given in (111) by χ_ρ . Note that in general the relative spin density is not a conserved quantity, obviously because the spin-spin interaction $J_\perp S_1 \cdot S_2$ breaks the $SU(2) \times SU(2)$ symmetry of decoupled ladder down to the global $SU(2)$

symmetry. In contrary to this the four-spin interaction $\epsilon_1 \cdot \epsilon_2$ leaves this symmetry intact and only in this particular case ($J_\perp = 0$), in (111) one can set $\Delta = 0$ and χ_ρ vanishes at $q = 0$ and the relative spin density as well as total spin density is conserved.

- The dual of this function, i.e relative spin current

$$\mathbf{S}_1(n) \times \mathbf{S}_1(n+1)|^\alpha - \mathbf{S}_2(n) \times \mathbf{S}_2(n+1)|^\alpha \sim i(\xi_a \xi_0 - \bar{\xi}_a \bar{\xi}_0). \quad (63)$$

which its correlator is given in (111) by χ_J . This is also not a conserved quantity except at the the special point

$$H_{12} \sim \mathbf{n}_1 \cdot \mathbf{n}_1 - \epsilon_1 \epsilon_2 \quad (64)$$

which corresponds to setting $m = m_t + m_s = 0$ in χ_j .

- The transverse spin current

$$\tilde{\mathbf{J}}_\perp^\alpha \sim \mathbf{S}_1 \times \mathbf{S}_2|^\alpha \sim i(\xi_0 \bar{\xi}_a - \bar{\xi}_0 \xi_a) \quad (65)$$

shows a singularity in its correlation function, only in the rung-singlet and Haldane phases. The z-component of the transverse spin current is $\sin \sqrt{4\pi} \Theta_-$. The correlation function is given in (112). In the non-Haldane phase this propagator is not singular and just shows a square root threshold.

- The three-spin function

$$\begin{aligned} & (\mathbf{S}_1(n) \cdot \mathbf{S}_1(n+1))\mathbf{S}_2(n) - (\mathbf{S}_2(n) \cdot \mathbf{S}_2(n+1))\mathbf{S}_1(n) \\ & = \epsilon_1 \mathbf{n}_2 - \epsilon_2 \mathbf{n}_1 \sim \epsilon_- \mathbf{n}_+ - \epsilon_+ \mathbf{n}_- \sim i(\xi_0 \bar{\xi}_a + \bar{\xi}_0 \xi_a) \end{aligned} \quad (66)$$

has a singular propagator only in the non-Haldane phase. In this phase from (52) one infers that the propagator of this function effectively reduces to the structure factor at $q_\perp = \pi$ and $q = \pi$, namely $\langle \mathbf{n}_-(\mathbf{r}) | \mathbf{n}_-(\mathbf{0}) \rangle$. So one arrives at the result of (54).

How two-particle interaction modifies those correlation functions? In (51) the two lines at which the signs of two-particle interaction terms change are not those which separate rung-singlet phase from dimerized spin liquid phase. To avoid complication here we study the extreme case of each phase: in the rung-singlet phase we assume that $|J_\perp| \gg |u|$ and in the non-Haldane phase we assume that $|J_\perp| \ll |u|$ but still both weak compared to J_\parallel . Let us start from the rung-singlet phase with antiferromagnetic interaction [area

(A) in Fig(3)]. In this phase as a consequence of triplet-triplet interaction a bound state can be formed below $s = 2|m_t|$, so the singularity in the correlation function of total spin density (42), $S^{zz}(q \sim 0, q_{\perp} \sim 0, \omega)$, total spin current (57) and also (61) will be removed in favor of a coherent peak followed by a nonsingular broad continuum Fig(5). The same is true for those propagators which are singular at $s = |m_t| + |m_s|$ namely the relative spin density (43), $S^{zz}(q \sim 0, q_{\perp} \sim \pi, \omega)$, the relative spin current (63) and the transverse spin current (65).

The situation remains almost the same deep inside the dimerized spin liquid phase with $u < 0$ (area (B) in Fig(3)), but instead of transverse spin current (65) we must consider (66).

In other two extreme cases namely inside the Haldane phase with ferromagnetic inter-chain exchange (area C) and dimerized spin liquid phase with $u > 0$ (area D) no bound state can be formed and the above mentioned function keeps their singular character.

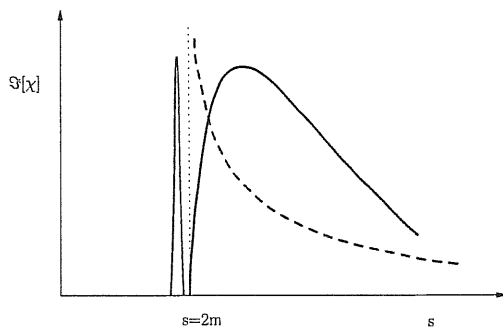


Figure 5: The bare singular correlation function at $s = 2m$ (dashed line). In the presence of the interaction, instead of singularity a bound state will appear (solid line).

Now we try to present a simple physical picture of the low energy excitations. We start from the dimerized spin liquid phases. In the dimerized ground state the excitations are kink-like which connect two degenerate vacua as shown in Fig(6). As at the position of each kind $\epsilon_1 \rightarrow -\epsilon_1$ and $\epsilon_2 \rightarrow -\epsilon_2$, or equivalently $\Phi_{1(2)} \rightarrow \Phi_{1(2)} + \sqrt{\pi/2}$, we have either

$\Phi_+ \rightarrow \Phi_+ + \sqrt{\pi}$, $\Phi_- \rightarrow \Phi_-$ or $\Phi_- \rightarrow \Phi_- + \sqrt{\pi}$, $\Phi_+ \rightarrow \Phi_+$. In the extreme case $J_\perp = 0$ according to (49) this correspond to a soliton kink either in the (+) or (-) channel sine-Gordon model respectively. In the first case we have a kink of total spin $\Delta S_+^z = \frac{1}{\sqrt{\pi}} \int \Delta \Phi_+ dx = 1$ and in the second case a kink of relative spin $\Delta S_-^z = \frac{1}{\sqrt{\pi}} \int \Delta \Phi_- dx = 1$, Fig(6). Assuming a peri-

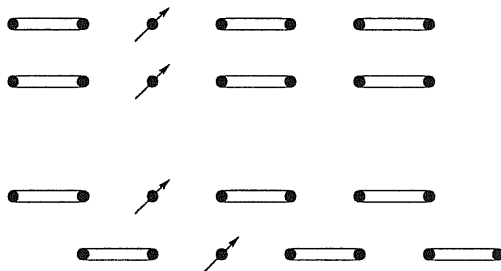


Figure 6: The kink excitations of the in-phase dimerized spin liquid (the above figure) and the alternating dimerized phase (the lower figure).

odic boundary condition the kinks can appear only in pairs and, as long as the interaction is not considered, they propagate freely without making any bound state. However, in the in-phase dimerized ladder a small attraction between kinks and anti-kinks in the (+) sector confine them and creates a bound state at $s < 2|m_t|$. In the same way, a kink anti-kink pair in the (-) sector binds at $s < |m_t| + |m_s|$.

A very similar picture can be seen the rung-singlet phase. The kink excitations are schematically shown in Fig(7). The ground state of the rung singlet (Haldane) phases consists of $\mathbf{n}_1 + \mathbf{n}_2$ ($\mathbf{n}_1 - \mathbf{n}_2$) singlets, similar to $\epsilon_1 \pm \epsilon_2$. The kink excitations are shown in Fig(7). An antiferromagnetic inter-chain coupling can bind a kink and antikink excitation only in the rung-singlet phase.

3.3 Conclusion

We have studied the generalized standard spin ladder in which, besides the inter-chain exchange coupling J_\perp , the four spin interaction (48) with strength u is included, both of them in the weak coupling regime $u \ll J_\parallel, J_\perp \ll J_\parallel$.

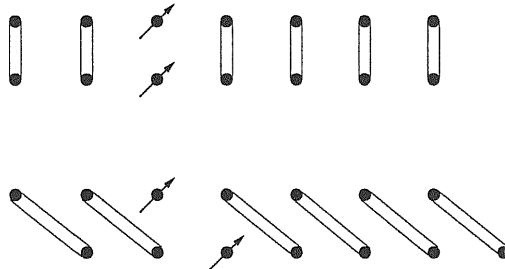


Figure 7: The triplet excitations in the rung-singlet phase (the above figure) and in the Haldane phase (the lower figure). Along the line spins have a tendency to form singlets.

The spin ladder can move from rung-singlet or Haldane phases towards spin-dimerized phases, either through the Ising transition line $3J_{\perp} + u = 0$ or through the KT transition line $J_{\perp} - u = 0$. We have shown that deep inside the rung-singlet phase with antiferromagnetic inter-chain coupling and deep inside the in-phase dimerized spin liquid, with $u < 0$, bound states of total and relative spin-1 excitations appear respectively below $s = 2|m_t|$ and $s = |m_t| + |m_s|$. For ferromagnetic coupling, $J_{\perp} < 0$, and for $u > 0$ one instead observes a two particle mass threshold singularity at those two values in accordance with Ref. [2].

4 Appendix I: Quantum Ising chain

The quantum Ising chain is the 1D Ising model in a transverse magnetic field:

$$H[\sigma] = -J \sum_{n=1}^N (\sigma_n^z \sigma_{n+1}^z + \lambda \sigma_n^x). \quad (67)$$

By duality transformation:

$$\mu_{n+1/2}^z = \prod_{j=1}^n \sigma_j^x, \quad \mu_{n+1/2}^x = \sigma_n^z \sigma_{n+1}^z \quad (68)$$

we equivalently get

$$H[\mu] = -J \sum_{n=1}^N (\lambda \mu_{n-1/2}^z \mu_{n+1/2}^z + \mu_{n+1/2}^x) \quad (69)$$

Comparing to (67) we see that $H[\sigma, \lambda] = \lambda H[\mu, 1/\lambda]$ which implies that $\lambda_c = 1$ is the self-duality critical point. So $\lambda < 1$ is the ordered phase in which $\langle \sigma^z \rangle \neq 0$, $\langle \mu^z \rangle = 0$ and $\lambda > 1$ is the disordered phase in which $\langle \mu^z \rangle \neq 0$, $\langle \sigma^z \rangle = 0$ and near the critical point the mass gap is

$$m(\lambda) \sim |1 - \lambda| \sim |T - T_c|/T_c. \quad (70)$$

The Jordan-Wigner transformation

$$\sigma_n^x = 2a_n^\dagger a_n - 1, \quad \sigma_n^z = (-1)^n \exp[\pm i\pi \sum_{j=1}^{n-1} a_j^\dagger a_j] (a_n^\dagger a_n) \quad (71)$$

transforms the model onto

$$H = \sum_n [J(a_n^\dagger - a_n)(a_{n+1}^\dagger + a_{n+1}) - \Delta(a_n^\dagger - a_n)(a_n^\dagger + a_n)]$$

By introducing the real lattice Majorana fermions:

$$\zeta_n = a_n^\dagger + a_n \quad \eta_n = -i(a_n^\dagger - a_n)$$

the Hamiltonian transforms to

$$H = i \sum_n [J\eta_n(\zeta_{n+1} - \zeta_n) - (\Delta - J)\eta_n\zeta_n]$$

which in the continuum limit is

$$H = \int dx [iv\eta(x)\partial_x\zeta(x) - im\eta(x)\zeta(x)].$$

Here $2Ja = v$, $2(\Delta - J) = m$ and the continuum fields $\eta_n = \sqrt{2a}\eta(x)$, $\zeta_n = \sqrt{2a}\zeta(x)$ satisfy the anti-commutation relations

$$\{\eta(x), \eta(x')\} = \{\zeta(x), \zeta(x')\} = \delta(x - x'), \quad \{\zeta(x), \eta(x')\} = 0.$$

Finally by introducing the chiral Majorana $\xi_R = (\eta - \zeta)/\sqrt{2}$ and $\xi_L = (\eta + \zeta)/\sqrt{2}$ we arrive the free massive Majorana Hamiltonian

$$\mathcal{H}(x) = \frac{iv}{2}(\xi_L\partial_x\xi_L - \xi_R\partial_x\xi_R) - im\xi_R\xi_L \quad (72)$$

in which m is given in (70). As Majorana fermions are real the Fourier space of the fields is restricted to $k > 0$ and $\xi(k)^\dagger = \xi(-k)$.

The Green Function of Majorana fermion is given by

$$\begin{aligned} \hat{G}(\varepsilon, k) &= \begin{pmatrix} \langle \bar{\xi}, \bar{\xi} \rangle & \langle \bar{\xi}, \xi \rangle \\ \langle \xi, \bar{\xi} \rangle & \langle \xi, \xi \rangle \end{pmatrix} \\ &= -\frac{1}{\varepsilon^2 + k^2 + m^2} \begin{pmatrix} i\varepsilon + k, & -im \\ im, & i\varepsilon - k \end{pmatrix}. \end{aligned} \quad (73)$$

Yet our goal is to map the bosonic operators which appear in the sine-Gordon model onto Ising-like operators. Since the bosonic fields are related to Dirac fermion fields, we start by writing a single Dirac fermion $\psi = (R, L)$ in term of two real (Majorana) fermions

$$\psi(x) = \frac{\xi_1(x) + i\xi_2(x)}{\sqrt{2}}$$

As the Bosonization of Dirac fermion is know one can write

$$[\xi^1(x) + i\xi^2(x)]_{R,L} = \frac{1}{\sqrt{\pi\alpha}} \exp[\pm\Phi_{R,L}(x)] \quad (74)$$

where α is the short distance cut off of the bosonic theory. The chiral currents are expressed as

$$\partial_x\Phi = i\sqrt{\pi}(\xi_R^1\xi_R^2 + \xi_L^1\xi_L^2), \quad \partial_x\Theta = i\sqrt{\pi}(-\xi_R^1\xi_R^2 + \xi_L^1\xi_L^2) \quad (75)$$

The mass bilinears $R^\dagger L = -\frac{i}{2\pi\alpha} \exp[-i\sqrt{4\pi}\Phi]$ and $R^\dagger L^\dagger = \frac{i}{2\pi\alpha} \exp[i\sqrt{4\pi}\Theta]$ is written as

$$\begin{aligned}\cos\sqrt{4\pi}\Phi &= i\pi\alpha(\xi_R^2\xi_L^2 + \xi_R^1\xi_L^1) \\ \cos\sqrt{4\pi}\Theta &= i\pi\alpha(\xi_R^2\xi_L^2 - \xi_R^1\xi_L^1) \\ \sin\sqrt{4\pi}\Phi &= -i\pi\alpha(\xi_R^1\xi_L^2 + \xi_L^1\xi_R^2) \\ \sin\sqrt{4\pi}\Theta &= i\pi\alpha(\xi_R^1\xi_L^2 - \xi_L^1\xi_R^2)\end{aligned}\quad (76)$$

The important relation between the sine-Gordon model at $\beta^2 = 4\pi$ and free massive Dirac can then be established as

$$\begin{aligned}\mathcal{H}_M(\vec{\xi}) &= \mathcal{H}(x) = \frac{iv}{2} \sum_{a=1,2} (\xi_L^a \partial_x \xi_L^a - \xi_R^a \partial_x \xi_R^a) - im\xi_R^a \xi_L^a \\ \mathcal{H}_{SG} &= \frac{v_s}{2} [(\partial_x \Phi)^2 + (\Pi)^2] - \frac{m}{\pi\alpha} \cos\sqrt{4\pi}\Phi(x)\end{aligned}\quad (77)$$

Now we are able to fully exploit the relationship among the quantum Ising chain and the sine-Gordon model[2]. We start considering the sine-Gordon model Eq. (77) in the *disordered* phase, $m > 0$. In the Ising language that implies $\langle \sigma_1 \rangle = \langle \sigma_2 \rangle = 0$ and $\langle \mu_1 \rangle = \langle \mu_2 \rangle \neq 0$, which translated into the sine-Gordon language means $\langle \cos\sqrt{\pi}\Phi \rangle \neq 0$, $\langle \sin\sqrt{\pi}\Phi \rangle = 0$.

On the contrary, in the *ordered* phase, $m < 0$, $\langle \sigma_1 \rangle = \langle \sigma_2 \rangle \neq 0$, $\langle \mu_1 \rangle = \langle \mu_2 \rangle = 0$ and equivalently $\langle \cos\sqrt{\pi}\Phi \rangle = 0$, $\langle \sin\sqrt{\pi}\Phi \rangle \neq 0$. Therefore

$$\sigma_1\sigma_2 \sim \sin\sqrt{\pi}\Phi, \quad \mu_1\mu_2 \sim \cos\sqrt{\pi}\Phi. \quad (78)$$

By making the duality transformation

$$\Phi \rightarrow \Theta, \quad \xi_R^1 \rightarrow -\xi_R^1, \quad \sigma_1 \leftrightarrow \mu_1$$

we get

$$\mu_1\sigma_2 \sim \sin\sqrt{\pi}\Theta, \quad \sigma_1\mu_2 \sim \cos\sqrt{\pi}\Theta \quad (79)$$

The correlation function of noncritical $T > T_c$ Ising operator in long distance $|m|r \rightarrow \infty$ is given in [48]:

$$\langle \sigma(\mathbf{r})\sigma(\mathbf{0}) \rangle \approx A \left[1 + \frac{1}{8\pi(mr)^2} e^{-2|m|r} \right] \quad \langle \mu(\mathbf{r})\mu(\mathbf{0}) \rangle \approx \frac{A}{\pi} K_0(|m|r) \sim \frac{1}{\sqrt{(mr)}} e^{-|m|r} \quad (80)$$

in which the Mac-Donald function $K_0(|m|r)$ is the real space propagator of a free massive boson

$$K_0(|m|r) \leftrightarrow \frac{1}{\omega^2 + q^2 + m^2}$$

5 Appendix II: Breathers in the sine-Gordon model

The sine-Gordon model (77) contains quantum solitons and antisolitons in its spectrum, in the massive region $\beta^2 < 8\pi$. Below the Luther-Emery point $\beta^2 = 4\pi$ the bound states of soliton and antisoliton, known as breathers can be formed with the mass spectrum

$$M_n = 2m_s \sin \pi \nu n / 2 \quad n = 1, 2, \dots, < 1/\nu \quad (81)$$

in which m_s is the mass of a soliton, and

$$\frac{1}{\nu} = \frac{8\pi}{\beta^2} - 1. \quad (82)$$

The number of the breathers and their masses depend on β . We are interested, in the vicinity of Luther-Emery point, when only the first breather is present. It's well known that exactly at this point $\Im[\langle \sin \beta\Phi | \sin \beta\Phi \rangle]$ shows a square root singularity at the two-mass threshold $s = \sqrt{\omega^2 - q^2} = 2m$. Below $\beta^2 < 4\pi$ the first breather mass show itself as a coherent peak in this correlation function slightly below the two mass threshold and moreover the singularity will disappear. The fact that the first breather is odd under charge conjugation can explain why the the breather peak must be searched in the correlation of $\sin \beta\Phi$ operator: if the correlation function of the operator \mathcal{O} is going to show an excitonic pole, then its expectation value between the vacuum and the first breather state $\langle 0 | \mathcal{O} | \mathcal{B} \rangle$ must be nonzero which is valid only for odd operators like $\sin \beta\Phi$, the density operator ρ and the current operator J .

Here we discuss that the appearance of the first breather mass can explained using the particle-hole (soliton-antisoliton) content of the model and and their interaction. To this end, by first rescaling the fields

$$\Phi \rightarrow \sqrt{\frac{4\pi}{\beta^2}} \Phi, \quad \Theta \rightarrow \sqrt{\frac{\beta^2}{4\pi}} \Theta$$

one maps the sine-Gordon model to

$$H = \frac{v}{2} [(\partial_x \Phi)^2 + (\partial_x \Theta)^2] - \frac{m}{\pi a} \cos \sqrt{4\pi} \Phi + \frac{g_0}{2\pi} [(\partial_x \Phi)^2 - (\partial_x \Theta)^2]$$

$$\frac{4\pi}{\beta^2} = 1 + \frac{g_0}{\pi v}. \quad (83)$$

in which g_0 is a small parameter which goes to zero at the Luther-Emery point. The first term describes the model of free fermions (77) and g_0 -term plays the role of small interacting term. Written in the Majorana fermion language the interaction is

$$H_{int} = -2g_0\xi_1\xi_2\bar{\xi}_1\bar{\xi}_2 \quad (84)$$

At $\beta^2 = 4\pi$ (or $g_0 = 0$) the model consists of free massive fermions. In the whole region $4\pi < \beta^2 < 8\pi$ for which the interaction term is attractive $g_0 < 0$ no bound state can be present. In contrary when $\beta^2 < 4\pi$ the interaction between massive fermions is repulsive $g_0 > 0$, implying that the solitons (particles) and antisolitons (holes) can attract each other and form breathers. Note that from (81) and (82) for small value of g_0 the first breather mass is given by

$$M_1 = 2m_s(1 - \frac{g_0^2}{2}) \quad (85)$$

which shows that the difference between the breather mass and soliton-antisoliton mass $2m_s$ is of the second order in g_0 . The interaction will also re-normalize the single soliton mass m_s which in the first loop approximation gives $m_s = m_s(1 + \frac{g_0}{\pi} \ln \frac{\Lambda}{m_s})$. We assume that this correction is already taken into account in the fermion mass. Below we first calculate those two-particle correlation functions like density-density and current-current which show a singular behavior near the two-mass threshold. Switching on the interaction we keep the most divergent terms in the RPA perturbation series of these propagators, and show that the first breather appears as a true pole of them.

5.1 Bare propagators

From (75) density-density correlation $\chi_\rho = \frac{1}{\pi} \langle \partial_x \Phi(0) | \partial_x \Phi(x) \rangle$ and current-current correlation $\chi_J = \frac{1}{\pi} \langle \partial_x \Theta(0) | \partial_x \Theta(x) \rangle$ are given by


$$\chi_{\rho/J} = \text{---} + \text{---} \pm \text{---} \pm \text{---} = D + \bar{D} \pm 2C. \quad (86)$$

For free massless fermions these two correlations are the same and is just the sum of two anomalous terms in (17). This is because the Hamiltonian of the free fermions (6) is invariant under *independent* $U(1) \otimes U(1)$ transformation

$$R \rightarrow e^{i\alpha_R} R, \quad L \rightarrow e^{i\alpha_L} L \quad (87)$$

which implies that the right and left current density J_R, J_L are independently conserved and so the continuity equation does not distinguish between the density and the current:

$$\partial_t \rho + \partial_x J = 0 \longleftrightarrow \partial_x \rho + \partial_t J = 0. \quad (88)$$

The mass term $m(R^\dagger L + L^\dagger R)$ violates independent chiral-currents conservation. Now (87) is valid only if $\alpha_R = \alpha_L$ and so only the total density is conserved. In this case as $\rho\rho - JJ$ is Lorentz-invariant we first calculate $\chi_\rho - \chi_J = 4C = 4$ . Using (73) we get

$$C = \text{} = -m^2 \chi \quad (89)$$

in which χ can be written in a compact form

$$\chi = -\frac{1}{2\pi \tilde{s}_m \tilde{s}} \ln\left(\frac{\tilde{s}_m + \tilde{s}}{\tilde{s}_m - \tilde{s}}\right)$$

where $s^2 = (i\omega)^2 - q^2$, $s_m = \sqrt{(i\omega)^2 - 4m^2 - q^2}$ and $\tilde{s}_m = \sqrt{4m^2 + q^2 - (i\omega)^2}$. The real part of it is given by


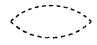
$$\Re[\chi] \approx - \begin{cases} \frac{1}{\pi s \tilde{s}_m} \tan^{-1}(s/\tilde{s}_m) & s < 2m \\ -\frac{1}{\pi s s_m} \tanh^{-1}(s_m/s) & 2m < s \end{cases} \quad (90)$$


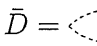
which is singular when s goes to $2m$ from below

$$\Re[\chi] = -\frac{1}{2s\tilde{s}_m} \quad s \rightarrow 2m \quad (91)$$

while the imaginary part is singular when s approach the two-mass threshold from the above $2m \rightarrow s$

$$\Im[\chi] \approx -\frac{1}{2ss_m} \theta(s - 2m). \quad (92)$$

The chiral graph $D = \text{}$ and its dual $\bar{D} = \text{}$ are not Lorentz invariant and contain anomalous term:

$$\begin{aligned} D = \text{} &= -\frac{1}{2\pi} \frac{q}{i\omega + q} + m^2 \frac{i\omega - q}{i\omega + q} \chi \\ \bar{D} = \text{} &= \frac{1}{2\pi} \frac{q}{i\omega - q} + m^2 \frac{i\omega + q}{i\omega - q} \chi \end{aligned} \quad (93)$$

The mass correction (second term) contains the singular function χ . Now the bare density-density and current-current propagators can be calculated

$$\begin{aligned}
\chi_\rho &= \langle \partial_x \Phi_+ | \partial_x \Phi_+ \rangle \approx \text{diagram 1} + \text{diagram 2} + \text{diagram 3} + \text{diagram 4} \\
&= \frac{q^2}{\pi s^2} (1 + 4\pi m^2 \chi) \\
\chi_j &= \langle \partial_x \Theta_+ | \partial_x \Theta_+ \rangle \approx \text{diagram 5} + \text{diagram 6} - \text{diagram 7} - \text{diagram 8} \\
&= \frac{q^2}{\pi s^2} \left(1 + \frac{(i\omega)^2}{q^2} 4\pi m^2 \chi \right)
\end{aligned} \tag{94}$$

The vanishing of χ_ρ at $q = 0$ reflects the fact that spin density is a conserved quantity. The total spin current is not conserved and so it does not vanish at $q = 0$. The current-current and density-density correlation functions are related to each other by continuity equation

$$\omega^2 \chi_\rho - q^2 \chi_j = q^2 / \pi. \tag{95}$$

Note that the 'shift' term q^2/π is originated exactly from the anomaly term.

From (76) the correlation function of $\chi_{\sin \phi} = \langle \sin \sqrt{4\pi} \Phi(x) | \sin \sqrt{4\pi} \Phi(0) \rangle$ and $\chi_{\sin \theta} = \langle \sin \sqrt{4\pi} \Theta(x) | \sin \sqrt{4\pi} \Theta(0) \rangle$ is:

$$\chi_{\sin \phi} / \sin \theta = \text{diagram 9} + \text{diagram 10} \pm \text{diagram 11} \pm \text{diagram 12} \tag{96}$$

Obviously $\text{diagram 11} = -\text{diagram 12} = -C$ so we need to calculate only $L = \text{diagram 9} = \text{diagram 10}$. Note that all of them are Lorentz-invariant.

$$L = \text{diagram 9} = -\ell/2 + \frac{s^2 - 2m^2}{2} \chi \tag{97}$$

with $\ell = \frac{1}{\pi} \ln \frac{\Lambda}{m}$. So

$$\begin{aligned}
\chi_{\sin \theta} &= 2(L + C) = -\ell + s_m^2 \chi \\
\chi_{\sin \phi} &= 2(L - C) = -\ell + s^2 \chi
\end{aligned} \tag{98}$$

Note that as near the threshold $\chi \sim 1/\tilde{s}_m$ the correlation function $\chi_{\sin \theta}$ shows only the square root threshold $\Im[\chi_{\sin \phi}] \sim \sqrt{s^2 - 4m^2}$. In contrary to this, $\chi_{\sin \phi}$ shows a square root singularity $\Im[\chi_{\sin \theta}] \sim 1/\sqrt{s^2 - 4m^2}$ near $s = 2m$.

These are the bare graphs which appear in different propagator of physical quantities. All of them are even function of incoming momenta (ω, q) and in each of them the chirality of two incoming fermions is either intact or both changed. In the perturbation series one encounters new graphs which are odd function of (ω, q) :

$$R = \begin{array}{c} \text{---} \text{---} \\ \text{---} \text{---} \end{array} = \begin{array}{c} \text{---} \text{---} \\ \text{---} \text{---} \end{array} = - \begin{array}{c} \text{---} \text{---} \\ \text{---} \text{---} \end{array} = - \begin{array}{c} \text{---} \text{---} \\ \text{---} \text{---} \end{array} = -\frac{1}{2}im(i\omega - q)\chi$$

$$\bar{R} = \begin{array}{c} \text{---} \text{---} \\ \text{---} \text{---} \end{array} = \begin{array}{c} \text{---} \text{---} \\ \text{---} \text{---} \end{array} = - \begin{array}{c} \text{---} \text{---} \\ \text{---} \text{---} \end{array} = - \begin{array}{c} \text{---} \text{---} \\ \text{---} \text{---} \end{array} = -\frac{1}{2}im(i\omega + q)\chi$$

As it's clear from the structure of these graphs they connect the current-current type diagrams to Lorentz-invariant type like $\chi_{\sin \phi}$, $\chi_{\sin \theta}$.

5.2 Perturbation Series

We have identified all singular propagators of the sine-Gordon model. Now we switch on the interaction and calculate the above correlation in RPA approximation. In the perturbation series keep only the most singular terms and drop the rest, so in the n-th order only $g^n \chi^n$ terms are retained and for example $g^{n+1} \chi^n$ is neglected.

We rewrite the current-current interacting Hamiltonian (84) as

$$\mathcal{H}_{int} = -g\xi_2\xi_1\bar{\xi}_1\bar{\xi}_2$$

Note that in compare to (84)

$$g = -2g_0. \tag{99}$$

In general considering two Majorana each with two chirality there are 16 graphs and so 16 equations. But obviously some original symmetries of the bare graphs must be restored to the end. Consequently they can be classified to four different and independent groups. The first two groups contain full graphs of the current and density operators :

$$\begin{array}{l} \begin{array}{c} \text{---} \text{---} \\ \text{---} \text{---} \end{array} + g \begin{array}{c} \text{---} \text{---} \\ \text{---} \text{---} \end{array} + g \begin{array}{c} \text{---} \text{---} \\ \text{---} \text{---} \end{array} + g \begin{array}{c} \text{---} \text{---} \\ \text{---} \text{---} \end{array} - g \begin{array}{c} \text{---} \text{---} \\ \text{---} \text{---} \end{array} - g \begin{array}{c} \text{---} \text{---} \\ \text{---} \text{---} \end{array} = \begin{array}{c} \text{---} \text{---} \\ \text{---} \text{---} \end{array} \\ \begin{array}{c} \text{---} \text{---} \\ \text{---} \text{---} \end{array} + g \begin{array}{c} \text{---} \text{---} \\ \text{---} \text{---} \end{array} + g \begin{array}{c} \text{---} \text{---} \\ \text{---} \text{---} \end{array} + g \begin{array}{c} \text{---} \text{---} \\ \text{---} \text{---} \end{array} - g \begin{array}{c} \text{---} \text{---} \\ \text{---} \text{---} \end{array} - g \begin{array}{c} \text{---} \text{---} \\ \text{---} \text{---} \end{array} = \begin{array}{c} \text{---} \text{---} \\ \text{---} \text{---} \end{array} \\ \begin{array}{c} \text{---} \text{---} \\ \text{---} \text{---} \end{array} + g \begin{array}{c} \text{---} \text{---} \\ \text{---} \text{---} \end{array} + g \begin{array}{c} \text{---} \text{---} \\ \text{---} \text{---} \end{array} + g \begin{array}{c} \text{---} \text{---} \\ \text{---} \text{---} \end{array} - g \begin{array}{c} \text{---} \text{---} \\ \text{---} \text{---} \end{array} - g \begin{array}{c} \text{---} \text{---} \\ \text{---} \text{---} \end{array} = \begin{array}{c} \text{---} \text{---} \\ \text{---} \text{---} \end{array} \end{array}$$

$$\text{Diagram 1} + g \text{Diagram 2} + g \text{Diagram 3} - g \text{Diagram 4} - g \text{Diagram 5} = \text{Diagram 6}$$

and its dual:

$$\text{Diagram 7} + g \text{Diagram 8} + g \text{Diagram 9} - g \text{Diagram 10} - g \text{Diagram 11} = \text{Diagram 12}$$

$$\text{Diagram 13} + g \text{Diagram 14} + g \text{Diagram 15} - g \text{Diagram 16} - g \text{Diagram 17} = \text{Diagram 18}$$

$$\text{Diagram 19} + g \text{Diagram 20} + g \text{Diagram 21} - g \text{Diagram 22} - g \text{Diagram 23} = \text{Diagram 24}$$

$$\text{Diagram 25} + g \text{Diagram 26} + g \text{Diagram 27} - g \text{Diagram 28} - g \text{Diagram 29} = \text{Diagram 30}$$

The next two groups contains Lorentz-invariant full graphs, from which the correlation function of the $\sin \sqrt{4\pi}\Phi$ and $\sin \sqrt{4\pi}\Theta$ can be derived:

$$\text{Diagram 31} - g \text{Diagram 32} - g \text{Diagram 33} + g \text{Diagram 34} + g \text{Diagram 35} = \text{Diagram 36}$$

$$\text{Diagram 37} - g \text{Diagram 38} - g \text{Diagram 39} + g \text{Diagram 40} + g \text{Diagram 41} = \text{Diagram 42}$$

$$\text{Diagram 43} - g \text{Diagram 44} - g \text{Diagram 45} + g \text{Diagram 46} + g \text{Diagram 47} = \text{Diagram 48}$$

$$\text{Diagram 49} - g \text{Diagram 50} - g \text{Diagram 51} + g \text{Diagram 52} + g \text{Diagram 53} = \text{Diagram 54}$$

By interchanging $\xi_1 \leftrightarrow \xi_2$ we get

$$\text{Diagram 55} - g \text{Diagram 56} - g \text{Diagram 57} + g \text{Diagram 58} + g \text{Diagram 59} = \text{Diagram 60}$$

$$\text{Diagram 61} - g \text{Diagram 62} - g \text{Diagram 63} + g \text{Diagram 64} + g \text{Diagram 65} = \text{Diagram 66}$$

$$\text{Diagram 67} - g \text{Diagram 68} - g \text{Diagram 69} + g \text{Diagram 70} + g \text{Diagram 71} = \text{Diagram 72}$$

$$\text{Diagram 73} - g \text{Diagram 74} - g \text{Diagram 75} + g \text{Diagram 76} + g \text{Diagram 77} = \text{Diagram 78}$$

These equations can be written as

$$\mathbf{M} \cdot X = X_0 \tag{100}$$

in which X contains all sixteen graphs and \mathbf{M} is a 16×16 matrix, but block diagonalized, each block a 4×4 matrix, all are related to each other by a unitary transformation. So basically we need only one of them, let say the first group. By defining $\text{Diagram 1} = \mathbf{D}$, $\text{Diagram 2} = \mathbf{C}$, $\text{Diagram 3} = -\mathbf{R}_2$, $\text{Diagram 4} =$

$-\mathbf{R}_1$, the dressed graphs $X = (\mathbf{D}, \mathbf{C}, \mathbf{R}_1, \mathbf{R}_2)$ can be expressed in term of bare correlators $X = M^{-1} \cdot X_0$, in which

$$M = \begin{pmatrix} 1 + gC & gD & -gR_1 & -gR_2 \\ g\bar{D} & 1 + gC & g\bar{R}_2 & g\bar{R}_1 \\ g\bar{R}_1 & -gR_2 & 1 + gC & -gL \\ g\bar{R}_2 & -gR_1 & -gL & 1 + gC \end{pmatrix} \quad (101)$$

The inverse matrix can be found and from that the full correlation functions is derived:

$$\begin{aligned} \chi_{\sin\theta} &= 2 \frac{L + C}{1 + gC + gL} = \frac{\chi_{\sin\theta}^0}{1 + g\chi_{\sin\theta}^0} \\ \chi_\rho &= \frac{2}{g} + \frac{(1 + gC - gL)(D + \bar{D} - 2C - 2/g) - 2g(R + \bar{R})^2}{Q} \\ \chi_J &= -\frac{2}{g} + \frac{(1 + gC - gL)(D + \bar{D} + 2/g + 2C) - 2g(R - \bar{R})^2}{Q} \\ \chi_{\sin\phi} &= -\frac{1}{g} + \frac{(1 + gC)^2 - g^2 D \bar{D}}{gQ} \end{aligned} \quad (102)$$

The propagator of $\chi_{\sin\theta}$ has a trivial RPA form which could be derived simply by subtracting two first equations of the third (or fourth) group. This function doesn't have any pole because near the mass threshold $L + C \approx \frac{2m}{s}$ doesn't show any singularity. All other three correlation functions have a common pole. The function Q is the common denominator of all of them and is given by:

$$Q = (1 + gC - gL) \left((1 + gC)^2 - g^2 D \bar{D} \right) + 2g^2 \left(gD\bar{R}^2 + g\bar{D}R^2 + 2(1 + gC)R\bar{R} \right) \quad (103)$$

Actually $\det|M| = (1 + gC + gL)Q$. As there is no singularity in $1 + gC + gL = 1 + g\frac{2m}{s}\chi$ this factor is not important.

Now we will show that Q is only the first order function of $g\chi$. Keeping only the singular terms $g^n\chi^n$: perturbation

$$(1 + gC)^2 - g^2 D \bar{D} \approx 1 - 2gm^2\chi$$

$$1 + gC - gL \approx 1 - g\frac{s^2}{2}\chi$$

$$g^3 D\bar{R}^2 + g^3 \bar{D}R^2 + g^2 2R\bar{R}(1 + gC) \approx -g^2 m^2 \frac{s^2}{2} \chi^2.$$

Finally

$$Q \approx 1 - g\frac{s^2 + 4m^2}{2}\chi = 1 + g_0(s^2 + 4m^2)\chi \quad (104)$$

The position of the pole is given by $Q = 0$. Note that near the mass threshold $\Re[\chi] < 0$, for $g_0 < 0$ no pole exists. For $g_0 > 0$ the pole is located at

$$s^2 = 4m^2(1 - g_0^2) \quad (105)$$

in agreement with (85).

The bound state coherent δ function will smear out the square root singularity of the singular correlation functions:

$$\begin{aligned} \chi_\rho &= \frac{q^2}{\pi s^2} \left(1 + \frac{g}{2\pi}\right) \frac{(1 + 4\pi m^2 \chi - g\frac{s^2}{2}\chi)}{Q} \\ \chi_J &= \frac{q^2}{\pi s^2} \frac{\left[\left(1 - \frac{g}{2\pi}\right)(1 - g\frac{s^2}{2}\chi) + \left(\frac{\omega^2}{q^2} - \frac{g}{2\pi}\right)4\pi m^2 \chi\right]}{Q} \\ \chi_{\sin\phi} &= \frac{s^2 \chi \left(1 + g^2 \frac{m^2 q^2}{4\pi^2 s^2}\right)}{Q} \end{aligned} \quad (106)$$

We demonstrate this only for the $\chi_{\sin\phi}$ as an example. The pole at $Q = 0$ contributes a δ peak to the imaginary part of $\chi_{\sin\phi}$ for $s^2 < 4m^2$. However for $s^2 > 4m^2$ the imaginary part of the correlation is given by:

$$\Im[\chi_{\sin\phi}] \approx \frac{s^2 |\chi|}{1 + g^2 \left(\frac{s^2 + 4m^2}{2}\right)^2 |\chi|^2} \theta(s - 2m)$$

which near $s = 2m$ is

$$\Im[\chi_{\sin\phi}] \approx \frac{s^3 s_m}{s^2 s_m^2 + g^2 \left(\frac{s^2 + 4m^2}{2}\right)^2} \theta(s - 2m) \quad (107)$$

which indicates that near the threshold, instead of square root singularity, this propagator shows a square root threshold. Fig(5).

The same is true for χ_ρ and χ_J . Moreover in the presence of interaction the continuity equation reads:

$$\frac{\omega^2}{1 - g_0\pi}\chi_\rho - q^2(1 - g_0\pi)\chi_j = q^2/\pi \quad (108)$$

• **Duality Transformation** It's instructive to see what happens if we make the duality transformation $\Phi \rightarrow \Theta$. First in the Hamiltonian (83) instead of the mass term we have the superconducting term ($R^\dagger L^\dagger + LR$) which now reduce the $U(1) \otimes U(1)$ symmetry (87) to $U(1)$ symmetry $\alpha_R = -\alpha_L$ and so this time only the total spin current J is conserved. On the other hand we expect that this time $\chi_{\sin\theta}$ will be the singular function instead of $\chi_{\sin\theta}$. These two expectations come true if we note that as the consequence of duality, $\bar{\xi}_1 \rightarrow -\bar{\xi}_1$ and so only the sign of C graph will change $C \rightarrow -C$. Moreover this transformation changes the sign of the interacting term in (83) $g_0 \rightarrow -g_0$.

We should repeat above calculations when the mass of two fermions are different. This is useful because in (41) beside the CDW term $m \cos \sqrt{4\pi}\Phi_-$ the superconducting term $\Delta \cos \sqrt{4\pi}\Theta_-$ is also present. In term of Majorana we have two fermions with different masses:

$$H = i\frac{v}{2} \sum_{a=1}^2 (\xi_a \partial_x \xi_a - \bar{\xi}_a \partial_x \bar{\xi}_a) - im_a \bar{\xi}_a \xi_a$$

$$m_1 = m + \Delta, \quad m_2 = m - \Delta \quad (109)$$

We assume that $\Delta < m$ so both Majorana have positive masses, if not we just need to apply the duality.

Clearly the RPA is intact and only the bare propagators had to be recalculated. First we derive density and current propagator. The Lorentz invariant part of them (the graph C) is given by

$$\langle \text{graph C} \rangle = C = -m_1 m_2 \chi = \frac{s_m^2 - s_\Delta^2}{4} \chi$$

The singular function χ is

$$\Re[\chi] \approx - \begin{cases} \frac{1}{\pi \tilde{s}_\Delta \tilde{s}_m} \tanh^{-1}(\tilde{s}_\Delta/\tilde{s}_m) & s < 2\Delta < 2m \\ \frac{1}{\pi s_\Delta \tilde{s}_m} \tan^{-1}(s_\Delta/\tilde{s}_m) & 2\Delta < s < 2m \\ -\frac{1}{\pi s_\Delta s_m} \tanh^{-1}(s_m/s_\Delta) & 2\Delta < 2m < s \end{cases} \quad (110)$$

the singularity is near $s = 2m$ ($\chi \rightarrow \frac{1}{\tilde{s}_m}$).

The chiral graphs read

$$D = \text{loop} = -\frac{q}{2\pi} \frac{1}{i\omega + q} + \frac{i\omega - q}{i\omega + q} \left(\frac{m\Delta}{s^2} \ln \left| \frac{m + \Delta}{m - \Delta} \right| + \frac{m^2 s_\Delta^2 + \Delta^2 s_m^2}{s^2} \chi \right)$$

$$\bar{D} = \text{loop} = \frac{q}{2\pi} \frac{1}{i\omega - q} + \frac{i\omega + q}{i\omega - q} \left(\frac{m\Delta}{s^2} \ln \left| \frac{m + \Delta}{m - \Delta} \right| + \frac{m^2 s_\Delta^2 + \Delta^2 s_m^2}{s^2} \chi \right)$$

which lead to the following result for the current and density propagators

$$\chi_\rho \sim \frac{m^2 q^2 s_\Delta^2 + \Delta^2 \omega^2 s_m^2}{s^4} \chi + \frac{q^2}{\pi s^2}$$

$$\chi_J \sim \frac{m^2 \omega^2 s_\Delta^2 + \Delta^2 q^2 s_m^2}{s^4} \chi + \frac{q^2}{\pi s^2} \quad (111)$$

None of these propagators vanishes at $q = 0$ and the continuity equation is not valid anymore as the $U(1) \otimes U(1)$ (87) is broken totally by mass and superconducting term. The bare density-density and current-current propagators (111) have singularity at $s = |m_1| + |m_2| = 2\max\{m, \Delta\}$.

To calculate $\chi_{\sin\phi}$ and $\chi_{\sin\theta}$ we need

$$\text{loop} = L = -\frac{\ell}{2} + \frac{1}{2}(s^2 - 2m^2 - 2\Delta^2)\chi = -\frac{\ell}{2} + \frac{s_m^2 + s_\Delta^2}{4}\chi$$

here $\ell = \frac{1}{\pi} \ln \frac{\Lambda}{\sqrt{|m_1 m_2|}}$

$$\chi_{\sin\theta} = 2(L + C) = -\ell + s_m^2 \chi \quad \chi_{\sin\phi} = 2(L - C) = -\ell + s_\Delta^2 \chi \quad (112)$$

so for $\Delta < m$ ($\Delta > m$) only $\chi_{\sin\phi}$ (respectively $\chi_{\sin\theta}$) is singular at $s = 2m$ (at $s = 2\Delta$).

Lastly we need R_1 and R_2 :

$$\text{loop} = R_{2(1)} = -\frac{im_{2(1)}}{2}(i\omega - q)\chi \quad \text{loop} = \bar{R}_{2(1)} = -\frac{im_{2(1)}}{2}(i\omega + q)\chi$$

In the perturbation series only the most singular terms $g^n \chi^n$ has to be kept:

$$\begin{aligned}
(1 + gC)^2 - g^2 D\bar{D} &\approx 1 + 2g \frac{s_m^2 - s_\Delta^2}{4} \chi - g^2 \chi^2 \frac{4m^2 \Delta^2 s_m^2 s_\Delta^2}{s^4} \\
(1 + gC)^2 - g^2 L^2 &\approx 1 - g^2 \chi^2 \frac{s_m^2 s_\Delta^2}{4} + 2g \frac{s_m^2 - s_\Delta^2}{4} \chi \\
g^3 D\bar{R}^2 + g^3 \bar{D}R^2 + 2g^2 R\bar{R}(1 + gC) &\approx -g^2 \frac{s^2}{2} \chi^2 - g^3 \Delta^2 s_m^2 \chi^3 \\
g^3 D\bar{R}^2 + g^3 \bar{D}R^2 - 2g^2 R\bar{R}(1 + gC) &\approx +g^2 \frac{s^2}{2} \chi^2 - g^3 m^2 s_\Delta^2 \chi^3 \\
16g^4 m^2 \Delta^2 R^2 \bar{R}^2 &= g^4 m^2 \Delta^2 s^4 \chi^4
\end{aligned}$$

The determinant of M is given by

$$\begin{aligned}
Q &= \left((1 + gC)^2 - g^2 L^2 \right) \left((1 + gC)^2 - g^2 D\bar{D} \right) + 16g^4 m^2 \Delta^2 R^2 \bar{R}^2 \\
&+ 2m^2 (1 + gL + gC) (g^3 D\bar{R}^2 + g^3 \bar{D}R^2 + 2g^2 (1 + gC) R\bar{R}) \\
&- 2\Delta^2 (1 - gL + gC) (g^3 D\bar{R}^2 + g^3 \bar{D}R^2 - 2g^2 (1 + gC) R\bar{R}) \quad (113)
\end{aligned}$$

This function can be simplified as:

$$\begin{aligned}
Q &\approx \left(1 - g \frac{s_\Delta^2 (s^2 + 4m^2)}{2s^2} \chi - g^2 \frac{8m^2 \Delta^2 (s^2 - 2\Delta^2)}{s^2} \chi^2 \right) \\
&\times \left(1 + g \frac{s_m^2 (s^2 + 4\Delta^2)}{2s^2} \chi - g^2 \frac{8m^2 \Delta^2 (s^2 - 2m^2)}{s^2} \chi^2 \right) \quad (114)
\end{aligned}$$

When $\Delta \rightarrow 0$ the second order term χ^2 vanishes and the first line reduces to (104) and the second one becomes a non-singular propagator $\chi_{\sin\theta}$. Depending on the ratio $\frac{m}{\Delta}$ this function can have a pole for only one sign of g . Here we assume that $\Delta < m$ then the pole near the mass threshold $s = m_1 + m_2 = 2m$ is ($g = -2g_0$)

$$s^2 = 4m^2 \left(1 - g_0^2 \left(1 + \frac{\Delta^4}{m^2(m^2 - \Delta^2)} \right) \right) \quad (115)$$

6 Appendix III: The bosonized form of four-spin interaction

The relevant part of the 4-spin interaction is given by:

$$(\mathbf{S}_1 \cdot \mathbf{S}'_1)(\mathbf{S}_2 \cdot \mathbf{S}'_2) = \left(\frac{3}{\pi a}\right)^2 \epsilon_1 \epsilon_2$$

(\mathbf{S} is $\mathbf{S}(n)$ and \mathbf{S}' is $\mathbf{S}(n+1)$) which has the bosonized form:

$$= \frac{9}{\pi^2 a^2} \frac{\lambda^2}{\pi^2 a^2} \cos \sqrt{2\pi} \Phi_1 \cos \sqrt{2\pi} \Phi_2 = \frac{9}{\pi^2 a^2} \frac{\lambda^2}{2\pi^2 a^2} (\cos \sqrt{4\pi} \Phi_+ + \cos \sqrt{4\pi} \Phi_-)$$

In term of Majorana it reads

$$= \frac{9}{\pi^2 a^2} \frac{i\lambda^2}{2\pi a} (\bar{\xi}_0 \xi_0 + \bar{\xi} \xi).$$

The marginal term is given by

$$(\mathbf{S}_1 \cdot \mathbf{S}'_1)(\mathbf{S}_2 \cdot \mathbf{S}'_2) = (\mathbf{M}_1 \cdot \mathbf{M}'_1)(\mathbf{M}_2 \cdot \mathbf{M}'_2) =$$

in which $\mathbf{M} = \mathbf{J} + \bar{\mathbf{J}}$ is the total magnetization. We just need to calculate the $z-z$ component interaction and then use the $SU(2)$ symmetry to drive the rest:

$$M_1^z M_1'^z = (J_1^z + \bar{J}_1^z)(J_1'^z + \bar{J}_1'^z) = J_1^z J_1'^z + \bar{J}_1^z \bar{J}_1'^z + J_1^z \bar{J}_1'^z + \bar{J}_1^z J_1'^z$$

Using the relation

$$J^3(z) J^3(w) = \frac{1}{8\pi^2} \frac{1}{(z-w)^2}, \quad \bar{J}^3(\bar{z}) \bar{J}^3(\bar{w}) = \frac{1}{8\pi^2} \frac{1}{(\bar{z}-\bar{w})^2}$$

we get:

$$= -\frac{2}{8\pi^2 a^2} + \frac{1}{\pi} \partial_x \phi \partial_x \bar{\phi}$$

From this one concludes:

$$\mathbf{M}_1 \cdot \mathbf{M}'_1 = -\frac{3}{4\pi^2 a^2} + \frac{1}{\pi} \partial_x \phi_1 \partial_x \bar{\phi}_1 - \frac{2}{(2\pi a)^2} \cos \sqrt{8\pi} \Phi$$

so that

$$(\mathbf{M}_1 \cdot \mathbf{M}'_1)(\mathbf{M}_2 \cdot \mathbf{M}'_2) = \left(-\frac{3}{4\pi^2 a^2} + \frac{1}{\pi} \partial_x \phi_1 \partial_x \bar{\phi}_1 + \dots\right) \left(-\frac{3}{4\pi^2 a^2} + \frac{1}{\pi} \partial_x \phi_2 \partial_x \bar{\phi}_2 + \dots\right)$$

$$\begin{aligned}
&= -\frac{3}{4\pi^2 a^2} \frac{1}{\pi} \left[\partial_x \phi_1 \partial_x \bar{\phi}_1 + \partial_x \phi_2 \partial_x \bar{\phi}_2 + \dots \right] \\
&= -\frac{3}{4\pi^2 a^2} \frac{1}{2\pi} \left[\partial_x (\phi_+ + \phi_-) \partial_x (\bar{\phi}_+ + \bar{\phi}_-) + \partial_x (\phi_+ - \phi_-) \partial_x (\bar{\phi}_+ - \bar{\phi}_-) + \dots \right] \\
&= -\frac{3}{4\pi^2 a^2} \frac{1}{\pi} \left[\partial_x \phi_+ \partial_x \bar{\phi}_+ + \partial_x \phi_- \partial_x \bar{\phi}_- + \dots \right]
\end{aligned}$$

in which ellipsis represent the transverse components.

In the fermionic form

$$(\mathbf{M}_1 \cdot \mathbf{M}'_1)(\mathbf{M}_2 \cdot \mathbf{M}'_2) = \frac{3}{4\pi^2 a^2} \left[\xi_1 \xi_2 \bar{\xi}_1 \bar{\xi}_2 + \xi_2 \xi_3 \bar{\xi}_2 \bar{\xi}_3 + \xi_3 \xi_1 \bar{\xi}_3 \bar{\xi}_1 + \vec{\xi} \xi_0 \vec{\xi} \cdot \bar{\xi}_0 \right]$$

In whole we have

$$\begin{aligned}
\kappa(\mathbf{S}_1 \cdot \mathbf{S}'_1)(\mathbf{S}_2 \cdot \mathbf{S}'_2) &\approx ui \left(\frac{\lambda^2}{2\pi} \right) (3\bar{\xi}_0 \xi_0 - \vec{\xi} \cdot \vec{\xi}) \\
&+ \frac{ua}{12} (\xi_1 \xi_2 \bar{\xi}_1 \bar{\xi}_2 + \xi_2 \xi_3 \bar{\xi}_2 \bar{\xi}_3 + \xi_3 \xi_1 \bar{\xi}_3 \bar{\xi}_1) + a \vec{\xi} \xi_0 \vec{\xi} \cdot \bar{\xi}_0 \quad (116)
\end{aligned}$$

in which $u = \frac{9\kappa}{\pi^2 a^2}$.

Now for comparison we do the same for $\mathbf{S}_1 \cdot \mathbf{S}_2$ interaction. The marginal term is given by:

$$\begin{aligned}
M_1^z M_2^z &= \frac{1}{2\pi} (\partial_x \phi_1 \partial_x \bar{\phi}_2 + \partial_x \phi_2 \partial_x \bar{\phi}_1) \\
&= \frac{1}{2\pi} \frac{1}{2} [\partial_x (\phi_+ + \phi_-) \partial_x (\bar{\phi}_+ - \bar{\phi}_-) + \partial_x (\phi_+ - \phi_-) \partial_x (\bar{\phi}_+ + \bar{\phi}_-)] \\
&= \frac{1}{2\pi} (\partial_x \phi_+ \partial_x \bar{\phi}_+ - \partial_x \phi_- \partial_x \bar{\phi}_-) = -\frac{\xi_1 \xi_2 \bar{\xi}_1 \bar{\xi}_2 - \xi_3 \xi_0 \bar{\xi}_3 \bar{\xi}_0}{2}
\end{aligned}$$

So

$$\mathbf{M}_1 \cdot \mathbf{M}_2 = \frac{-\xi_1 \xi_2 \bar{\xi}_1 \bar{\xi}_2 - \xi_2 \xi_3 \bar{\xi}_2 \bar{\xi}_3}{2} - \xi_3 \xi_1 \bar{\xi}_3 \bar{\xi}_1 + \vec{\xi} \xi_0 \vec{\xi} \cdot \bar{\xi}_0$$

The relevant part is simply:

$$\begin{aligned}
\mathbf{n}_1 \cdot \mathbf{n}_2 &= \frac{\lambda^2}{\pi^2 a^2} (\cos \sqrt{4\pi} \Theta_- + \frac{1}{2} \cos \sqrt{4\pi} \Phi_- - \frac{1}{2} \cos \sqrt{4\pi} \Phi_+) \\
&= \frac{i\lambda^2}{2\pi a} (3\bar{\xi}_0 \xi_0 - \vec{\xi} \cdot \vec{\xi})
\end{aligned}$$

Adding this contribution to the four-spin term we get (51).

Part II

Ordered phase of XXZ-zigzag spin-1/2 Heisenberg ladder

In this part using bosonization approach, we derive an effective low-energy theory for XXZ-symmetric spin-1/2 zigzag ladders and discuss its phase diagram by a variational approach. A spin nematic phase emerges in a wide part of the phase diagram, either critical or massive. Possible crossovers between the spontaneously dimerized and spin nematic phases are discussed, and the topological excitations in all phases identified.

7 The model and its low-energy limit

We consider a frustrated spin-1/2 Heisenberg chain with $2L$ sites, described by the Hamiltonian

$$H = \sum_{a=x,y,z} \sum_{n=1}^{2L} [J'_a S_n^a S_{n+1}^a + J_a S_n^a S_{n+2}^a], \quad (117)$$

where

$$\begin{aligned} J_x = J_y = J > 0, & \quad J_z = J\Delta, \\ J'_x = J'_y = J' > 0, & \quad J'_z = J'\Delta'. \end{aligned} \quad (118)$$

In what follows, Δ and Δ' will be treated as independent anisotropy parameters. Upon the transformation

$$\mathbf{S}_{2n} \rightarrow \mathbf{S}_1(n), \quad \mathbf{S}_{2n+1} \rightarrow \mathbf{S}_2(n),$$

the model (117) is mapped onto the zig-zag spin-1/2 ladder Hamiltonian

$$\begin{aligned} H = & \sum_{a=x,y,z} \sum_{n=1}^L \sum_{i=1,2} J_a S_i^a(n) S_i^a(n+1) \\ & + \sum_{a=x,y,z} \sum_n J'_a [S_1^a(n) + S_1^a(n+1)] S_2^a(n) \end{aligned} \quad (119)$$

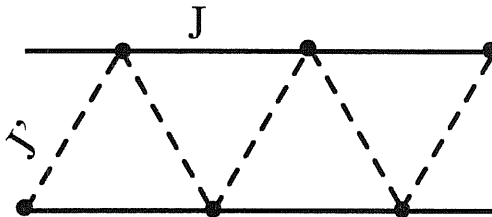


Figure 8: The zigzag ladder with in-chain coupling J and inter-chain coupling J' . For small J it can be viewed as a single ladder (along the dashed line) with next nearest neighbor interaction.

Let us discuss some general properties of this model. In the limit $J = 0$, (117) describes a standard Heisenberg antiferromagnetic chain where the spin-spin correlations are modulated with wavevector $q = \pi$. On the contrary, when $J' = 0$, the equivalent model (119) describes two decoupled spin chains. The modulating wavevector in this case is $q = \pi/2$. When both J and J' are finite, we may expect two possible behaviors of the spin structure factor $S(q) = (2L)^{-1} \sum_{n,m} \langle \mathbf{S}_n \cdot \mathbf{S}_m \rangle e^{iq(n-m)}$: either it is peaked at $q = \pi$ and $q = \pi/2$, or it shows a single peak at an incommensurate q_0 which smoothly moves from $q = \pi/2$ at $J \gg J'$ towards $q = \pi$ when $J' \gg J$. Translated into the zig-zag ladder language, the former case implies that, for n large,

$$\begin{aligned} \langle \mathbf{S}_1(n) \cdot \mathbf{S}_1(0) \rangle &= \langle \mathbf{S}_2(n) \cdot \mathbf{S}_2(0) \rangle \\ &= F_0(|2n|) + F_\pi(|2n|) + (-1)^n F_{\pi/2}(|n|), \\ \langle \mathbf{S}_1(n) \cdot \mathbf{S}_2(0) \rangle &= F'_0(|2n+1|) - F'_\pi(|2n+1|), \\ \langle \mathbf{S}_2(n) \cdot \mathbf{S}_1(0) \rangle &= F'_0(|2n-1|) - F'_\pi(|2n-1|), \end{aligned}$$

where $F_0(|n|)$, $F_\pi(|n|)$ and $F_{\pi/2}(|n|)$, as well as the primed ones, are smooth real functions describing the contributions of the $q = 0$, $q = \pi$ and $q = \pi/2$ modes, respectively. The difference between the 1-2 and 2-1 spin-spin correlators, as well as the absence of inversion symmetry $n \rightarrow -n$, reflect the fact that the zigzag ladder lacks two Z_2 symmetries – the $1 \leftrightarrow 2$ interchange symmetry and site parity P_S (understood as $P_S^{(1)} \otimes P_S^{(2)}$). However, if the model is gap-less or possesses a small spectral gap inducing a macroscopically large correlation length, then site-parity is effectively restored at long distances.

If, apart from $q = 0$, the spin structure factor has a peak at an incommensurate wave vector $q_0 \in [\pi/2, \pi]$, then we expect that

$$\begin{aligned} \langle \mathbf{S}_1(n) \cdot \mathbf{S}_1(0) \rangle &= \langle \mathbf{S}_2(n) \cdot \mathbf{S}_2(0) \rangle \\ &= F_0(|2n|) + F_{q_0}(|2n|) \cos 2nq_0, \\ \langle \mathbf{S}_1(n) \cdot \mathbf{S}_2(n) \rangle &= F'_0(|2n+1|) \\ &\quad + F'_{q_0}(|2n+1|) \cos q_0(2n+1), \end{aligned} \tag{120}$$

$$\begin{aligned} \langle \mathbf{S}_2(0) \cdot \mathbf{S}_1(n) \rangle &= F'_0(|2n-1|) \\ &\quad + F'_{q_0}(|2n-1|) \cos q_0(2n-1). \end{aligned} \tag{121}$$

We notice that the presence of the modulating factors in (120),(121) makes the the breakdown of P_S even more pronounced and, contrary to the commensurate case, this breakdown will survive the continuum limit we are going

to adopt. Thus, the two different types of spin correlations – commensurate or incommensurate – can be distinguished within a continuum, low-energy description by an asymptotic restoration or breakdown of the site-parity symmetry.

As discussed in the Introduction, in this paper we are going to study the model (119), or equivalently (117), in the limit $J \gg J'$ of weakly coupled chains. That allows us to adopt the well-known continuum description of each XXZ chain based on the bosonization approach, as discussed in section 2.2 (see also Ref. [16, 32] and then treat the inter-chain coupling as a weak perturbation. Bosonization of the XXZ zigzag spin-1/2 ladder has already been discussed in Ref.[33].

The universal, low-energy properties of a single XXZ spin-1/2 chain, in the gap-less Luttinger liquid phase ($-1 < \Delta \leq 1$) are adequately described by the Gaussian model for a massless scalar field $\varphi(x) = \varphi_R(x) + \varphi_L(x)$ (31). The dependence $Q = Q(\Delta)$ in the whole range $-1 < \Delta \leq 1$ is given in (30). Note that Q varies in the range $\infty > Q \geq 1$ when Δ takes values within the interval $-1 < \Delta \leq 1$. In particular, $Q = 2$ at the XX point ($\Delta = 0$), and $Q = 1$ at the SU(2)-symmetric (Heisenberg) point ($\Delta = 1$). Throughout this paper it will be assumed that $\Delta < 1$ (i.e. $Q > 1$). In this case the perturbation to the Gaussian model (31), $\lambda_U \cos \sqrt{8\pi}\varphi$ ($\lambda_U \sim J\Delta$), which in terms of the Jordan-Wigner fermions originates from Umklapp processes, is strongly irrelevant and will be dropped in what follows.

Since for each chain only the uniform and staggered low-energy modes survive the continuum limit, the corresponding spin densities can be parametrized as follows:

$$\mathbf{S}_i(n) \rightarrow a_0 \mathbf{S}_i(x), \quad (x = na_0) \tag{122}$$

$$\mathbf{S}_i(x) = \mathbf{J}_{i,R}(x) + \mathbf{J}_{i,L}(x) + (-1)^n \mathbf{n}_i(x) \quad (i = 1, 2). \tag{123}$$

Here a_0 is the lattice spacing, $\mathbf{J}_{i,R,L}$ are chiral components of the smooth part of the magnetization of the i -th chain, and \mathbf{n}_i is the staggered magnetization. The latter is even under site parity transformation (P_S) and odd under link parity transformation (P_L). A distinctive feature of the zigzag ladder is that it is invariant under mixed parity: $P_S^{(1)} \otimes P_L^{(2)}$ and $P_L^{(1)} \otimes P_S^{(2)}$. By this symmetry, strongly relevant terms, $n_1^a n_2^a$, which determine the spin-liquid properties of the unfrustrated spin-1/2 ladders [2], are instead forbid-

den in model (119). As a result, in the low-energy limit, the inter-chain perturbation, $\mathcal{H}' = \mathcal{H}_{JJ} + \mathcal{H}_{\text{twist}}$, is contributed by the “current-current” interaction[21, 34]

$$\mathcal{H}_{JJ} = 2 \sum_{a=x,y,z} g_a J_1^a J_2^a, \quad (124)$$

and also by “twist” terms[24] allowed by the $P_S^{(1)} \otimes P_L^{(2)}$ symmetry:

$$\mathcal{H}_{\text{twist}} = \frac{1}{2} \sum_{a=x,y,z} g_a a_0 T^a + \frac{1}{2} g_0 a_0 T^0, \quad (125)$$

Here

$$T^a = n_1^a \partial_x n_2^a - n_2^a \partial_x n_1^a, \quad T^0 = \epsilon_1 \partial_x \epsilon_2 - \epsilon_2 \partial_x \epsilon_1, \quad (126)$$

are chirally asymmetric operators with conformal spin 1, and $\epsilon_i \simeq (-1)^n \mathbf{S}_i(n) \cdot \mathbf{S}_i(n+1)$ represent the continuum limit of the dimerization operators. (Note that for a single chain $\epsilon(x)$ is even under P_L and odd under P_S .) The coupling constants are given by $g_x = g_y \equiv g_{\perp} = J' a_0$, $g_z \equiv g_{\parallel} = J' \Delta' a_0$.

The “current-current” and twist perturbations are of different nature. The former are parity [i.e. $P_{S(L)}^{(1)} P_{S(L)}^{(2)}$] symmetric. If acting alone, provided that the inter-chain exchange is antiferromagnetic, these lead to spontaneous dimerization of the ground state (see section III), the existence of massive topological excitations (spinons), and the onset of short-ranged *commensurate* inter-chain spin correlations [21, 35]. The twist terms, whose appearance stems from the frustrated nature of inter-chain interaction, explicitly break parity. However, by the previous discussion, parity can be broken either in a mild way, which is the case when the leading asymptotics of spin-spin correlations are still commensurate, or more profoundly, i.e. explicitly inducing *incommensurations* in the spin correlations. Both patterns of the low-energy behavior of the system will be discussed below.

In model (119), only the vector part of the twist perturbation, $g_a T^a$, emerges in the continuum limit. The scalar part, $g_0 T^0$, although absent in the bare Hamiltonian, is generated in the course of RG flow[24].

For this reason we will assume that such a term is present at the outset, with a bare amplitude g_0 .

Let us first bosonize \mathcal{H}_{JJ} . In terms of the rescaled fields, $\phi_i = (1/\sqrt{Q})\varphi_i$ and $\theta_i = \sqrt{Q}\vartheta_i$, the “currents” $J_i^a = J_{i,R}^a + J_{i,L}^a$, are given by [36]

$$J_i^z = \sqrt{\frac{Q}{2\pi}} \partial_x \phi_i, \quad J_i^+ = -\frac{\zeta}{\pi\alpha} e^{i\sqrt{\frac{2\pi}{Q}}\theta_i} \cos \sqrt{2\pi Q} \phi_i, \quad (127)$$

where α is the short-distance cutoff of the bosonic theory, and $\zeta(Q)$ is a nonuniversal (and yet unknown) positive constant approaching the value 1 in the SU(2) limit. Using the definitions (127) and passing to the symmetric and antisymmetric combinations of the fields, $\phi_{\pm} = (\phi_1 \pm \phi_2)/\sqrt{2}$, $\theta_{\pm} = (\theta_1 \pm \theta_2)/\sqrt{2}$, we find that the longitudinal (zz) part of \mathcal{H}_{JJ} adds to the Gaussian part of the model transforming the latter into

$$\mathcal{H}_G \rightarrow \sum_{\sigma=\pm} \frac{v_{\sigma}}{2} \left[R_{\sigma} (\partial_x \theta_{\sigma})^2 + R_{\sigma}^{-1} (\partial_x \phi_{\sigma})^2 \right], \quad (128)$$

with

$$\frac{1}{R_{\pm}} = \frac{v_{\pm}}{v_s} = \sqrt{1 \pm \frac{g_{\parallel} Q}{\pi v_s}} = 1 \pm \frac{g_{\parallel} Q}{2\pi v_s} + O(g_{\parallel}^2). \quad (129)$$

The exact dependence of R_{\pm} on the dimensionless parameter $g_{\parallel} Q/\pi v_s$ is unknown. Therefore we will restrict ourselves to the case $|g_{\parallel}|Q/\pi v_s \ll 1$ and keep only linear terms in the expansion (129). For a weak inter-chain interaction ($|g_{\parallel}|/\pi v_s \ll 1$), this is justified almost for the whole range $|\Delta| < 1$ except for a narrow region $\Delta + 1 \sim (g_{\parallel}/\pi v_s)^2$ close to the ferromagnetic transition point. The parameters R_{\pm} then satisfy the relation $R \equiv R_+ = 1/R_-$ which considerably simplifies the perturbative analysis.

Performing an additional rescaling of the fields, $\phi_{\pm} = \sqrt{R_{\pm}} \Phi_{\pm}$, $\theta_{\pm} = \sqrt{R_{\mp}} \Theta_{\pm}$, for the transverse (xx, yy) part of \mathcal{H}_{JJ} one finds:

$$\mathcal{H}_{JJ;\perp} = 2g_{\perp} \sum_{a=x,y} J_1^a J_2^a = \frac{\lambda_{\perp}}{\pi\alpha} (\mathcal{D} + \mathcal{F}), \quad (130)$$

$$\mathcal{D} = \cos \sqrt{4\pi K_+} \Phi_+ \cos \sqrt{4\pi K_-} \Theta_-, \quad (131)$$

$$\mathcal{F} = \cos \sqrt{4\pi/K_-} \Phi_- \cos \sqrt{4\pi K_-} \Theta_-, \quad (132)$$

where $\lambda_{\perp} = g_{\perp} \zeta^2/\pi\alpha$, and

$$K_+ = QR, \quad K_- = R/Q. \quad (133)$$

To bosonize the twist perturbation (125), we use the bosonization formulas for the staggered magnetization of the S=1/2 XXZ chain (see section 2.2):

$$n_i^z = -(C_z/\pi\alpha) \sin \sqrt{2\pi Q} \phi_i \quad (134)$$

$$n_i^{\pm} = (C_x/\pi\alpha) \exp(\pm i \sqrt{2\pi/Q} \theta_i), \quad (135)$$

where $C_a(Q)$ ($a = x, z$) are nonuniversal parameters (their exact dependence on Q was recently found in Refs. [37, 38]). Then, in terms of the fields Φ_{\pm} , Θ_{\pm} , the twist term becomes:

$$\mathcal{H}_{\text{twist}} = \sum_{i=1,2,3} \lambda_i \mathcal{O}_i, \quad (136)$$

with

$$\lambda_1 \sim C_x^2 g_{\perp} / \alpha, \quad \lambda_{2,3} \sim C_z^2 (\pm g_{\parallel} + g_0) / \alpha, \quad (137)$$

and three bosonized twist operators $\mathcal{O}_{1,2,3}$ related to T^i ($i = 0, 1, 2, 3$) as follows:

$$\mathcal{O}_1 = T^x + T^y = \frac{2}{\sqrt{K_+}} \partial_x \Theta_+ \sin \sqrt{4\pi K_-} \Theta_-, \quad (138)$$

$$\mathcal{O}_2 = \frac{T^0 + T^z}{2} = \sqrt{K_+} \partial_x \Phi_+ \sin \sqrt{\frac{4\pi}{K_-}} \Phi_-, \quad (139)$$

$$\mathcal{O}_3 = \frac{T^0 - T^z}{2} = \frac{1}{\sqrt{K_-}} \partial_x \Phi_- \sin \sqrt{4\pi K_+} \Phi_+. \quad (140)$$

Thus, the bosonized continuum version of our model, $\mathcal{H} = \mathcal{H}_0 + \mathcal{H}_{JJ;\perp} + \mathcal{H}_{\text{twist}}$, represents a Gaussian field theory of two scalar fields,

$$\mathcal{H}_0 = \sum_{\sigma=\pm} \mathcal{H}_0^{(\sigma)} = \sum_{\sigma=\pm} \frac{v_{\sigma}}{2} [(\partial_x \Phi_{\sigma})^2 + (\partial_x \Theta_{\sigma})^2], \quad (141)$$

with perturbations (130) and (136) which couple the (+) and (-) channels together. Since \mathcal{H}_0 is perturbed in a relevant way, the relationship between the coupling constants of the original model (117) and the parameters of \mathcal{H} , obtained within our weak-coupling approach, is not to be trusted. For this reason we will consider those parameters as independent. Namely, we will treat the Hamiltonian \mathcal{H} as a low-energy effective theory for a most general class of frustrated zigzag spin-1/2 ladders, sharing the same symmetry properties with the model (117).

The scaling dimensions of the perturbing operators are:

$$d_{\mathcal{D}} = K_+ + K_-, \quad d_{\mathcal{F}} = K_- + \frac{1}{K_-}, \quad (142)$$

$$d_1 = 1 + K_-, \quad d_2 = 1 + \frac{1}{K_-}, \quad d_3 = 1 + K_+. \quad (143)$$

Their relevance ($d < 2$) or irrelevance ($d > 2$) can be understood from Fig.(7) where the plane (K_-, K_+) is shown. The point $K_+ = K_- = 1$ corresponds to the SU(2)-symmetric zig-zag ladder where all perturbations (including the Umklapp term) are marginal[24]. This point and its close vicinity will not be discussed in this paper. Due to the condition $K_+/K_- = Q^2 \geq 1$, the physical part of the (K_-, K_+) plane lies above the line $K_+ = K_-$ and can be divided into four sectors in which at least one twist operator is relevant:

$$\text{sector A : } d_1 < 2, \quad d_{\mathcal{F}} \geq 2, \quad d_2, d_3, d_{\mathcal{D}} > 2, \quad (144)$$

$$\text{sector B : } d_1 < d_{\mathcal{D}} < 2, \quad d_2, d_3, d_{\mathcal{F}} > 2, \quad (145)$$

$$\text{sector C : } d_{\mathcal{D}} < d_1 < d_3 < 2, \quad d_2, d_{\mathcal{F}} > 2, \quad (146)$$

$$\text{sector D : } d_2 < 2, \quad d_{\mathcal{F}} \geq 2, \quad d_1, d_3, d_{\mathcal{D}} > 2. \quad (147)$$

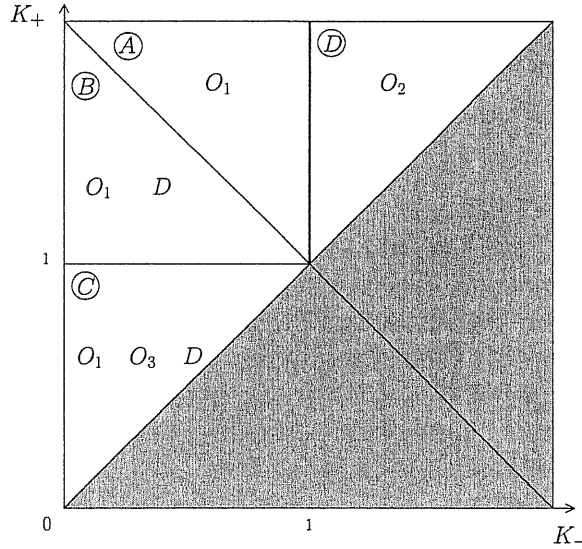


Figure 9: The parameter space of the model

Notice that, except for the operator \mathcal{D} , all other perturbing operators have a nonzero Lorentz spin: $S_{1,2,3} = 1$, $S_{\mathcal{F}} = 2$. Strictly speaking, the

conventional criterion of relevance does not apply to such operators (see e.g. Ref. [32]) because in higher orders of perturbation theory they can generate relevant scalar perturbations. Using standard fusion rules for the Gaussian model, we have analyzed the structure of various terms appearing in the second order of perturbation theory. There are marginal terms leading to small corrections to the parameters K_{\pm} and the velocities v_{\pm} , as well as those which renormalize the already existing coupling constants. Besides, new scalar operators $\cos 2\sqrt{4\pi K_+}\Phi_+$, $\cos 2\sqrt{4\pi/K_-}\Phi_-$, $\cos 3\sqrt{4\pi K_-}\Theta_-$ and $\cos 2\sqrt{4\pi K_-}\Theta_-$ are generated. The first two of them have scaling dimensions $4QR$ and $4Q/R$, respectively, and are therefore strongly irrelevant (since $Q > 1$, $R \sim 1$). The third operator has dimension $9K_- = 9R/Q$ and becomes relevant roughly at $Q > 9/2$, which is a region of the ferromagnetic intrachain exchange, far away from the XX point. This region will not be considered here. Finally, the last perturbation $\sim \cos 2\sqrt{4\pi K_-}\Theta_-$ has dimension $4K_- = 4R/Q$ and thus becomes relevant at $K_- < 1/2$, which corresponds to a vicinity of the XX point $Q = 2$. However, even in that case its role is subdominant, as we will show later.

Thus, the continuum model we will be dealing with in the remainder of this paper reads:

$$\mathcal{H} = \mathcal{H}_0 - (\lambda_{\perp}/\pi\alpha)\mathcal{D} + \sum_{i=1,2,3} \lambda_i \mathcal{O}_i. \quad (148)$$

where \mathcal{H}_0 is given by (141). For later purposes, we have suitably inverted the sign of the coupling constant λ_{\perp} by making a shift of the field Φ_+ : $\Phi_+ \rightarrow \Phi_+ + \sqrt{\pi/4K_+}$. In what follows, we will analyze possible phases of this model in the four sectors A,B,C,D by using a generalization of the standard variational approach [39] that accounts for ground states with nonzero values of topological charges, $\langle \partial_x \Theta_- \rangle$ and $\langle \partial_x \Phi_{\pm} \rangle$. The very possibility to incorporate such states within the variational method stems from the fact that the twist operators (138)–(140) are products of fields belonging to different Gaussian models \mathcal{H}_0^{\pm} .

8 Twistless ladder

Before addressing the role of the twist terms in (148) it is instructive first to apply the variational approach to a simpler frustrated two-leg ladder

model[40, 35] which, in the continuum limit, is free from parity-breaking perturbations yet being spontaneously dimerized. This model is the two leg-ladder version of the standard J_1 - J_2 frustrated Heisenberg plane, in which the inter-chain coupling includes besides the usual on-rung coupling, J_\perp , a frustrating exchange, J_\times , across the diagonals of the plaquettes. In the XXZ case its Hamiltonian reads:

$$H_{\text{gen}} = \sum_{a,n} \sum_{i=1,2} J_a S_i^a(n) S_i^a(n+1) + \sum_{a,n} J'_a S_1^a(n) S_2^a(n) \quad (149)$$

$$+ \sum_{a,n} J''_a [S_1^a(n) S_2^a(n+1) + S_1^a(n+1) S_2^a(n)], \quad (150)$$

where J_a are defined as in (118), and

$$J'_x = J'_y = J_\perp, \quad J'_z = J_\perp \Delta', \quad (151)$$

$$J''_x = J''_y = J_\times, \quad J''_z = J_\times \Delta'. \quad (152)$$

The $P_{S(L)}^{(1)} \otimes P_{S(L)}^{(2)}$ reflection symmetry of the model (150) forbids the marginal twist perturbations to appear in the continuum limit. The additional condition $J_\perp = 2J_\times$ eliminates the $n_1^a n_2^a$ part of the inter-chain coupling and thus makes the two decoupled Gaussian models only perturbed by the current-current inter-chain interaction (124) with coupling constants $g_\perp = 2J_\times \Delta' a_0$ and $g_\parallel = 2J_\times a_0$. So the bosonized continuum Hamiltonian has the structure of Eq.(148) with $\lambda_\perp \neq 0$ and $\lambda_{1,2,3} = 0$. As we shall see below, the dimerized phase it describes also occurs in the most part of sector C of the zigzag ladder, Eq.(148), where \mathcal{D} is the most relevant perturbation to the Gaussian models (141).

To implement Coleman's variational procedure[39], we introduce a trial ground state,

$$|\text{vac}\rangle = |0; m_+, m_-\rangle = |0; m_+\rangle \otimes |0; m_-\rangle, \quad (153)$$

which describes free bosons in the (\pm) sectors with masses m_\pm . These are regarded as variational parameters. To estimate the variational ground-state energy density, $E_0(m_+, m_-) = \langle \text{vac} | \mathcal{H} | \text{vac} \rangle$, one needs to normal order the

Hamiltonian with the prescription that, in the normal-mode expansions of $\Phi_{\pm}(x)$ and $\Theta_{\pm}(x)$, m_{\pm} should be treated as infrared regulator masses.

Upon normal ordering[39]

$$\mathcal{H}_0^{(\pm)} = \mathcal{N}_{m_{\pm}} \left[\mathcal{H}_0^{(\pm)} \right] \quad (154)$$

$$+ \frac{1}{8\pi v_{\pm}} \left[2 \left(\frac{v_{\pm}}{\alpha} \right)^2 + m_{\pm}^2 + O \left(\frac{m_{\pm}^2 \alpha^2}{v_{\pm}^2} \right) \right], \quad (155)$$

$$\cos \sqrt{4\pi K_+} \Phi_+ = \left(\frac{|m_+| \alpha}{v_+} \right)^{K_+} \mathcal{N}_{m_+} \left[\cos \sqrt{4\pi K_+} \Phi_+ \right], \quad (156)$$

$$\cos \sqrt{4\pi K_-} \Theta_- = \left(\frac{|m_-| \alpha}{v_-} \right)^{K_-} \mathcal{N}_{m_-} \left[\cos \sqrt{4\pi K_-} \Theta_- \right], \quad (157)$$

where $\mathcal{N}_{m_{\pm}}$ are the normal ordering symbols. Subtracting from (155) the diverging contribution of the zero-point motion when $\alpha \rightarrow 0$, ignoring for simplicity the difference between the velocities v_{\pm} and defining the dimensionless quantities,

$$\mathcal{E} = \frac{4\pi\alpha^2}{v} E_0, \quad M_{\pm} = \frac{m_{\pm}\alpha}{v}, \quad z_{\perp} = \frac{4\lambda_{\perp}\alpha}{v}, \quad (158)$$

we find that

$$\mathcal{E}(M_+, M_-) = \frac{M_+^2 + M_-^2}{2} - z_{\perp} |M_+|^{K_+} |M_-|^{K_-}. \quad (159)$$

Without loss of generality we choose M_{\pm} to be positive. With the condition $z_{\perp} \ll 1$ in mind, it should be understood that the masses M_{\pm} , obtained upon minimization of \mathcal{E} , should satisfy $M_{\pm} \ll 1$.

At $d_{\mathcal{D}} > 2$ only a trivial solution exists, $M_{\pm} = 0$, corresponding to a critical regime in which the inter-chain interaction is irrelevant and the two chains asymptotically decouple in the low-energy limit. At $d_{\mathcal{D}} = K_+ + K_- < 2$ we find a nontrivial solution,

$$\frac{M_+}{\sqrt{K_+}} = \frac{M_-}{\sqrt{K_-}} = K_+^{\frac{K_+}{2(2-d_{\mathcal{D}})}} K_-^{\frac{K_-}{2(2-d_{\mathcal{D}})}} z_{\perp}^{\frac{1}{2-d_{\mathcal{D}}}}, \quad (160)$$

with ground state energy given by:

$$\mathcal{E}_D = -\left(\frac{1-K_+}{2K_+}\right)M_+^2 - \left(\frac{1-K_-}{2K_-}\right)M_-^2 \quad (161)$$

$$= -\left(\frac{2-d_D}{2K_+}\right)M_+^2 \quad (162)$$

This solution describes a strong-coupling, massive phase in which the fields Φ_+ and Θ_- are locked in one of infinitely degenerate minima of the potential $\mathcal{U}(\Phi_+, \Theta_-) = -(\lambda_\perp/\pi\alpha)\mathcal{D}$. Since $\lambda_\perp > 0$, these minima decouple into “even” and “odd” sets:

$$\Phi_+ = \sqrt{\frac{\pi}{4K_+}}2n_+, \quad \Theta_- = \sqrt{\frac{\pi}{4K_-}}2n_-; \quad (163)$$

$$\Phi_+ = \sqrt{\frac{\pi}{4K_+}}(2n_+ + 1), \quad \Theta_- = \sqrt{\frac{\pi}{4K_-}}(2n_- + 1), \quad (164)$$

where $n_\pm = 0, \pm 1, \pm 2, \dots$. The existence of these two inequivalent sets reflects two-fold degeneracy of the spontaneously dimerized ground state. Transverse dimerization is the order parameter; it is defined as $\langle \epsilon_\perp(x) \rangle$ where [21, 35]

$$\epsilon_\perp(x) = \mathbf{n}_1(x) \cdot \mathbf{n}_2(x) \propto C_x^2 \cos \sqrt{4\pi K_-} \Theta_- \quad (165)$$

$$+ \frac{1}{2}C_z^2 \left(\cos \sqrt{4\pi K_+} \Phi_+ + \cos \sqrt{4\pi/K_-} \Phi_- \right). \quad (166)$$

Since the field Θ_- is locked, its dual Φ_- is disordered and, hence, the expectation value of the last term in (166) vanishes. Hence,

$$\langle \epsilon_\perp \rangle = \pm \epsilon_0, \quad \epsilon_0 \propto C_x^2 |M_-|^{K_-} + \frac{1}{2}C_z^2 |M_+|^{K_+}, \quad (167)$$

with the two signs of ϵ corresponding to the even and odd vacua, respectively.

The discrete (Z_2) symmetry that is spontaneously broken in the ground state is generated by even-odd intersite transitions of the fields,

$$\Delta \Phi_+ = \pm \sqrt{\pi/4K_+}, \quad \Delta \Theta_- = \pm \sqrt{\pi/4K_-}, \quad (168)$$

and is related to translations by one lattice spacing on one chain only. This is not an exact symmetry of the microscopic Hamiltonian (150) but rather appears as an important property of the corresponding low-energy model with a “current-current” perturbation. The excitation spectrum of the model consists of pairs of massive topological kinks (spinons) interpolating between two adjacent minima of the potential \mathcal{U} . The kinks carry two topological quantum numbers – the total spin

$$S_+^z = \sqrt{\frac{K_+}{\pi}} \int_{-\infty}^{\infty} dx \partial_x \Phi_+(x), \quad (169)$$

and the relative longitudinal spin current

$$j_-^z/u = -\sqrt{\frac{K_-}{\pi}} \int_{-\infty}^{\infty} dx \partial_x \Theta_-(x), \quad (170)$$

which, according to (168), take fractional values $\pm 1/2$ [41].

9 Critical spin nematic phase

Now we are coming back to the continuum model (148) for the XXZ zig-zag ladder. We begin our discussion with sector A where the twist operator \mathcal{O}_1 is the only relevant perturbation to the two decoupled Gaussian models $\mathcal{H}_0^{(\pm)}$. Making a shift $\Theta_- \rightarrow \Theta_- + (1/4)\sqrt{\pi/K_-}$ we write the low-energy model in sector A as follows:

$$\mathcal{H}_A = \mathcal{H}_0^{(+)} + \mathcal{H}_0^{(-)} + \frac{2\lambda_1}{\sqrt{K_+}} \partial_x \Theta_+ \cos \sqrt{4\pi K_-} \Theta_-. \quad (171)$$

This model has the same structure as that for the XX zigzag ladder considered in Ref.[24]. Not surprisingly, the variational procedure we will follow now leads to qualitatively the same results as those obtained for the XX case within a symmetry-preserving mean-field approach[24].

The interaction term in (171) couples the vertex operator in the $(-)$ channel to the topological current density $\partial_x \Theta_+$ in the $(+)$ channel. The latter determines the z -component of the spin current which flows along the chain direction, \hat{j}_{\parallel}^z ,

$$\hat{j}_+^z \equiv \hat{j}_{\parallel}^z = -v \sqrt{\frac{K_+}{\pi}} \partial_x \Theta_+. \quad (172)$$

We observe that a finite λ_1 , see Eq. (171), generates an additional contribution to the spin current, \hat{j}_\perp^z , which flows along the inter-chain bonds. By the continuity equation related to the conservation of the z -component of the total spin, one finds that

$$\hat{j}_\perp^z = -\frac{2}{\sqrt{\pi}} \lambda_1 \cos \sqrt{4\pi K_-} \Theta_-. \quad (173)$$

The total spin current is therefore $\hat{j}^z = \hat{j}_\parallel^z + \hat{j}_\perp^z$, and the twist operator \mathcal{O}_1 is nothing but a coupling term $\hat{j}_\parallel^z \hat{j}_\perp^z$.

The structure of the perturbation in the model (171) suggests that the ground state admits finite values of the mass gap in the $(-)$ channel and the spin current in the $(+)$ channel. So one needs to treat both of these two quantities as variational parameters. To this end, we keep boundary conditions periodic for the field $\Theta_-(x)$ but impose twisted boundary conditions for the field $\Theta_+(x)$:

$$\Theta_+(x) = \Theta_+^0(x) - \frac{1}{v} \sqrt{\frac{\pi}{K_+}} j_+^z x. \quad (174)$$

Here $\Theta_+^0(x)$ is a massless harmonic Bose field satisfying periodic boundary conditions, and j_+^z is the average value of the current operator (172) which is to be determined self-consistently. The variational procedure is the same as in the previous section with the exception that the ground state energy in the $(+)$ channel will acquire a piece proportional to $(j_+^z)^2$. Otherwise this sector remains gap-less: $M_+ = 0$. Using dimensionless notations,

$$\mathcal{J}_+ = \frac{2\pi\alpha}{\sqrt{K_+}v} j_+^z, \quad z_1 = 4\sqrt{\frac{\pi}{K_+}} \frac{\lambda_1\alpha}{v}, \quad (175)$$

for the variational energy density \mathcal{E} we obtain:

$$\mathcal{E}(\mathcal{J}_+, M_-) = \frac{1}{2} (M_-^2 + \mathcal{J}_+^2) \mp z_1 \mathcal{J}_+ M_-^{K_-}. \quad (176)$$

As before, we have chosen M_- to be positive. The (\mp) signs in the interaction term correspond to two sets of vacuum expectation values of the field Θ_- : $\Theta_- = \sqrt{\pi/K_-}n$ and $\Theta_- = \sqrt{\pi/K_-}(n+1/2)$, respectively.

Minimizing \mathcal{E} with respect to M_\pm and \mathcal{J}_+ we find that the $(-)$ channel is gapped,

$$M_- = K_-^{\frac{1}{2(1-K_-)}} z_1^{\frac{1}{1-K_-}}, \quad (177)$$

if $K_- < 1$. This is actually the condition $d_1 < 2$ for the twist operator \mathcal{O}_1 to be a relevant perturbation, which is satisfied in sector A. At the same time, the gap supports a finite value of the spin current in the (+) channel:

$$\mathcal{J}_+ = \pm \frac{M_-}{\sqrt{K_-}} = \pm K_-^{\frac{K_-}{2(1-K_-)}} z_1^{\frac{1}{1-K_-}}. \quad (178)$$

We notice that the dimensionless transverse current defined by

$$\hat{\mathcal{J}}_{\perp} = -\frac{2\pi\alpha}{\sqrt{K_+u}} \hat{j}_{\perp}^z = z_1 \cos \sqrt{4\pi K_-} \Theta_-, \quad (179)$$

also acquires a finite ground-state expectation value

$$\mathcal{J}_{\perp} = \langle \hat{\mathcal{J}}_{\perp} \rangle = \mp z_1 M_-^{K_-}, \quad (180)$$

which exactly cancels $\mathcal{J}_{\parallel} = \mathcal{J}_+$, so that the total spin current is zero. This results in a spin nematic (or a staggered spin-flux) phase characterized by local spin currents circulating around elementary plaquettes in an alternating way. This type of ordering does not break time reversal symmetry. In sector A the spin nematic phase is critical because the spin-density fluctuations in the (+) channel remain gap-less.

We notice that the transverse current can be associated with the chirality order parameter. The latter is defined as

$$\kappa_z = \langle \kappa_z(x) \rangle, \quad \kappa_z(x) = [\mathbf{n}_1(x) \times \mathbf{n}_2(x)]_z, \quad (181)$$

and, according to bosonization rules (135), transforms in the continuum limit to

$$\kappa_z(x) \propto \cos \sqrt{4\pi K_-} \Theta_-(x) \propto \hat{j}_{\perp}(x). \quad (182)$$

As the dimerized phase discussed in sec.III, the spin nematic phase is doubly degenerate because the mixed parity symmetry $P_{S(L)}^{(1)} P_{L(S)}^{(2)}$ is spontaneously broken in the ground state. The two degenerate phases differ in the signs of the longitudinal and transverse currents. Consequently, apart from the massless bosonic mode describing low-energy fluctuations of the total magnetization, there exist massive topological Z_2 kinks corresponding to vacuum-vacuum transitions,

$$\mathcal{J}_+ \rightarrow -\mathcal{J}_+, \quad \Theta_- \rightarrow \Theta_- \pm \sqrt{\pi/4K_-},$$

and thus carrying the relative spin current $j^z/u = \pm 1/2$; see Eq.(170).

The presence of a finite longitudinal spin current in the ground state makes the transverse (xy) spin correlations incommensurate. Since the (+) channel is massless and described by a Gaussian field with a K_+ dependent compactification radius, the correlations will decay algebraically with a nonuniversal exponent. Making use of bosonization rules (135), Eq. (174) and the fact that the field Θ_- is locked, one easily finds the asymptotic behaviour of the transverse spin correlation function:

$$\langle S_1^+(x)S_{1,2}^- \rangle \propto \frac{(-1)^{x/a_0}}{|x|^{1/2K_+}} e^{-iq_0x} \quad (183)$$

where the wave vector $q_0 = \pi\mathcal{J}_{\parallel}/uK_+$. At the XX point ($Q = 2$, $R = 1$, $K_+ = 2$) the spin correlations decay according to the power law $|x|^{1/2}$, in agreement with Ref. [24].

The ground state energy of the critical spin nematic (CSN) phase is given by

$$\mathcal{E}_{\text{CSN}} = - \left(\frac{1 - K_-}{2K_-} \right) M_-^2 \quad (184)$$

Before closing this section, we would like to briefly discuss the role of the scalar operator $\cos 2\sqrt{4\pi K_-}\Theta_-$, which is generated in a higher orders and becomes relevant at $K_- < 1/2$. In the presence of a finite spin current in (+) channel, this term transforms the effective Hamiltonian in (-) channel to a double-frequency sine-Gordon model: $\mathcal{H}_0 - \lambda_{\text{eff}} \sin \sqrt{4\pi K_-}\Theta_- - g \cos 2\sqrt{4\pi K_-}\Theta_-$, where $\lambda_{\text{eff}} \propto \lambda_1 \langle j_+^z \rangle$. It is known [42, 43] that the g -term can induce an Ising transition to a new massive phase if $g > 0$ and $g^{1/2(1-2K_-)} > \lambda_{\text{eff}}^{1/(2-K_-)}$. The last inequality, however, is not satisfied since the amplitude $g \sim \lambda_{\text{eff}}^2$ is rather small and, hence, the presence of the second harmonics does not qualitatively affect the above results.

10 Massive spin nematic and dimerized phases

Let us now move to sectors B and C where the properties of the systems are determined by the interplay between two most relevant perturbations, \mathcal{O}_1 and \mathcal{D} . The second twist perturbation, \mathcal{O}_3 , is either irrelevant (as in sector B) or the least relevant (as in sector C). In Appendix A we explicitly

show that its role is indeed subdominant in sectors B and C far from the SU(2)-symmetric point, $K_+ = K_- = 1$,

Thus, the effective Hamiltonian reads:

$$\mathcal{H}_{B/C} = \mathcal{H}_0^{(+)} + \mathcal{H}_0^{(-)} \quad (185)$$

$$- \frac{\lambda_{\perp}}{\pi\alpha} \cos \sqrt{4\pi K_+} \Phi_+ \cos \sqrt{4\pi K_-} \Theta_- \quad (186)$$

$$+ \frac{2\lambda_1}{\sqrt{K_+}} \partial_x \Theta_+ \sin \sqrt{4\pi K_-} \Theta_- \quad (187)$$

The potential in (187) contains both the sine and cosine of the field Θ_- ; so its vacuum value Θ_-^* is expected to be located somewhere within the interval $(0, \sqrt{\pi/4K_-})$ and must be such that in a massive phase with $M_- \neq 0$

$$\langle \text{vac} | \cos \sqrt{4\pi K_-} \Theta_-^* | \text{vac} \rangle = M_-^{K_-}, \quad (188)$$

$$\langle \text{vac} | \sin \sqrt{4\pi K_-} \Theta_-^* | \text{vac} \rangle = 0. \quad (189)$$

Setting $\Theta_- = \Theta_-^* - \gamma/\sqrt{4\pi K_-}$, we arrive at the following expression of the dimensionless variational energy:

$$\mathcal{E}(\mathcal{J}_{\parallel}, M_+, M_-, \gamma) = \frac{1}{2} (M_+^2 + M_-^2 + \mathcal{J}_+^2) \quad (190)$$

$$\mp z_{\perp} \mathcal{J}_+ M_-^{K_-} \sin \gamma - z_{\perp} M_+^{K_+} M_-^{K_-} \cos \gamma. \quad (191)$$

Its minimization with respect to M_{\pm} , \mathcal{J}_+ and the angle γ yields the following set of equations:

$$M_-^{K_-} (z_{\perp} M_+^{K_+} \sin \gamma \mp z_{\perp} \mathcal{J}_+ \cos \gamma) = 0, \quad (192)$$

$$\mathcal{J}_+ \mp z_{\perp} M_-^{K_-} \sin \gamma = 0, \quad (193)$$

$$M_+ (1 - z_{\perp} K_+ M_+^{K_+ - 2} M_-^{K_-} \cos \gamma) = 0, \quad (194)$$

$$M_- (1 - z_{\perp} K_- M_+^{K_+} M_-^{K_- - 2} \cos \gamma) \quad (195)$$

$$\mp z_{\perp} K_- \mathcal{J}_+ M_-^{K_- - 2} \sin \gamma = 0. \quad (196)$$

There are two obvious solutions of these equations in which only one of the two perturbing operators is effective. In these solutions the angle γ takes two values: 0 and $\pi/2$. The corresponding phases are, respectively: (i) a fully gapped D phase already described in sec.III, with zero current ($\mathcal{J}_+ = 0$) and nonzero masses M_{\pm} given by Eq.(160), and (ii) a CSN phase with nonzero \mathcal{J}_+ and M_- given by Eqs. (178) and (177).

Eqs. (192)-(196) admit one more solution where the combined effect of the two relevant perturbations leads to an intermediate value of the mixing angle γ ,

$$\cos \gamma = \frac{M_+}{M_-} \sqrt{\frac{K_-}{K_+}}, \quad (197)$$

and a finite mass gap in the (+) channel,

$$M_+ = (z_{\perp} \sqrt{K_+}/z_1)^{\frac{1}{1-K_+}}. \quad (198)$$

This is a noncritical or massive spin nematic (MSN) phase characterized by the coexistence of a reduced spin current \mathcal{J}_+

$$\mathcal{J}_+ = [\mathcal{J}_+]_{\text{CSN}} \sin \gamma \quad (199)$$

and a nonzero dimerization

$$\epsilon_{\perp} \propto \pm \left[C_x^2 M_-^{K_-} \cos \gamma + \frac{1}{2} C_z^2 M_+^{K_+} \right]. \quad (200)$$

An important observation is that the minimal value of the variational energy (191) is still given by expression (161). Therefore, the energies of the MSN and CSN phases are related as

$$\mathcal{E}_{\text{MSN}} = \mathcal{E}_{\text{CSN}} + \frac{K_+ - 1}{2K_+} M_+^2.$$

So in sector B ($K_+ > 1$) the MSN phase is energetically less favorable than the CSN phase, and the ground state should be chosen between CSN and D phases. Accordingly, in sector C ($K_+ < 1$) the competing phases are MSN and D.

Consider first sector B. Here we need to compare the ground state energies of the D and CSN phases given by Eqs.(162) and (184). These are of the same order when the mass gaps of the two phases, Eqs. (160) and (177),

become comparable. Notice that the coupling constants z_1 and z_\perp are both proportional to g_\perp and, hence are of the same order of magnitude; their ratio is

$$z_\perp/z_1 = C\sqrt{K_+}, \quad (201)$$

where C is a nonuniversal number. Therefore, the condition

$$z_\perp^{\frac{2}{2-d_D}} \sim z_1^{\frac{2}{2-d_1}} \quad (202)$$

can be satisfied only in some vicinity of the line $K_+ = 1$ where scaling dimensions of the operators \mathcal{D} and \mathcal{O}_1 become equal.

As already mentioned, it is not possible to establish a precise relationship between the parameters of the original, microscopic model (119) and the effective low-energy theory (148). As a result, the parameter C in (201) is unknown. Therefore we are forced to consider two cases, $z_1 > z_\perp$ and $z_1 < z_\perp$, on equal footing and draw plausible scenarios for each of them, leaving the final choice to future numerical work.

Setting $K_+ = 1 + \delta$ with $|\delta| \ll 1$, we find that the condition (202) translates to the relation

$$\delta = (1 - K_-) \frac{\ln(z_\perp/z_1)}{\ln(1/z_1)}. \quad (203)$$

This relation determines a line $\delta = \delta(K_-)$ which lies entirely in sector B ($\delta > 0$) and is located very close to the line $K_+ = 1$ only if $z_1 < z_\perp$. Under this condition the relation (203) determines a phase boundary between the CSN and D states. The transition is of first order, associated with discontinuities of the spin current and dimerization order parameters. It can be easily shown that in the case $z_1 < z_\perp$ the D phase, occupying a narrow region close to the line $K_+ = 1$, extends over the whole C phase.

In the opposite case, $z_1 \geq z_\perp$, Eq.(203) has no solution for $\delta > 0$, implying that CSN is a stable ground state in the whole sector B. Moving to sector C opens a possibility for the MSN phase. If $1 - K_+ \ll 1$, the condition $z_1 \geq z_\perp$ admits a small nonzero mass M_+ given by (198). Thus in sector C the upper boundary for the MSN phase is $K_+ = 1$. The lower boundary is found from the requirement $\cos \gamma < 1$ (see Eq. (197)). Within the logarithmic accuracy, this brings us again to Eq.(203), this time for $\delta(K_-) < 0$.

Thus, if the ratio $z_1/z_\perp > 1$, then the CSN and D phases are “sandwiched” by the MSN phase occupying a narrow region in sector C

$$1 - (1 - K_-) \frac{\ln(z_1/z_\perp)}{\ln(1/z_1)} < K_+ < 1 \quad (204)$$

attached to the line K_+ (see Fig. 10). In all this region $\mathcal{E}_{\text{MSN}} < \mathcal{E}_{\text{D}}$. The transitions that occur on the upper and lower boundaries of the MSN phase are continuous. When moving from sector B to sector C through the MSN phase, the mixing angle γ varies from $\pi/2$ to 0. Correspondingly, the current \mathcal{J}_+ decreases from its nominal value $[\mathcal{J}_+]_{\text{CSN}}$ and vanishes at the lower boundary, whereas the transverse dimerization ϵ_\perp increases from zero at the upper boundary and reaches its value ϵ_0 , Eq.(167), in the pure D phase at the lower boundary (see Fig. 10). A possible way of driving the ladder to pass through these phases is shown in Fig. 11.

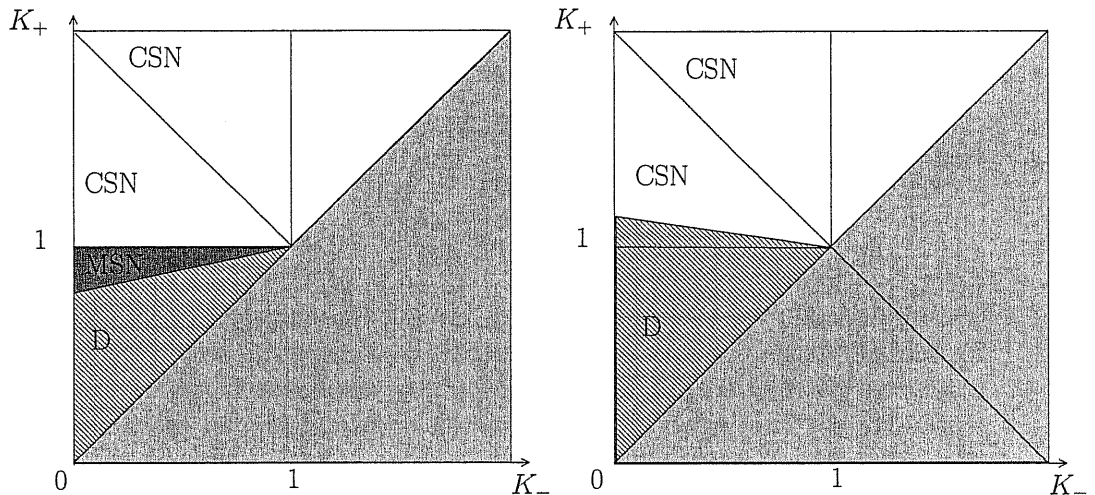


Figure 10: Possible phase transitions in the ladder: the left one is when $z_\perp < z_1$, MSN phase is very narrow, and the right one is for $z_\perp > z_1$

11 Ferromagnetic phase

Let us now consider sector D where $K_+ > K_- > 1$. This condition implies that $K_+K_- = R^2 > 1$, and so this sector corresponds to the case of

a ferromagnetic inter-chain interaction ($g_{\parallel} < 0$). The effective low-energy model

$$\mathcal{H}_D = \mathcal{H}_0^{(+)} + \mathcal{H}_0^{(-)} + \lambda_2 \sqrt{K_+} \partial_x \Phi_+ \sin \sqrt{4\pi/K_-} \Phi_- \quad (205)$$

contains only one relevant twist operator and is dual to model (171) describing the SN phase in sector A: mapping between these two models is achieved by duality transformations

$$2\lambda_1 \rightarrow \lambda_2, \quad K_{\pm} \rightarrow 1/K_{\pm}, \quad \Phi_{\pm} \rightarrow \Theta_{\pm} \quad (206)$$

Using this correspondence, we can readily translate the results of sec.IV to the present case. In particular, the spontaneously generated spin current \mathcal{J}_+ of the SN phase transforms to the z-component of the uniform spin density. So the ground state of the system in sector D is *ferromagnetic* (F). Contrary to the spin nematic phase, the F phase breaks time reversal invariance but preserves parity $P_S^{(1)} \otimes P_L^{(2)}$.

Shifting the field Φ_- by $\sqrt{\pi K_-}/4$ and passing to dimensionless notations for the coupling constant,

$$z_2 = 2\sqrt{\pi K_+} \frac{\lambda_2 \alpha}{v}$$

and total magnetization

$$\mathcal{S}_+ = \frac{2\pi\alpha}{\sqrt{K_+}} m^z,$$

we write the variational energy density as

$$\mathcal{E} = \frac{1}{2} (M_-^2 + \mathcal{S}_+^2) \mp z_2 \mathcal{S}_+ M_-^{1/K_-}. \quad (207)$$

Its minimization yields a finite gap in the (-) channel,

$$M_- = K_-^{-\frac{K_-}{2(K_- - 1)}} z_2^{\frac{K_-}{K_- - 1}} \quad (208)$$

which supports a nonzero magnetization directed along the exchange anisotropy axis:

$$\mathcal{S}_+ = \pm \sqrt{K_-} M_- = \pm K_-^{-\frac{1}{2(K_- - 1)}} z_2^{\frac{K_-}{K_- - 1}} \quad (209)$$

The (+) channel remains gap-less. Together with the finite spontaneous magnetization this circumstance makes the longitudinal spin correlations algebraic *and* incommensurate:

$$\langle S_1^z(x) S_{1,2}^z(0) \rangle = \langle S^z \rangle^2 - \frac{K_+}{8\pi^2} \frac{1}{x^2} \quad (210)$$

$$+ \text{const} \frac{(-1)^{x/a_0}}{|x|^{K_+/2}} \cos q_0 x, \quad (211)$$

where $q_0 = \mathcal{S}_+ \sqrt{K_+}/2\alpha$. The transverse spin correlations are short-ranged.

The ground state is doubly degenerate: the two vacua transforming to each other under time reversal. The corresponding topological kinks have a finite mass gap and carry the relative spin

$$S_-^z = \frac{1}{\sqrt{\pi K_-}} \int_{-\infty}^{\infty} dx \partial_x \Phi_- = \pm \frac{1}{2}. \quad (212)$$

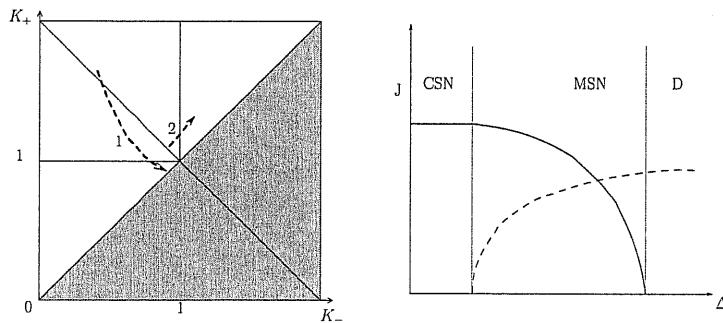


Figure 11: The first path shows one possible way of going through CSN, MSN and D phases when $z_\perp < z_1$, by increasing Δ and keeping Δ' to be a constant. The right figure shows the qualitative change of the spin current (solid line) and the dimerization order parameter (dashed line) following this path. In the second path by decreasing Δ' and keeping Δ at constant value, the ladder enters the F phase.

12 RG approach at A-D boundary

The results of sections IV and VI are valid far enough from the boundary between sectors A and D where one of the two twist operators, $\mathcal{O}_{1,2}$, is strongly relevant while the other is strongly irrelevant. On the boundary $K_- = 1$ separating these sectors both twist operators become marginal. Therefore we can expect that in the immediate vicinity of the boundary,

$$K_- = 1 - \delta_-, \quad |\delta_-| \ll 1, \quad (213)$$

far away from the SU(2)-symmetric point, i.e. $K_+ > 1$ in the sense that $K_+ - 1 = O(1)$, the infrared behavior of model will be controlled by the interplay between the two parity-breaking operators with a nonzero conformal spin, $\mathcal{O}_{1,2}$, and the longitudinal (conformal-scalar) terms $\partial_x \Phi_R^\pm \partial_x \Phi_L^\pm$ responsible for renormalization of the coupling constants. So the starting low-energy model should therefore contain both twist terms:

$$\mathcal{H} = \mathcal{H}_0^{(+)} + \mathcal{H}_0^{(-)} \quad (214)$$

$$+ \gamma_1 \partial_x \Theta_+ \sin \tilde{\beta} \Theta_- + \gamma_2 \partial_x \Phi_+ \sin \beta \Phi_- \quad (215)$$

Here $\gamma_{1,2}$ differ from $\lambda_{1,2}$ by some multiplicative factors, and

$$\tilde{\beta} = \frac{4\pi}{\beta} = \sqrt{4\pi K_-} = \sqrt{4\pi} \left[1 + \frac{\delta_-}{2} + O(\delta_-^2) \right] \quad (216)$$

Notice that the two twist terms in (215) contain vertex operators (the sines) of mutually dual and *nonlocal* fields, Θ_- and Φ_- . Models of this kind cannot be treated by the variational method used in the preceding sections. This is why in this section we address the RG flow of this model which will be studied using a mapping of the bosonic Hamiltonian (215) onto a theory of four interacting real (Majorana) fermions (c.f. Ref.[24]).

Let us first make all perturbations in (215) strictly marginal. This can be done by the following rescaling of the fields in the (-) and (+) sectors:

$$\Phi_- \rightarrow \sqrt{K_-} \Phi_-, \quad \Theta_- \rightarrow (1/\sqrt{K_-}) \Theta_- \quad (217)$$

$$\Phi_+ \rightarrow \sqrt{q_+} \Phi_+, \quad \Theta_+ \rightarrow (1/\sqrt{q_+}) \Theta_+ \quad (218)$$

The meaning of the first rescaling is transparent: we enforce the twist operators in (215) to have the scaling dimension 2. This rescaling generates

a current-current term in the $(-)$ channel. On the other hand, fusing the two twist operators, one generates a similar term in the $(+)$ sector; that will renormalize the parameter K_+ , $K_+ \rightarrow \bar{K}_+ = K_+ q_+$. Below we will set $q_+ = 1 - \delta_+$ assuming that $|\delta_+| \ll 1$. The Hamiltonian (215) then acquires the form:

$$\mathcal{H} = \frac{u}{2} \sum_{s=\pm} [(\partial_x \Phi_s)^2 + (\partial_x \Theta_s)^2] - 2u \sum_{s=\pm} \delta_s \partial_x \Phi_{sR} \partial_x \Phi_{sL} \quad (219)$$

$$+ \gamma_1 \partial_x \Theta_+ \sin \sqrt{4\pi} \Theta_- + \gamma_2 \partial_x \Phi_+ \sin \sqrt{4\pi} \Phi_- \quad (220)$$

where δ_{\pm} satisfy the initial conditions

$$\delta_+^{(0)} = 0, \quad \delta_-^{(0)} = \delta_- \quad (221)$$

It is understood that extra factors appearing due to rescaling of K_+ are absorbed into a redefinition of the coupling constants γ_1 and γ_2 .

The structure of (220) immediately suggests mapping onto four real (Majorana) fermions, ξ^a ($a = 0, 1, 2, 3$). This can be done using a correspondence

$$(\Phi_+, \Theta_+) \Rightarrow (\xi_1, \xi_2), \quad (\Phi_-, \Theta_-) \Rightarrow (\xi_3, \xi_0).$$

and standard fermionization rules for the currents and vertex operators. The resulting theory is given by the Euclidean action describing four degenerate massless fermions with a *chirally asymmetric* interaction:

$$S = \sum_{a=0}^3 \int d^2 z (\xi^a \bar{\partial} \xi^a + \bar{\xi}^a \partial \bar{\xi}^a) \quad (222)$$

$$+ 2\pi v \int d^2 z [\delta_+ \xi_1 \xi_2 \bar{\xi}_1 \bar{\xi}_2 + \delta_- \xi_3 \xi_0 \bar{\xi}_3 \bar{\xi}_0] \quad (223)$$

$$+ \gamma_+ (\xi_1 \xi_2 \xi_3 \bar{\xi}_0 + \bar{\xi}_1 \bar{\xi}_2 \bar{\xi}_3 \xi_0) \quad (224)$$

$$+ \gamma_- (\xi_1 \xi_2 \xi_0 \bar{\xi}_3 + \bar{\xi}_1 \bar{\xi}_2 \bar{\xi}_0 \xi_3). \quad (225)$$

Here $\xi_a(z)$ and $\bar{\xi}_a(\bar{z})$ are holomorphic (left) and antiholomorphic (right) components of the Majorana fields, $z = v\tau + ix$ and $\bar{z} = v\tau - ix$ are complex coordinates, $\partial = \partial/\partial z$, $\bar{\partial} = \partial/\partial \bar{z}$, and

$$\gamma_{\pm} = \frac{\pi^{3/2} \alpha}{2\pi u} (\gamma_1 \pm \gamma_2) \quad (226)$$

Due to its chiral asymmetry, the interaction in (225) gives rise to renormalization of the velocities already on the one-loop level. For this reason we will discriminate between the velocities of different Majorana species, and set $v_a = v(1 - 4\pi\rho_a)$ ($a = 0, 1, 2, 3$), where the dimensionless parameters ρ_a are subject to renormalization with initial conditions $\rho_a^{(0)} = 0$.

Using the standard fusion rules for fermion fields[45], one can easily derive the following one-loop RG equations:

$$\dot{\delta}_+ = -2\gamma_+\gamma_-, \quad \dot{\delta}_- = 0, \quad (227)$$

$$\dot{\gamma}_+ = \delta_-\gamma_-, \quad \dot{\gamma}_- = \delta_-\gamma_+, \quad (228)$$

$$\dot{\rho}_1 = \dot{\rho}_2 = \gamma_+^2 + \gamma_-^2, \quad (229)$$

$$\dot{\rho}_3 = \gamma_+^2, \quad \dot{\rho}_0 = \gamma_-^2, \quad (230)$$

where $\dot{g} \equiv dg(l)/dl$, $l = \ln(L/\alpha)$.

First of all, we observe that the coupling constant δ_- stays unrenormalized:

$$\delta_-(l) = \delta_-(0) = \delta_- \quad (231)$$

Representing λ_{\pm} as

$$\gamma_{\pm} = g_1 \pm g_2, \quad g_{1,2} = (\pi^{3/2}\alpha/2\pi u)\gamma_{1,2}$$

we rewrite the first, third and fourth RG equations as

$$\dot{\delta}_+ = -2(g_1^2 - g_2^2) \quad (232)$$

$$\dot{g}_1 = \delta_-g_1, \quad \dot{g}_2 = -\delta_-g_2 \quad (233)$$

We see that, depending on the sign of δ_- , either $g_1(l)$ or $g_2(l)$ grow up upon renormalization:

(a) $\delta_- > 0$

$$g_1(l) = g_1^{(0)}e^{\delta_-l}, \quad g_2(l) = g_2^{(0)}e^{-\delta_-l} \rightarrow 0 \quad (234)$$

Strong-coupling behavior of $g_1(l)$ in (234) is associated with a dynamical generation of a mass gap

$$m_1 \propto |g_1|^{1/\delta_-}. \quad (235)$$

(b) $\delta_- < 0$

$$g_2(l) = g_2^{(0)}e^{|\delta_-|l}, \quad g_1(l) = g_1^{(0)}e^{-|\delta_-|l} \rightarrow 0 \quad (236)$$

Here the mass gap is estimated as

$$m_2 \propto |g_2|^{1/|\delta_-|}. \quad (237)$$

The cases (a) and (b) describe the CSN and F phases, respectively. Estimations (235), (237) are consistent with the power-law scaling of the corresponding mass gaps, Eqs.(177) and (208). In both cases, $|\delta_+(l)|$ flows to strong coupling. It goes to large negative values in the case (a), implying that K_+ becomes even larger upon renormalization. In the case (b) it flows to large positive values; so the effective K_+ significantly reduces, and that might indicate the importance of the neglected twist operator \mathcal{O}_3 . Stability of the F phase is therefore under question.

Exactly at the boundary between sectors A and D $\delta_- = 0$. In this case both g_1 and g_2 stay unrenormalized. Moreover,

$$\delta_+(l) = -2(g_1^2 - g_2^2)l. \quad (238)$$

So, if in addition we set $g_1 = g_2$, the 1-loop RG will display a weak-coupling regime for all coupling constants. This is the self-dual point of the model where the interaction is not renormalized: for all effective couplings parametrizing interaction the β -function vanishes. Amazingly, in this case the Majorana action (225) decouples into two chirally asymmetric, independent parts, $S = S_I + S_{II}$, where

$$S_I = \int d^2z \left(\sum_{a=1}^3 \xi^a \bar{\partial} \xi^a + \bar{\xi}^0 \partial \xi^0 + g \xi^1 \xi^2 \xi^3 \bar{\xi}^0 \right) \quad (239)$$

and S_{II} is obtained from S_I by reversing the chiralities of all the fields. Notice that even though the present case corresponds to an essentially anisotropic regime (remember that we are far away from the SU(2)-symmetric point of the model), the effective theory on the boundary between sectors A and D ($K_- = 1$) with the self-duality condition $g_1 = g_2$ exhibits an enlarged, chiral SO(3) \otimes SO(3) symmetry. Consistent with this symmetry is renormalization of the velocities. The velocity of the singlet fermion, $\bar{\xi}^0$, stays intact: $\dot{\rho}_0 = 0$. However, the triplet velocity is renormalized. The RG equation $\dot{\rho}_i = 4g^2$ ($\rho_i \equiv \rho_i$ $i = 1, 2, 3$) shows that $4\pi\rho_i(l)$ increases upon renormalization and reaches values of the order of 1 in the region where $g^2 l \sim 1$. This sets up an infrared energy scale in the problem, $\omega_0 \sim \Lambda \exp(-\text{const}/g^2)$, at which the triplet collective excitations soften significantly. This is in agreement

with the exact results for the spectrum of model (239), recently obtained by Tsvetik [44].

Interestingly enough, the exact solution [44] shows that the chiral SO(3) symmetry of the action (239) is spontaneously broken at $T=0$, and the ground state of the model represents a “chiral ferromagnet” characterized by a nonzero expectation value of the vector current:

$$\langle \mathbf{I} \rangle \neq 0, \quad I^a = -(i/2)\epsilon^{abc}\xi_b\xi_c.$$

Similarly, for action S_{II}

$$\langle \bar{\mathbf{I}} \rangle \neq 0, \quad \bar{I}^a = -(i/2)\epsilon^{abc}\bar{\xi}_b\bar{\xi}_c.$$

As long as the actions S_{I} and S_{II} are decoupled, there is no correlation between $\langle \mathbf{I} \rangle$ and $\langle \bar{\mathbf{I}} \rangle$, or equivalently, between the magnetization $\mathbf{m} = \langle \mathbf{I} \rangle + \langle \bar{\mathbf{I}} \rangle$ and spin current $\mathbf{j} = \langle \mathbf{I} \rangle - \langle \bar{\mathbf{I}} \rangle$. Such correlation appears upon deviation from the A–D boundary since in this case chirally-symmetric terms that couple the actions S_{I} and S_{II} (and also introduce a finite XXZ anisotropy) are generated. Thus, in the A-vicinity of the A–D boundary $m_z \neq 0$, $j_z = 0$, whereas in the D-vicinity the situation is just inverted: $m_z = 0$, $j_z \neq 0$. So, the resulting picture at the A–D boundary depends on the side from which this boundary is approached, implying that the CSN – F transition is first-order.

Even though the action $S = S_{\text{I}} + S_{\text{II}}$ provides the simplest field-theoretical model for a frustrated ladder with a chirally asymmetric interaction and, hence, is quite interesting in its own right, we will refrain from its further discussion because it does not account for the low-energy properties of the zigzag spin-1/2 ladder with the *generic* SU(2) symmetry (the point $K_+ = K_- = 1$).

13 Conclusions

In this part of the thesis we have analyzed the phase diagram of the spin-1/2 anisotropic zigzag ladder with a weak inter-chain coupling ($J' \ll J$). Using the Abelian bosonization method combined with a variational approach, we have found that, depending on the anisotropy parameters, the system occurs either in the parity and time-reversal symmetric, spontaneously dimerized phase, or in one of those phases in which either parity is spontaneously

broken while time reversal preserved, or vice versa. These are the critical and massive spin nematic phases (CSN,MSN) and the critical ferromagnetic (F) phase. We have shown that the CSN phase extends well beyond the XX limit and covers broad regions A and B in the parameter space of the XXZ model (see Fig.10). Each of these phases is characterized by topological excitations carrying fractional quantum numbers.

Starting from a vicinity of the XX point, we addressed the nature of the transition between the CSN and D phases taking place upon increasing the intra-chain anisotropy parameter Δ , say, at a fixed positive value of Δ' . Typical curves are shown in Fig.11. In these two Figures we show two possible scenarios whose realization depends on the ratio (z_{\perp}/z_{\parallel}) between the amplitudes of the main competing perturbations – the twist operator \mathcal{O}_1 and the dimerization field \mathcal{D} . The reason we considered each of these scenarios on equal footing is due to the fact that the relationship between the parameters of our bosonized model, Eq.(148), and those of the microscopic Hamiltonian (119) is nonuniversal and, hence, known only by the order of magnitude. If $z_{\perp} > z_{\parallel}$, the CSN – D transition is first order. In the opposite case, $z_{\perp} < z_{\parallel}$, the CSN and D phases are sandwiched by the MSN phase characterized by the coexistence of a finite spin current with dimerization. Then the variational approach unambiguously shows that CSN–MSN and MSN – D transitions are continuous, even though it is inadequate to identify their universality classes. We believe that the final choice between the two possibilities discussed in this paper will be made in future numerical work (The accuracy of the recent DMRG calculations [25, 26] for the S=1/2 zigzag ladders was reported to be inadequate to resolve this issue. Moreover, the non-linear σ model approach of Ref. [31], which excludes the massive chiral phase for half integer spins, is only valid in the vicinity of the classical Lifshitz point $j = 1/4$.)

Starting from the region A occupied by the CSN phase, one can also keep the in-chain anisotropy intact and vary continuously the inter-chain anisotropy. In particular, one can smoothly go from the case of an anti-ferromagnetic inter-chain coupling ($g_{\parallel} > 0$) to the case of a ferromagnetic coupling ($g_{\parallel} < 0$) (see Fig.7). We have shown that in such situation the ladder crosses over from the CSN phase to the F phase, the latter being dual to the former.

14 Appendix I: More about sector C

In this Appendix we address the role of the so far neglected twist perturbation $\lambda_3 \mathcal{O}_3$ which becomes relevant in sector C. Adding this term to the effective Hamiltonian leads us to the following theory:

$$\mathcal{H}_C = \mathcal{H}_0^{(+)} + \mathcal{H}_0^{(-)} \quad (240)$$

$$- \frac{\lambda_\perp}{\pi\alpha} \cos \sqrt{4\pi K_+} \Phi_+ \cos \sqrt{4\pi K_-} \Theta_- \quad (241)$$

$$+ \frac{2\lambda_1}{\sqrt{K_+}} \partial_x \Theta_+ \sin \sqrt{4\pi K_-} \Theta_- \quad (242)$$

$$+ \frac{\lambda_3}{\sqrt{K_-}} \partial_x \Phi_- \sin \sqrt{4\pi K_+} \Phi_+. \quad (243)$$

It is convenient to introduce dimensionless notations for the coupling constant

$$z_3 = 2\sqrt{\frac{\pi}{K_-}} \frac{\lambda_3 \alpha}{v}$$

and the z-component of the relative spin density,

$$\mathcal{Q}_- = 2\sqrt{\pi}\alpha \partial_x \Phi_-.$$

The variational approach we followed in section V is straightforwardly generalized for the present case. As compared to section V, here we have two additional variational parameters: the relative spin density \mathcal{Q}_- and a mixing angle ζ for the field Φ_+ . The variational energy then depends on six variables:

$$\mathcal{E}_C = \frac{1}{2}(M_+^2 + M_-^2 + \mathcal{J}_+^2 + \mathcal{Q}_-^2) \quad (244)$$

$$\mp z_1 \mathcal{J}_+ M_-^{K-} \sin \gamma \mp z_3 \mathcal{Q}_- M_+^{K+} \sin \zeta \quad (245)$$

$$- z_\perp M_+^{K+} M_-^{K-} \cos \gamma \cos \zeta. \quad (246)$$

Its minimization yields the following set of equations:

$$M_-^{K-}(z_\perp M_+^{K+} \sin \gamma \cos \zeta \mp z_1 \mathcal{J}_+ \cos \gamma) = 0, \quad (247)$$

$$M_+^{K+}(z_\perp M_-^{K-} \cos \gamma \sin \zeta \mp z_3 \mathcal{Q}_- \cos \zeta) = 0, \quad (248)$$

$$\mathcal{J}_+ \mp z_1 M_-^{K-} \sin \gamma = 0, \quad (249)$$

$$\mathcal{Q}_- \mp z_3 M_+^{K+} \sin \zeta = 0, \quad (250)$$

$$M_-(1 \mp z_1 \mathcal{J}_+ K_- M_-^{K-2} \sin \gamma \quad (251)$$

$$- z_\perp K_- M_+^{K+} M_-^{K-2} \cos \gamma \cos \zeta) = 0, \quad (252)$$

$$M_+(1 \mp z_3 \mathcal{Q}_- K_+ M_+^{K+2} \sin \zeta \quad (253)$$

$$- z_\perp K_+ M_+^{K-} M_+^{K+2} \cos \gamma \cos \zeta) = 0 \quad (254)$$

There exist solutions of these equations in which the second twist perturbation $\lambda_3 \mathcal{O}_3$ plays no role:

- (i) $\gamma = \zeta = 0$, $\mathcal{J}_+ = \mathcal{Q}_- = 0$ - D phase;
- (ii) $\gamma = \pi/2$, $\zeta = 0$, $\mathcal{Q}_- = 0$ - CSN phase;
- (iii) $0 < \gamma < \pi/2$, $\zeta = 0$, $\mathcal{Q}_- = 0$ - MSN phase.

There exists a pair of solutions which are “dual” to (ii) and (iii), i.e. can be obtained from the latter by the replacements $z_1 \rightarrow z_3$, $\mathcal{J}_+ \rightarrow \mathcal{Q}_-$, $M_+ \leftrightarrow M_-$:

(iv) $\gamma = 0$, $\zeta = \pi/2$, $\mathcal{J}_+ = 0$. This is a critical phase with a nonzero relative magnetization (CRM), $\mathcal{Q}_- \neq 0$;

(v) $\gamma = 0$, $0 < \zeta < \pi/2$, $\mathcal{J}_+ = 0$ - the massive version of the above phase (MRM). In these two phases the twist operator \mathcal{O}_1 plays no role.

There also exist solutions in which both twist perturbations are effective. One of them corresponds to the case

(vi) $\gamma = \pi/2$, $\zeta = \pi/2$, in which the z_\perp -perturbation is ineffective and the variational energy decouples into a direct sum $\mathcal{E}_{CSN} + \mathcal{E}_{CRM}$. The resulting phase is fully gapped and represents a mixture of CSN and CRM phases - mixed (M) phase with nonzero \mathcal{J}_+ and \mathcal{Q}_- .

The case of arbitrary values of the mixing angles, $\gamma, \zeta \neq 0, \pi/2$, should be abandoned because, as follows from Eqs.(254), it requires that $z_1^2 z_3^2 = z_\perp^2$, – a condition which represents just a point in the parameter space of the model and which, on the other hand, cannot be satisfied for all coupling constants being of the same order.

The minimal value of the variational energy is again given by Eq.(161). From this expression it is obvious that in sector C ($K_\pm < 1$) the M phase has a lower energy than each of its “constituents”, i.e. CSN and CRM phases. So we are left to find out if the M and MRM phases can compete with the D and MSN phase.

Consider the MRM phase assuming the most favorable condition $z_3 > z_\perp$. Since the MRM phase is “dual” to the MSN phase, from Eq.(204) we can read off the range where it can exist:

$$1 - (1 - K_+) \frac{\ln(z_3/z_\perp)}{\ln(1/z_3)} < K_- < 1. \quad (255)$$

We see that, except for an extremely unrealistic case $z_3^2 > z_\perp$, the condition (255) determines a vicinity of the negative semiaxis $K_- = 1$, $K_+ < 1$, which is located in the unphysical part of the (K_+, K_-) plane, well beyond sector C. Thus the MRM phase should be abandoned.

Let us compare the energies of the M and MSN phases. In both cases the mass M_- is given by the same expression, so we only need to compare the masses in the (+) channel. Comparing the mass M_+ in the M phase, $M_+ \sim z_3^{1/(1-K_+)}$, with that in the MSN phase, Eq. (198), we find that, except for extremely small values of z_\perp , namely $z_\perp < z_1 z_3$, the MSN phase is always more favorable.

Finally, we are left to compare the energies of the M and D phases. On one hand, in the D phase we are below the line (204). This means that $z_\perp^{\frac{1}{2-k_D}} > z_1^{\frac{1}{1-K_-}}$ implying that the mass gap of the D phase is greater than the mass M_- of the M phase. On the other hand, to the left of the MSD-D transition line (255) we have the condition $z_\perp^{\frac{1}{2-k_D}} > z_3^{\frac{1}{1-K_+}}$ that tells us that the mass of the D phase is greater than the mass M_+ of the M phase. Consequently, the D phase is energetically more favorable than the M phase.

15 Appendix II: Twist Interacting Term

In this section is our last attempts to treat the twist term as a perturbing term to the Hamiltonian of standard ladder (41), as what we did for the current-current interaction. So we assume that both interactions are present. In each normal current-current interaction vertex we have only one pair of fermions and its dual. Contrary to this each twist interacting vertex contains all four fermions and so each block diagonal matrix is 8×8 . Below we represent only one of these eight matrices. Here $\langle \xi_1 \xi_2 | \xi_1 \xi_2 \rangle$ and four new graphs are those in which all fermions are present so for example $\langle \xi_3 \xi_0 | \xi_1 \xi_2 \rangle$. The twist vertex z_1 represents the vertex in which $\bar{\xi}_1$ has different chirality i.e $\bar{\xi}_1 \xi_2 \xi_3 \xi_0$ and so on.

$$\begin{aligned}
 & \langle \xi_1 \xi_2 | \xi_1 \xi_2 \rangle + g \langle \xi_1 \xi_2 | \xi_1 \xi_2 \rangle + g \langle \xi_1 \xi_2 | \xi_1 \xi_2 \rangle - g \langle \xi_1 \xi_2 | \xi_1 \xi_2 \rangle - g \langle \xi_1 \xi_2 | \xi_1 \xi_2 \rangle \\
 & + z_0 \langle \xi_1 \xi_2 | \xi_1 \xi_2 \rangle + z_3 \langle \xi_1 \xi_2 | \xi_1 \xi_2 \rangle + z_3 \langle \xi_1 \xi_2 | \xi_1 \xi_2 \rangle + z_0 \langle \xi_1 \xi_2 | \xi_1 \xi_2 \rangle \\
 & + z_2 \langle \xi_1 \xi_2 | \xi_1 \xi_2 \rangle + z_1 \langle \xi_1 \xi_2 | \xi_1 \xi_2 \rangle + z_1 \langle \xi_1 \xi_2 | \xi_1 \xi_2 \rangle + z_2 \langle \xi_1 \xi_2 | \xi_1 \xi_2 \rangle = \langle \xi_1 \xi_2 | \xi_1 \xi_2 \rangle \\
 \\
 & g \langle \xi_1 \xi_2 | \xi_1 \xi_2 \rangle + \langle \xi_1 \xi_2 | \xi_1 \xi_2 \rangle + g \langle \xi_1 \xi_2 | \xi_1 \xi_2 \rangle - g \langle \xi_1 \xi_2 | \xi_1 \xi_2 \rangle - g \langle \xi_1 \xi_2 | \xi_1 \xi_2 \rangle \\
 & + z_0 \langle \xi_1 \xi_2 | \xi_1 \xi_2 \rangle + z_3 \langle \xi_1 \xi_2 | \xi_1 \xi_2 \rangle + z_3 \langle \xi_1 \xi_2 | \xi_1 \xi_2 \rangle + z_0 \langle \xi_1 \xi_2 | \xi_1 \xi_2 \rangle \\
 & + z_2 \langle \xi_1 \xi_2 | \xi_1 \xi_2 \rangle + z_1 \langle \xi_1 \xi_2 | \xi_1 \xi_2 \rangle + z_1 \langle \xi_1 \xi_2 | \xi_1 \xi_2 \rangle + z_2 \langle \xi_1 \xi_2 | \xi_1 \xi_2 \rangle = \langle \xi_1 \xi_2 | \xi_1 \xi_2 \rangle \\
 \\
 & g \langle \xi_1 \xi_2 | \xi_1 \xi_2 \rangle + g \langle \xi_1 \xi_2 | \xi_1 \xi_2 \rangle + \langle \xi_1 \xi_2 | \xi_1 \xi_2 \rangle - g \langle \xi_1 \xi_2 | \xi_1 \xi_2 \rangle - g \langle \xi_1 \xi_2 | \xi_1 \xi_2 \rangle \\
 & + z_0 \langle \xi_1 \xi_2 | \xi_1 \xi_2 \rangle + z_3 \langle \xi_1 \xi_2 | \xi_1 \xi_2 \rangle + z_3 \langle \xi_1 \xi_2 | \xi_1 \xi_2 \rangle + z_0 \langle \xi_1 \xi_2 | \xi_1 \xi_2 \rangle \\
 & + z_2 \langle \xi_1 \xi_2 | \xi_1 \xi_2 \rangle + z_1 \langle \xi_1 \xi_2 | \xi_1 \xi_2 \rangle + z_1 \langle \xi_1 \xi_2 | \xi_1 \xi_2 \rangle + z_2 \langle \xi_1 \xi_2 | \xi_1 \xi_2 \rangle = \langle \xi_1 \xi_2 | \xi_1 \xi_2 \rangle \\
 \\
 & g \langle \xi_1 \xi_2 | \xi_1 \xi_2 \rangle + g \langle \xi_1 \xi_2 | \xi_1 \xi_2 \rangle - g \langle \xi_1 \xi_2 | \xi_1 \xi_2 \rangle + \langle \xi_1 \xi_2 | \xi_1 \xi_2 \rangle - g \langle \xi_1 \xi_2 | \xi_1 \xi_2 \rangle \\
 & + z_0 \langle \xi_1 \xi_2 | \xi_1 \xi_2 \rangle + z_3 \langle \xi_1 \xi_2 | \xi_1 \xi_2 \rangle + z_3 \langle \xi_1 \xi_2 | \xi_1 \xi_2 \rangle + z_0 \langle \xi_1 \xi_2 | \xi_1 \xi_2 \rangle \\
 & + z_2 \langle \xi_1 \xi_2 | \xi_1 \xi_2 \rangle + z_1 \langle \xi_1 \xi_2 | \xi_1 \xi_2 \rangle + z_1 \langle \xi_1 \xi_2 | \xi_1 \xi_2 \rangle + z_2 \langle \xi_1 \xi_2 | \xi_1 \xi_2 \rangle = \langle \xi_1 \xi_2 | \xi_1 \xi_2 \rangle \\
 \\
 & + z_0 \langle \xi_1 \xi_2 | \xi_1 \xi_2 \rangle + z_3 \langle \xi_1 \xi_2 | \xi_1 \xi_2 \rangle + z_3 \langle \xi_1 \xi_2 | \xi_1 \xi_2 \rangle + z_0 \langle \xi_1 \xi_2 | \xi_1 \xi_2 \rangle
 \end{aligned}$$

$$\begin{aligned}
& +z_1 \text{ (diagram)} + z_2 \text{ (diagram)} + z_{\bar{1}} \text{ (diagram)} + z_2 \text{ (diagram)} \\
& + \text{ (diagram)} -g \text{ (diagram)} -g \text{ (diagram)} +g \text{ (diagram)} +g \text{ (diagram)} = 0 \\
& +z_3 \text{ (diagram)} + z_{\bar{0}} \text{ (diagram)} + z_3 \text{ (diagram)} + z_0 \text{ (diagram)} \\
& +z_2 \text{ (diagram)} + z_1 \text{ (diagram)} + z_{\bar{1}} \text{ (diagram)} + z_2 \text{ (diagram)} \\
& -g \text{ (diagram)} -g \text{ (diagram)} + \text{ (diagram)} +g \text{ (diagram)} +g \text{ (diagram)} = 0 \\
& +z_3 \text{ (diagram)} + z_{\bar{0}} \text{ (diagram)} + z_3 \text{ (diagram)} + z_0 \text{ (diagram)} \\
& +z_2 \text{ (diagram)} + z_1 \text{ (diagram)} + z_{\bar{1}} \text{ (diagram)} + z_2 \text{ (diagram)} \\
& -g \text{ (diagram)} -g \text{ (diagram)} + \text{ (diagram)} +g \text{ (diagram)} +g \text{ (diagram)} = 0 \\
& +z_3 \text{ (diagram)} + z_{\bar{0}} \text{ (diagram)} + z_3 \text{ (diagram)} + z_0 \text{ (diagram)} \\
& +z_2 \text{ (diagram)} + z_1 \text{ (diagram)} + z_{\bar{1}} \text{ (diagram)} + z_2 \text{ (diagram)} \\
& -g \text{ (diagram)} -g \text{ (diagram)} +g \text{ (diagram)} + \text{ (diagram)} +g \text{ (diagram)} = 0
\end{aligned}$$

Written in $M.X = X_0$ form M is given by

$$M = \begin{pmatrix} M_{11} & M_{12} \\ M_{21} & M_{22} \end{pmatrix} \quad (256)$$

Two matrices M_{11} and M_{22} is what we have derived before adding twist operator, for (1, 2) and (3, 0) fermions respectively:

$$M_{11} = \begin{pmatrix} 1 + gC & gD & -gR_1 & -gR_2 \\ g\bar{D} & 1 + gC & g\bar{R}_2 & g\bar{R}_1 \\ g\bar{R}_1 & -gR_2 & 1 + gC & -gL \\ g\bar{R}_1 & -gR_2 & 1 + gC & -gL \end{pmatrix} \quad (257)$$

$$M_{22} = \begin{pmatrix} 1 + gC' & -gL' & g\bar{R}_3 & -gR_0 \\ -gL' & 1 + gC' & g\bar{R}_0 & -gR_3 \\ -gR_3 & -gR_0 & 1 + gC' & gD' \\ g\bar{R}_0 & g\bar{R}_3 & g\bar{D}' & 1 + gC' \end{pmatrix} \quad (258)$$

Twist term appears only in M_{12} and M_{21} , those elements which connect (1, 2) fermions to (3, 0)

$$M_{12} = \begin{pmatrix} z_0 D + z_3 \bar{C} & z_3 \bar{D} + z_0 C & z_2 R_2 + z_1 \bar{R}_1 & z_1 R_2 + z_2 \bar{R}_1 \\ z_0 C + z_3 \bar{D} & z_3 C + z_0 \bar{D} & -z_2 \bar{R}_1 - z_1 \bar{R}_2 & -z_1 \bar{R}_1 - z_2 \bar{R}_2 \\ -z_0 R_2 + z_3 \bar{R}_1 & -z_3 R_2 + z_0 \bar{R}_1 & z_2 L - z_1 C & z_1 L - z_2 C \\ -z_0 R_1 + z_3 \bar{R}_2 & -z_3 R_1 + z_0 \bar{R}_2 & -z_2 C + z_1 L & -z_1 C + z_2 L \end{pmatrix} \quad (259)$$

$$M_{12} = \begin{pmatrix} z_0 L' - z_3 C' & z_3 L' - z_0 C' & z_1 \bar{R}_3 - z_2 R_0 & -z_1 R_0 + z_2 \bar{R}_3 \\ z_3 L' - z_0 C' & -z_3 C' + z_0 L' & -z_2 R_3 + z_1 \bar{R}_0 & -z_1 R_3 + z_2 \bar{R}_0 \\ z_3 R_3 + z_0 R_0 & z_3 R_0 + z_0 R_3 & z_2 D' + z_1 C' & z_1 D' + z_2 C' \\ -z_3 \bar{R}_0 - z_0 \bar{R}_3 & -z_3 \bar{R}_3 - z_0 \bar{R}_0 & z_2 C' + z_1 \bar{D}' & z_1 C' + z_2 \bar{D}' \end{pmatrix} \quad (260)$$

The effect of twist term is considered only in the symmetric case in which $m_s = -m_t$ which correspond to the standard ladder with additional four-spin interaction in which the most relevant term is $\mathbf{n}_1 \cdot \mathbf{n}_2 - \epsilon_1 \cdot \epsilon_2$. Equivalently the twist operator is

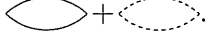
$$\mathbf{n}_1 \partial_x \mathbf{n}_2 - \epsilon_1 \partial_x \epsilon_2 + (1 \leftrightarrow 2) = -\bar{\xi}_0 \xi_1 \xi_2 \xi_3 + \xi_0 \bar{\xi}_1 \xi_2 \xi_3 + \xi_0 \xi_1 \bar{\xi}_2 \xi_3 + \xi_0 \xi_1 \xi_2 \bar{\xi}_3 + (R \leftrightarrow L) \quad (261)$$

so that $z_1 = z_2 = z_3 = -z_0 = z_0 = -z_1 = -z_2 = -z_3$. In this case the pole must be searched in:

$$W = (1 + gC - gL) \left((1 + gC)^2 - g^2 D \bar{D} \right) + 2 \left(g^3 D \bar{R}^2 + g^3 \bar{D} R^2 + 2g^2 R \bar{R} (1 + gC) \right) + 2z^2 \left((C - L)(D + \bar{D} - 2C + 2g(C^2 - D \bar{D})) - 2(R + \bar{R})^2 + 4g(D \bar{R}^2 + \bar{D} R^2 + 2C R \bar{R}) \right)$$

which simplifies to

$$W = 1 - (2gm^2 + g \frac{s^2}{2} + \frac{z^2 q^2}{\pi} + \frac{gz^2 q^2}{2\pi^2}) \chi. \quad (262)$$

The first two terms are those in (104). The effect of twist term is embodied in the correction to the current-current interaction as $z^2 \frac{q^2}{\pi s^2}$. This correction comes from the anomalous part of current-current term . Note that this correction always reduces the effective $g_0 \sim J_\perp$ i.e it's a ferromagnetic correction which opposes the formation of bound state. Moreover it breaks the Lorentz-invariance. In order to have a bound state the center of mass momentum of the pair must satisfy

$$q^2 < \frac{8\pi m^2 g_0}{z^2}. \quad (263)$$

When q exceed this limit the bound pairs break. In the absence of the twist term the bound states can basically move with any center of mass momenta q provided that $s^2 < 4m^2$. By breaking Lorentz invariance, in the presence of twist term only those two particles with almost opposite momentum can bind together. To see this we note that the position of the bound state is given by

$$\omega^2 \approx M_b^2 + q^2\left(1 + \frac{g_0 z^2}{\pi m}\right) + q^2 \frac{g_0^2 z^2}{\pi^2 m} - q^4 \frac{z^4}{16\pi^2 m^2} \left(1 - \frac{g_0}{\pi}\right)^2$$

($M_b = \sqrt{4m^2(1 - g_0^2)}$ is the bound state mass in the absence of twist term). The nontrivial solution (with $q \neq 0$) is

$$q^2 \approx \frac{16mg_0}{z^2} + \frac{16m^2\pi^2}{z^4} + \frac{32m^2g_0}{z^4}$$

which already exceeds the limit (263).

16 Conclusion

In this thesis we have studied the simplest spin ladders namely the standard ladder Fig.(2) and the frustrated zig-zag ladder Fig.(8). Ladders are important because there exist some compounds which can be best described by ladders [5, 7, 8, 14]. Moreover they are intermediate models between one dimensional (1D) spin chains and two dimensional spin systems. In one limit, the antiferromagnetic Heisenberg (AFH) spin chains is disordered by dominant quantum fluctuations, leading to a power-law falloff of the spin-spin correlations, and gapless spinon ($\Delta S = 1/2$) excitations. In the other limit, the 2D AFH systems is known to be long range ordered with gapless magnon ($\Delta S = 1$) excitations. Ladders lay in the route between these two limits which nevertheless is not a trivial route. The ladders with odd number of chains have gapless spin excitations and power-law falloff the spin-spin correlations (apart from logarithmic corrections); however the ladders with even number of the legs are gapped with short range spin-spin correlations although they are unfrustrated.

In the first part we have studied the simplest prototype of spin ladders namely the two-leg standard ladder with inchain coupling J and interchain coupling J_{\perp} , Fig.(2). The properties of the ladder is well understood in the strong interchain coupling limit $|J_{\perp}| \gg J$. In this limit for ferromagnetic interchain coupling, triplets are formed along each rung separated by a gap of the order J_{\perp} from singlet excitations. The ladder is effectively described by the well known gapped $S = 1$ Haldane chain. In the strong antiferromagnetic interchain coupling, singlets are formed along each rung, and interact weakly with each other through inchain coupling J , leading to the simple massive magnon dispersion $\omega(q) = J_{\perp} + J \cos(q)$. Even in the weak coupling limit magnons remain massive, as we will discuss soon. Moreover in the strong coupling limit, besides individual magnon excitations, bound states of two magnons were predicted to exist theoretically and observed experimentally [10, 11], slightly below the two-magnon continuum. As in the compounds the typical interchain coupling is of the order of the inchain coupling, it is interesting to address the fate of two magnon bound states in the weak coupling limit, also because they can change the nature of correlation function considerably.

In the weak interchain coupling limit the bosonization technique can be implemented to investigate the ground state and the excitations of the ladder[2]. In the continuum limit each spin is described by a slowly varying

smooth part (i.e total magnetization) and a staggered part. It is the interaction between the staggered part of spins along each rung which opens the gap of the order of J_{\perp} in the model. For ferromagnetic interchain coupling $J_{\perp} < 0$ the ladder is known to be in the Haldane phase at which two spins along each rung form a triplet. This fact is best illustrated in the total staggered magnetization correlation function or $S(q \approx \pi, q_{\perp} = 0, \omega)$ (see (55)), which shows a coherent magnon peak (45). For antiferromagnetic interchain coupling, the singlet is formed along the rung of each unit cell, the ladder being in the rung-singlet phase. This time the triplet excitations contribute a coherent δ -peak to the relative staggered magnetization correlation function i.e $S(q \approx \pi, q_{\perp} = \pi, \omega)$. In both cases magnons are optical, i.e they have spectral gap. At the same time the smooth part of the total and relative magnetization, $S(q \approx 0, q_{\perp} = 0, \omega)$ and $S(q \approx 0, q_{\perp} = \pi, \omega)$, show a two-particle mass threshold singularity respectively at two triplet mass $s = 2|m_t|$ and a triplet and singlet mass threshold $s = |m_t| + |m_s|$.

However, exactly here, the marginal interacting term between the smooth part of the spins along the rungs plays its role and cause an effective interaction among triplet excitations and between a triplet and a singlet excitation (47). While in the Haldane phase, $J_{\perp} < 0$, the interaction is 'repulsive' and just renormalizes the triplet and singlet masses, in the rung-singlet phase $J_{\perp} > 0$ it can create bound states; which in turn changes the behavior of spin-spin correlation functions.

The coherent bound state δ -peak can be observed in the correlation function of the smooth part of total (relative) magnetization, $S(q \approx 0, q_{\perp} = 0, \omega)$ ($S(q \approx 0, q_{\perp} = \pi, \omega)$). The peak is slightly below the two triplet masses $s = 2|m_t|$ (below the triplet and singlet mass threshold $s = |m_t| + |m_s|$). These peaks replace the square root singularity at these two points by a square root threshold Fig.(5). So in spite of both being a spin gap, we predict that there will be a clear distinction between the antiferromagnetic and ferromagnetic interchain coupling due to the formation of bound states. The difference is in principle observable in experiments by measuring the structure factor $S(q \approx 0, q_{\perp} = 0, \omega)$ and $S(q \approx 0, q_{\perp} = \pi, \omega)$.

Including the four-spin interaction (48) (which can be generated for example by phonons) can cause dimerization in the ladder. The picture of the two-fold degenerate ground state is simple Fig.(4) and consists of singlet pairs formed along each individual chain, which break the translation invariant symmetry. The singlet pairs in different chains are either in-phase or are out-of phase. In Fig.(3) we have shown the phase diagram of the standard

ladder including these so called dimerized spin liquid phases.

The excitations of two dimerized spin liquid phases differ from those of Haldane and rung-singlet phases. While in the latter phases the triplet excitations form a coherent magnon peak, the excitations of dimerized spin liquid phases are propagating massive topological singlets or triplets Fig.(6). For instance in the in-phase dimerized spin liquid, looking at the correlation function of the total and relative staggered magnetization i.e ($S(q = \pi, q_{\perp} = 0, \omega)$) and ($S(q = \pi, q_{\perp} = \pi, \omega)$), instead of a δ -peak, one observes a singular mass threshold at respectively $s = 2|m_t|$ and $s = |m_t| + |m_s|$ (54). For out of phase dimerized spin liquid, the role of total and relative staggered spin correlations is interchanged. (The correlation function of total and relative smooth magnetization i.e ($S(q = 0, q_{\perp} = 0, \omega)$), ($S(q = 0, q_{\perp} = \pi, \omega)$) have two-mass singularity at $s = 2|m_t|$ and respectively $s = |m_t| + |m_s|$ in all above mentioned four phases.)

Taking into account the interaction between excitations will change the nature of spin-spin correlation functions very similar to the case of the rung-singlet and Haldane phase. This time bound states are formed only in the in-phase spin dimerized phase below $s = 2|m_t|$ and $s = |m_t| + |m_s|$. Here in all spin-spin correlation functions instead of a singular threshold, one observes a bound state δ -peak followed by a nonsingular mass threshold. In the out of phase dimerized spin liquid, the interaction only renormalizes the excitations masses.

In the second part of the thesis we have included frustration. The interplay between frustration and quantum fluctuations makes the problem even more interesting. We have considered the simplest model, namely the AFH spin chain with nearest neighbor interaction J' and antiferromagnetic next nearest neighbor interaction J , which equivalently, when $J \gg J'$ can be viewed as the zig-zag Heisenberg ladder Fig.(8). The ladder has some realizations in compounds like Cs_2CuCl_4 . The classical ground state of the chain is the Néel ordered phase for $j = J/J' < 1/4$ with characteristic momentum $q = \pi$ and the spiral order for $j > 1/4$ with characteristic momentum $q = -\arccos(1/4j)$.

For small value of the next nearest neighbor interaction $j < j_c \simeq 0.241$, quantum fluctuations disorder the classical Néel order phase. Instead, for $j > j_c \simeq 0.241$, quantum fluctuations spoil out completely the spiral classical order, and induce a spontaneously dimerized phase. The transition

between these two phases is a Berezinskii-Kosterlitz-Thouless transition. In the dimerized phase a spin gap opens up in the system, whose value becomes maximum at the so-called Majumdar-Ghosh point $j = 1/2$ at which the exact ground state of the ladder is known. In the whole dimerized phase $j > j_c$, the excitations of the ladder are massive spinon dimerization kinks, carrying $S = 1/2$. So in comparison to standard ladder in which two spinons confine to form a massive coherent magnon, in the frustrated ladder one observes massive fractionalized spinons.

By further increasing j , the value of the mass decreases as expected since for $j \rightarrow \infty$ one approaches the two decoupled chains limit. Moreover the spin-spin correlation functions show another change in their nature namely they become incommensurate i.e their characteristic momentum is neither $q = \pi$ (in the limit of single chain) nor $q = \pi/2$ (in the limit of two decoupled chains). So the trace of the classical phase ordering is best observed in the large $j \gg 1$ limit.

In this limit, the interchain coupling, is a weak perturbative interaction added to the free Hamiltonian of two AFH chains. It is expected that this interaction will simultaneously induce incommensurability and dimerization in the ladder. In fact the interchain interaction of the smooth part of the spins can open up a gap in the system [21] while the interaction between the staggered part of the spins leads to the parity breaking twist term which is known to be responsible for incommensurate spin-spin correlations [24] (see (124,125)).

At the $SU(2)$ point the interplay between these two operators is still an unsolved problem. The authors of [24] has shown that in the strong anisotropic XX -limit the role of the twist term is dominant. In the two-fold degenerate ground state there is a finite spin current along two chains and (in opposite direction) along the zig-zag line. The spin current is nothing but the chirally vector operator $\mathbf{S}_n \times \mathbf{S}_{n+1}$ so that in the large spin limit one recovers the classical spiral long range order. In this ground state the time-reversal symmetry is preserved but the parity is broken. The presence of spin current induce incommensurability in spin-spin correlation function. The transverse spin-spin correlation shows an algebraic decay and moreover it is incommensurate (183). The existence of this so called critical spin nematic (CSN) phase is confirmed in numerical studies for integer and half-integer spins[25].

Far away from $SU(2)$ -symmetric point, we have used the Abelian bosonization method combined with a variational approach, to derive the phase di-

agram of the system and the possible crossover between these phases. The inchain and interchain spin anisotropy has been treated independently. By changing these two parameters we can cover various regions of the phase diagram at which the role of the dimerization operator, twist operator or both of them are dominant so that we can study the interplay between dimerization and incommensurability (see Fig.10).

We have shown that the CSN phase extends well beyond the XX limit and covers broad regions in the parameter space of the XXZ model.

Increasing the intra-chain anisotropy parameter, ultimately a phase transition occurs to a spontaneously dimerized phase with broken translational invariance symmetry. In the dimerized phase spin correlations decay exponentially but they are commensurate, so this is the extreme limit at which the role of dimerization is dominant and there is no trace of incommensurability.

We have shown that the transition from CSN to D phase can happen either directly or through an intermediate state called massive spin nematic *MSN* phase. The latter possibility is interesting because in the new phase both dimerization and twist operators play a role. The *MSN* phase is characterized by the coexistence of a finite spin current with dimerization. In another words even though the spin-spin correlation functions falloff exponentially they remain incommensurate. Recent numerical works show that in the case of integer spin such a phase can be seen in a narrow region between fully dimerized phase and CSN phase [25]. For half-integer spins the numerical precision is not enough to decide whether such possibility can exist or not. What we have shown here is that this possibility is not excluded for spin-1/2 ladder.

Finally we have shown that for the ferromagnetic coupling ($J' < 0$) the ladder can be in a new ferromagnetic phase (F phase). This ferromagnetic phase is the dual of the CSN phase. So while in the latter a finite spin current is induced in the system, in the former there appears a finite magnetization. Time reversal symmetry is broken in this phase but the parity is preserved. The ground state is two-fold degenerate and the massive kinks which interpolate between these two vacua carry relative spin $S_z = 1/2$ (212).

References

- [1] P.A. Lee, cond-mat/0307508

- [2] D. Shelton, A.A. Nersesyan, and A.M. Tsvelik, Phys.Rev B **53**, 8521 (1996).
- [3] A.A. Nersesyan and A.M. Tsvelik, Phys. Rev. Lett **78**, 3939 (1997)
- [4] F. D. M. Haldane, Phys. Rev. B **25**, 4925 (1982); Errata *ibid.* **26**, 5257 (1982).
- [5] E. Dagotto, T .M .Rice, Science 271 (1996) 618.
- [6] M. Fabrizio, Phys. Rev. B **54**, 10054 (1996)
- [7] S. E. Nagler, D. A. Tennant, R. A. Cowley, T. G. Perring, and S. K. Satija, Phys. Rev. B **44**, 12361 (1991); D. A. Tennant, T. G. Perring, R. A. Cowley, and S. E. Nagler, Phys. Rev. Lett. **70**, 4003 (1993); D. A. Tennant, R. A. Cowley, S. E. Nagler, and A. M. Tsvelik, Phys. Rev. B **52**, 13368 (1995).
- [8] S. Gopalan, T. M. Rice, and M. Sigrist, Phys. Rev. B **49**, 8901 (1994).
- [9] G. Chaboussant, M. H. Julien, Y. Fagot-Revurat, L. P. Levy, C. Berthier, M. Horvatic, and O. Piovesana, Phys. Rev. Lett **79** 925, (1997).
- [10] O. P. Sushkov and V. N. Kotov, Phys. Rev. Lett. **81**, 1941 (1998); V. N. Kotov, O. P. Sushkov and R. Eder, Phys. Rev. B **59**, 6266 (1999).
- [11] M. Windt, M. Grüninger, T. Nunner, C. Knetter, K. P. Schmidt, G. S. Uhrig, T. Kopp, A. Freimuth, U. Ammerahl, B. Büchner, and A. Revcolevschi, Phys. Rev. Lett. **87**, 127002 (2001).
- [12] S. Sachdev, Quantum Phase Transitions, Cambridge University Press, 1999.
- [13] P. Lecheminant, cond-mat/0306520.
- [14] R. Coldea, D.A. Tennant, R.A. Cowley, D.F. McMorrow, B. Dorner, and Z. Tylczynski, Phys. Rev. Lett. **79**, 151 (1997); R. Coldea, D.A. Tennant, A.M. Tsvelik, and Z. Tylczynski, Phys. Rev. Lett. **86**, 1335 (2001). R. Coldea, D.A. Tennant, and Z. Tylczynski, cond-mat/0307025 (unpublished).

- [15] A. Luther and I. Peschel, Phys. Rev. **B9**, 2911 (1974).
- [16] A. Luther and I. Peschel, Phys. Rev. B **12**, 3908 (1975).
- [17] I. Affleck, Nucl. Phys. B 265, 409 (1986); Also see I. Affleck and F. D. M. Haldane, Phys. Rev. B 36, 5291 (1987).
- [18] F.D.M. Haldane, Phys. Rev. B**25**, 4925 (1982).
- [19] S.Eggert, Phys. Rev. B **54**, 961 (1996).
- [20] K.Okamoto and K.Nomura, Phys. Lett. A **169**, 433 (1992)
- [21] S.R. White and I. Affleck, Phys. Rev B**54**, 9862 (1996)
- [22] C.K. Majumdar and D.K. Ghosh, J.Math. Phys **10**, 1388 (1969).
- [23] A.A. Aligia, C.D. Batista, and F.H.L. Essler, Phys. Rev. B **62**, 3259 (2000).
- [24] A.A. Nersesyan, A.O. Gogolin, and F.H.L. Essler, Phys. Rev. Lett. **81**, 910 (1998).
- [25] T. Hikihara, M. Kaburagi and H. Kawamura, Phys. Rev. B **63**, 174430 (2001).
- [26] T. Hikihara, M. Kaburagi and H. Kawamura, Prog. Theor. Phys. Suppl. **145**, 58 (2002).
- [27] P.D. Sacramento and V.R. Vieira, J.Phys.: Condens. Matter **14**, 591 (2002).
- [28] V. R. Vieira, N. Guihery, J. P. Rodriguez, and P. D. Sacramento, Phys. Rev. B 63, 224417 (2001).
- [29] H. Fukushima, H. Kikuchi, M. Chiba, Y. Fujii, Y. Yamamoto, and H. Hori, Prog. Theor. Phys. Suppl. **145**, 72 (2002).
- [30] P.Lecheminant, T.Jolicoeur and P.Azaria, Phys. Rev. B**63**, 174426 (2001).
- [31] A.K.Kolezhuk,Phys. Rev. B**62**, R6057 (2000).

- [32] A.O. Gogolin, A.A. Nersesyan, and A.M. Tsvelik, *Bosonization and Strongly Correlated Systems*, Cambridge Univ. Press, Cambridge, 1999.
- [33] D.C. Cabra, A. Honecker, and P. Pujol, *Eur. Phys. J. B* **13**, 55 (2000).
- [34] D. Allen and D. Senechal, *Phys. Rev. B* **55**, 299 (1997).
- [35] D. Allen, F.H.L. Essler, and A.A. Nersesyan, *Phys. Rev. B* **61**, 8871 (2000).
- [36] It should be remembered that it is only at the SU(2) point that all three components of the vector current satisfy the SU(2)₁ Kac-Moody algebra. In the XXZ case ($\Delta < 1$) $J_{R,L}^x$ and $J_{R,L}^y$ acquire anomalous dimensions, and only $J_{R,L}^z$ remain as the generators of U(1)_{R,L}.
- [37] S. Lukyanov and A.B. Zamolodchikov, *Nucl.Phys. B* **493**, 571 (1997).
- [38] S. Lukyanov, *Mod. Phys. Lett. A* **12**, 2543 (1997).
- [39] S. Coleman, *Phys. Rev. D* **11**, 2088 (1975). For an equivalent Self-Consistent Harmonic Approximation see Y. Suzumura, *Prog. Theor. Phys.* **61**, 1 (1979).
- [40] Z. Weihong, V. Kotov, and J. Oitmaa, *Phys. Rev. B* **57**, 11 439 (1998); X. Wang, cond-mat/9803290; A.K. Kolezhuk and H.-J. Mikeska, *Int. J. Mod. Phys. B* **5**, 2325 (1998).
- [41] Massive spinons carrying fractional quantum numbers have been recently shown to persist in a higher-dimensional version of the model (150); see A.A. Nersesyan and A.M. Tsvelik, *Phys. Rev. B* **67**, 024422 (2003).
- [42] G. Delfino and G. Mussardo, *Nucl. Phys. B* **516**, 675 (1998).
- [43] M. Fabrizio, A.O. Gogolin, and A.A. Nersesyan, *Nucl. Phys. B* **580**, 647 (2000).
- [44] A.M. Tsvelik, *Nucl. Phys. B* **612**, 479 (2001).
- [45] P. Di Francesco, P. Mathieu, and D. Senechal, *Conformal Field Theory*, NY, Springer-Verlag, 1996.

- [46] A. Lauchli, G. Schmid, and M. Troyer, cond-mat/0206153
- [47] S. R. White and D. A. Huse, Phys. Rev. B **48**, 3844 (1993); E. S. Sorensen and I. Affleck, Phys. Rev. Lett. **71**, 1633 (1993); Phys. Rev. B **49**, 15771 (1994).
- [48] T. T. Wu, B. McCoy, C. A. Tracy, and E. Barouch, Phys. Rev. B **13**, 316 (1976).
- [49] K. Damle and S. Sachdev, Phys. Rev. B **57**, 8307 (1998).
- [50] C. Jurecka and W. Brenig, Phys. Rev. B **61**, 14307 (2000).
- [51] S. Trebst, H. Monien, C. J. Hamer, Z. Weihong, and R. R. P. Singh, Phys. Rev. Lett. **85**, 4373 (2000); W. Zheng, C. J. Hamer, R. R. P. Singh, S. Trebst, and H. Monien, Phys. Rev. B **63**, 144410 (2001).